US009651533B2

(12) **United States Patent**
Islam

(10) **Patent No.: US 9,651,533 B2**
(45) **Date of Patent: *May 16, 2017**

(54) **SHORT-WAVE INFRARED SUPER-CONTINUUM LASERS FOR DETECTING COUNTERFEIT OR ILLICIT DRUGS AND PHARMACEUTICAL PROCESS CONTROL**

(71) Applicant: **OMNI MEDSCI, INC.**, Ann Arbor, MI (US)

(72) Inventor: **Mohammed N. Islam**, Ann Arbor, MI (US)

(73) Assignee: **Omni Medsci, Inc.**, Ann Arbor, MI (US)

(*) Notice: Subject to any disclaimer, the term of this patent is extended or adjusted under 35 U.S.C. 154(b) by 0 days.

This patent is subject to a terminal disclaimer.

(21) Appl. No.: **14/875,709**

(22) Filed: **Oct. 6, 2015**

(65) **Prior Publication Data**

US 2016/0047787 A1 Feb. 18, 2016

Related U.S. Application Data

(63) Continuation of application No. 14/108,986, filed on Dec. 17, 2013, now Pat. No. 9,164,032.
(Continued)

(51) **Int. Cl.**
G01J 5/20 (2006.01)
G01N 33/15 (2006.01)
(Continued)

(52) **U.S. Cl.**
CPC ***G01N 33/15*** (2013.01); ***A61B 5/0013*** (2013.01); ***A61B 5/0022*** (2013.01);
(Continued)

(58) **Field of Classification Search**
CPC G01N 33/15; G01N 21/359; G01N 33/49
(Continued)

(56) **References Cited**

U.S. PATENT DOCUMENTS

4,063,106 A 12/1977 Ashkin et al.
4,158,750 A 6/1979 Sakoe et al.
(Continued)

FOREIGN PATENT DOCUMENTS

CN 101849821 B 7/2013
DE 102010012987 A1 10/2010
(Continued)

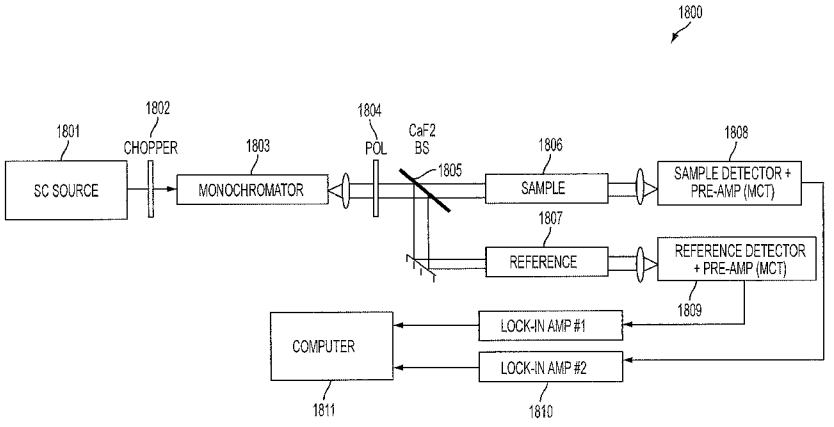
OTHER PUBLICATIONS

Istepanian, Robert H., "The Comparative Performance of Mobile Telemedical Systems based on the IS-54 and GSM Cellular Telephone Standards"; Journal of Telemedicine and Telecare 1999; pp. 97-104.
(Continued)

Primary Examiner — David Porta
Assistant Examiner — Abra Fein
(74) *Attorney, Agent, or Firm* — Brooks Kushman P.C.

(57) **ABSTRACT**

A measurement system includes a wearable measurement device for measuring one or more physiological parameters, including a light source comprising a plurality of light emitting diodes (LEDs) configured to generate an output optical beam with a near-infrared wavelength between 700 nanometers and 2500 nanometers. The light source is configured to increase signal-to-noise ratio by increasing a light intensity and pulse rate of the LEDs. The system includes a plurality of lenses configured to receive the output optical beam and to deliver an analysis output beam to a sample. The wearable measurement device includes a receiver configured to process the analysis output beam reflected or transmitted from the sample and to generate an output signal
(Continued)



Samsung Ex. 1081
Samsung v. Omni
PGR2025-00064
Page 00001

that may be transmitted to a remote device configured to process the received output status to generate processed data and to store the processed data.

18 Claims, 26 Drawing Sheets

Related U.S. Application Data

(60) Provisional application No. 61/747,487, filed on Dec. 31, 2012.

(51) **Int. Cl.**

A61B 5/1455	(2006.01)
A61B 5/00	(2006.01)
G01J 3/10	(2006.01)
G01J 3/28	(2006.01)
G01J 3/453	(2006.01)
G01N 21/359	(2014.01)
A61B 5/145	(2006.01)
G01N 33/49	(2006.01)
H01S 3/30	(2006.01)
G01J 3/14	(2006.01)
G01J 3/18	(2006.01)

(52) **U.S. Cl.**

CPC ***A61B 5/0075*** (2013.01); ***A61B 5/0086*** (2013.01); ***A61B 5/0088*** (2013.01); ***A61B 5/1455*** (2013.01); ***A61B 5/14532*** (2013.01); ***A61B 5/14546*** (2013.01); ***A61B 5/4547*** (2013.01); ***G01J 3/108*** (2013.01); ***G01J 3/28*** (2013.01); ***G01J 3/453*** (2013.01); ***G01N 21/359*** (2013.01); ***G01N 33/49*** (2013.01); *A61B 2562/0233* (2013.01); *A61B 2562/0238* (2013.01); *A61B 2562/146* (2013.01); *A61B 2576/02* (2013.01); *G01J 3/14* (2013.01); *G01J 3/1838* (2013.01); *G01J 2003/104* (2013.01); *G01J 2003/2826* (2013.01); *G01N 2201/061* (2013.01); *G01N 2201/062* (2013.01); *G01N 2201/12* (2013.01); *H01S 3/302* (2013.01)

(58) **Field of Classification Search**

USPC 250/338.4

See application file for complete search history.

(56) **References Cited**

U.S. PATENT DOCUMENTS

4,221,997	A	9/1980	Flemming
4,275,266	A	6/1981	Lasar
4,374,618	A	2/1983	Howard
4,403,605	A	9/1983	Tanikawa
4,462,080	A	7/1984	Johnstone et al.
4,516,207	A	5/1985	Moriyama et al.
4,523,884	A	6/1985	Clement et al.
4,605,080	A	8/1986	Lemelson
4,641,292	A	2/1987	Tunnell et al.
4,704,696	A	11/1987	Reimer et al.
4,728,974	A	3/1988	Nio et al.
4,762,455	A	8/1988	Coughlan et al.
4,776,016	A	10/1988	Hansen
4,958,910	A	9/1990	Taylor et al.
4,989,253	A	1/1991	Liang et al.
5,078,140	A	1/1992	Kwoh
5,084,880	A	1/1992	Esterowitz et al.
5,086,401	A	2/1992	Glassman et al.
5,134,620	A	7/1992	Huber
5,142,930	A	9/1992	Allen et al.
5,180,378	A	1/1993	Kung et al.
5,191,628	A	3/1993	Byron
5,218,655	A	6/1993	Mizrahi
5,230,023	A	7/1993	Nakano
5,246,004	A	9/1993	Clarke et al.
5,267,152	A	11/1993	Yang et al.
5,267,256	A	11/1993	Saruwatari et al.
5,267,323	A	11/1993	Kimura
5,300,097	A	4/1994	Lerner et al.
5,303,148	A	4/1994	Mattson et al.
5,305,427	A	4/1994	Nagata
5,313,306	A	5/1994	Kuban et al.
5,323,404	A	6/1994	Grubb
5,345,538	A	9/1994	Narayannan et al.
5,400,165	A	3/1995	Gnauck et al.
5,408,409	A	4/1995	Glassman et al.
5,458,122	A	10/1995	Hethuin
5,544,654	A	8/1996	Murphy et al.
5,572,999	A	11/1996	Funda et al.
5,617,871	A	4/1997	Burrows
5,631,758	A	5/1997	Knox et al.
5,687,734	A	11/1997	Dempsey et al.
5,695,493	A	12/1997	Nakajima et al.
5,696,778	A	12/1997	MacPherson
5,704,351	A	1/1998	Mortara et al.
5,718,234	A	2/1998	Warden et al.
5,747,806	A	5/1998	Khalil
5,748,103	A	5/1998	Flach et al.
5,792,204	A	8/1998	Snell
5,812,978	A	9/1998	Nolan
5,855,550	A	1/1999	Lai et al.
5,862,803	A	1/1999	Besson et al.
5,867,305	A	2/1999	Waarts et al.
5,912,749	A	6/1999	Harstead et al.
5,944,659	A	8/1999	Flach et al.
5,950,629	A	9/1999	Taylor et al.
5,957,854	A	9/1999	Besson et al.
5,970,457	A	10/1999	Brant et al.
6,014,249	A	1/2000	Fermann et al.
6,043,927	A	3/2000	Islam
6,115,673	A	9/2000	Malin
6,181,414	B1	1/2001	Raz et al.
6,185,535	B1	2/2001	Hedin et al.
6,200,309	B1	3/2001	Rice et al.
6,212,310	B1	4/2001	Waarts et al.
6,224,542	B1	5/2001	Chang et al.
6,246,707	B1	6/2001	Yin et al.
6,246,896	B1	6/2001	Dumoulin
6,273,858	B1	8/2001	Fox et al.
6,278,975	B1	8/2001	Brant et al.
6,281,471	B1	8/2001	Smart
6,285,897	B1	9/2001	Kilcoyne
6,289,238	B1	9/2001	Besson et al.
6,301,271	B1	10/2001	Sanders et al.
6,301,273	B1	10/2001	Sanders et al.
6,333,803	B1	12/2001	Kurotori et al.
6,337,462	B1	1/2002	Smart
6,340,806	B1	1/2002	Smart et al.
6,350,261	B1	2/2002	Domankevitz et al.
6,364,834	B1	4/2002	Reuss et al.
6,374,006	B1	4/2002	Islam et al.
6,381,391	B1	4/2002	Islam et al.
6,402,691	B1	6/2002	Peddicord et al.
6,407,853	B1	6/2002	Samson et al.
6,436,107	B1	8/2002	Wang et al.
6,441,747	B1	8/2002	Khair et al.
6,442,430	B1	8/2002	Ferek-Petric
6,443,890	B1	9/2002	Schulze et al.
6,450,172	B1	9/2002	Hartlaub et al.
6,453,201	B1	9/2002	Daum et al.
6,454,705	B1	9/2002	Cosentino et al.
6,458,120	B1	10/2002	Shen et al.
6,462,500	B1	10/2002	L'Hegarat et al.
6,463,361	B1	10/2002	Wang et al.
6,480,656	B1	11/2002	Islam et al.
6,512,936	B1	1/2003	Monfre
6,543,012	B1	4/2003	Viswanathan
6,549,702	B2	4/2003	Islam et al.
6,567,431	B2	5/2003	Tabirian et al.
6,587,702	B1	7/2003	Ruchti

(56) **References Cited**

U.S. PATENT DOCUMENTS

6,603,910	B2	8/2003	Islam et al.	
6,605,080	B1	8/2003	Altshuler et al.	
6,611,643	B2	8/2003	Birk	
6,619,835	B2	9/2003	Kita	
6,625,180	B2	9/2003	Bufetov et al.	
6,631,025	B2	10/2003	Islam et al.	
6,640,117	B2	10/2003	Makarewicz	
6,659,947	B1	12/2003	Carter et al.	
6,659,999	B1	12/2003	Anderson et al.	
6,738,652	B2	5/2004	Mattu	
6,760,148	B2	7/2004	Islam	
6,773,922	B2	8/2004	Jeng	
6,788,965	B2	9/2004	Ruchti	
6,802,811	B1	10/2004	Slepian	
6,816,241	B2	11/2004	Grubisic	
6,847,336	B1	1/2005	Lemelson	
6,864,978	B1	3/2005	Hazen	
6,885,498	B2	4/2005	Islam	
6,885,683	B1	4/2005	Fermann et al.	
6,943,936	B2	9/2005	Islam et al.	
6,990,364	B2	1/2006	Ruchti	
7,010,336	B2	3/2006	Lorenz	
7,027,467	B2	4/2006	Baev et al.	
7,060,061	B2	6/2006	Altshuler et al.	
7,105,823	B2	9/2006	Abrahamsson et al.	
7,133,710	B2	11/2006	Acosta	
7,167,300	B2	1/2007	Fermann et al.	
7,209,657	B1	4/2007	Islam	
7,233,816	B2	6/2007	Blank	
7,259,906	B1	8/2007	Islam	
7,263,288	B1	8/2007	Islam	
7,294,105	B1	11/2007	Islam	
7,299,080	B2	11/2007	Acosta	
7,317,938	B2	1/2008	Lorenz	
7,356,364	B1	4/2008	Bullock et al.	
7,395,158	B2	7/2008	Monfre	
7,433,116	B1	10/2008	Islam	
7,519,253	B2	4/2009	Islam	
7,519,406	B2	4/2009	Blank	
7,620,674	B2	11/2009	Ruchti	
7,697,966	B2	4/2010	Monfre	
7,771,320	B2	8/2010	Riley et al.	
7,787,503	B2	8/2010	Wadsworth	
7,787,924	B2	8/2010	Acosta	
7,800,818	B2	9/2010	Mattsson	
7,807,718	B2	10/2010	Hashim	
7,848,605	B2	12/2010	Ridder et al.	
7,890,158	B2	2/2011	Rowe et al.	
8,000,574	B2	8/2011	Buchter	
8,145,286	B2	3/2012	Arai	
8,157,730	B2	4/2012	LeBoeuf et al.	
8,158,493	B2	4/2012	Shah et al.	
8,180,422	B2	5/2012	Rebec	
8,213,007	B2	7/2012	Wang et al.	
8,430,310	B1	4/2013	Ho et al.	
8,472,108	B2	6/2013	Islam	
8,509,882	B2	8/2013	Albert et al.	
8,788,002	B2	7/2014	LeBoeuf et al.	
8,948,832	B2	2/2015	Hong et al.	
9,326,712	B1	5/2016	Kiani	
2002/0013518	A1	1/2002	West et al.	
2002/0019584	A1	2/2002	Schulze et al.	
2002/0032468	A1	3/2002	Hill et al.	
2002/0082612	A1	6/2002	Moll et al.	
2002/0109621	A1	8/2002	Khair et al.	
2002/0115914	A1	8/2002	Russ	
2002/0128846	A1	9/2002	Miller	
2002/0178003	A1	11/2002	Gehrke et al.	
2003/0022126	A1	1/2003	Buchalla	
2004/0174914	A1	9/2004	Fukatsu	
2004/0240037	A1	12/2004	Harter	
2005/0111500	A1	5/2005	Harter et al.	
2005/0133691	A1*	6/2005	Doppke	H04B 10/6933 250/214 A
2006/0058683	A1	3/2006	Chance	
2006/0198397	A1	9/2006	Korolev et al.	
2006/0223032	A1	10/2006	Fried	
2006/0245461	A1	11/2006	Islam	
2006/0268393	A1	11/2006	Islam	
2006/0283931	A1	12/2006	Polli et al.	
2007/0021670	A1	1/2007	Mandelis et al.	
2007/0078348	A1	4/2007	Holman	
2008/0086318	A1	4/2008	Gilley et al.	
2008/0105665	A1	5/2008	Kondo	
2009/0028193	A1	1/2009	Islam	
2009/0105605	A1	4/2009	Abreu	
2009/0204110	A1	8/2009	Islam	
2009/0244288	A1*	10/2009	Fujimoto	H04N 5/2256 348/164
2009/0287067	A1	11/2009	Dorogusker et al.	
2010/0046067	A1	2/2010	Fermann et al.	
2010/0160794	A1	6/2010	Banet et al.	
2010/0217102	A1	8/2010	LeBoeuf et al.	
2010/0322490	A1	12/2010	Pan	
2010/0331637	A1	12/2010	Ting	
2011/0040197	A1	2/2011	Welch et al.	
2011/0143364	A1	6/2011	Kim	
2011/0208015	A1	8/2011	Welch et al.	
2011/0267688	A1*	11/2011	Kleppe	G02B 21/0036 359/385
2011/0282167	A1	11/2011	Ridder et al.	
2011/0292376	A1	12/2011	Kukushkin et al.	
2012/0013722	A1	1/2012	Wong	
2012/0239013	A1	9/2012	Islam	
2012/0310062	A1	12/2012	Li et al.	
2012/0316455	A1	12/2012	Rahman et al.	
2013/0274569	A1	10/2013	Islam	
2013/0281795	A1	10/2013	Varadan	
2013/0327966	A1*	12/2013	Fidler	G02B 26/04 250/578.1
2014/0078510	A1*	3/2014	Rubio Guivernau	G01B 9/02091 356/479
2014/0081100	A1	3/2014	Muhsin et al.	
2014/0236021	A1	8/2014	Islam	
2014/0249427	A1*	9/2014	Liu	A61B 1/00167 600/477
2014/0275852	A1	9/2014	Hong et al.	
2014/0275854	A1	9/2014	Venkatraman et al.	
2015/0011851	A1	1/2015	Mehta et al.	
2016/0045118	A1	2/2016	Kiani	
2016/0327476	A1	11/2016	Islam	

FOREIGN PATENT DOCUMENTS

EP	1148666		10/2001
WO	WO9715240		5/1997
WO	WO9749340		12/1997
WO	WO0150959		7/2001
WO	0189362		11/2001
WO	0227640		4/2002
WO	0228123		4/2002
WO	2005013843	A2	2/2005
WO	2007061772	A2	5/2007
WO	2009130464	A1	10/2009
WO	2012135952	A1	10/2012
WO	WO2013012938	A1	1/2013
WO	WO2015084376	A1	6/2015

OTHER PUBLICATIONS

Aris, Ishak Bin, "An Internet-Based Blood Pressure Monitoring System for Patients"; Journal of Telemedicine and Telecare 2001; pp. 51-53.

"Application Brief AB-070: The role of infrared microprobe analysis in forensic drug analysis," www.smithsdetection.com, Jun. 27, 2005.

Jasco Application Note No. 200DR0188-E, "Rapid Identification of illegal drug using NIR (identification of MDMA tablet)", Sep. 4, 2008.

Palou, A. J. Cruz, M. Blanco, J. Tomas, J. De Los Rios, M. Alcala, "Determination of drug, excipients and coating distribution in

(56) **References Cited**

OTHER PUBLICATIONS

pharmaceutical tablets using NIR-CI," Journal of Pharmaceutical Analysis, vol. 2, No. 2, pp. 90-97 (2012).
Arnold, T., M. De Biasio, R. Leitner, "Near-Infrared Imaging Spectroscopy for Counterfeit Drug Detection," Next Generation Spectroscopic Technologies IV, edited by M. A. Druy, R.A. Crocombe, Proceedings of SPIE, vol. 8032, 80320Y-1 to 7, (2011).
Wedding, B.B., C. Wright, S. Grauf, R.D. White, "The application of near infrared spectroscopy for the assessment of avocado quality attributes," Infrared Spectroscopy—Life and Biomedical Sciences, pp. 211-230 (2011).
Michaels, C.A., T. Masiello, P.M. Chu, "Fourier transform spectrometry with a near infrared supercontinuum source," Optical Society of America, CLEO/IQEC Conference, paper CMDD6 (2009).
Michaels, C.A., T. Masiello, P.M. Chu, "Fourier transform spectrometry with a near-infrared supercontinuum source," Applied Spectroscopy, vol. 63, No. 5, pp. 538-543 (2009).
Moros,J., J. Kuligowski, G. Quintas, S. Garrigues, M. DeLa Guardia, "New cut-off criterion for uninformative variable elimination in multivariate calibration of near-infrared spectra for the determination of heroin in illicit street drugs," Analytica Chimica Acta, vol. 630, pp. 150-160 (2008).
Moros, J. N. Gallpienso, R. Vilches, S. Garrigues, M. DeLa Guardia, "Nondestructive direct determination of heroin in seized illicit street drugs by diffuse reflectance near-infrared spectroscopy," Analytical Chemistry, vol. 80, No. 19, pp. 7257-7265 (Oct. 1, 2008).
Roggo, Y. P. Chalus, L. Maurer, C. Lema-Martinez, A. Edmond, N. Jent, "A review of near infrared spectroscopy and chemometrics in pharmaceutical technologies," Journal of Pharmaceutical and Biomedical Analysis, vol. 44, pp. 683-700 (2007).
Pojic, M. J. Mastilovic, N. Majcen, "The application of near infrared spectroscopy in wheat quality control," Infrared Spectroscopy—Life and Biomedical Sciences, pp. 167-184 (2012).
Reich, G. "Near-infrared spectroscopy and imaging: basic principles and pharmaceutical applications," Advanced Drug Delivery Reviews, vol. 57, pp. 1109-1143 (2005).
Rodionova, O.Y., L.P. Houmoller, A.L. Pomerantsev, P. Geladi, J. Burger, V.L. Dorofeyev, A.P. Arzamastsev, "NIR spectrometry for counterfeit drug detection: a feasibility study," Analytica Chimica Acta, vol. 549, pp. 151-158 (2005).
Schneider, R.C., K.A. Kovar, "Analysis of ecstasy tablets: comparison of reflectance and transmittance near infrared spectroscopy," Forensic Science International, vol. 134, pp. 187-195 (2003).
Olsen, B.A., M.W. Borer, F.M. Perry, R.A. Forbes, "Screening for counterfeit drugs using near-infrared spectroscopy," Pharmaceutical Technology, pp. 62-71 (Jun. 2002).
Scafi, S.H.F., C. Pasquini, "Identification of counterfeit drugs using near-infrared spectroscopy," Analyst, vol. 126, pp. 2218-2224 (2001).
Sondermann, N., K.A. Kovar, "Identification of ecstasy in complex matrices using near-infrared spectroscopy," Forensic Science International, vol. 102, pp. 133-147 (1999).
Rambla, F.J., S. Garrigues, M. DeLa Guardia, "PLS-NIR determination of total sugar, glucose, fructose and sucrose in aqueous solutions of fruit juices," Analytica Chimica Acta, vol. 344, pp. 41-53 (1997).
Hori, Takashi, et al., "Flatly broadened, wideband and low noise supercontinuum generation in highly nonlinear hybrid fiber", Optics Express, vol. 12, No. 2, Jan. 26, 2004, pp. 317-324.
Wadsworth, W. J., et al., "Supercontinuum and four-wave mixing with Q-switched pulses in endlessly single-mode photonic crystal fibres", Optics Express, vol. 12, No. 2, Jan. 26, 2004, pp. 299-309.
Hilligsoe, Karen Marie, et al., "Supercontinuum generation in a photonic crystal fiber with two zero dispersion wavelengths", Optics Express, vol. 12, No. 6, Mar. 22, 2004, pp. 1045-1054.
Venugopalan, V., "Optical Society of America BIOMED Topical Meeting Tutorial on Tissue Optics", Apr. 27, 2004, pp. 1-32.
Slusher, Richart E., et al., "Large Raman gain and nonlinear phase shifts in high-purity As2So3 chalcogenide fibers", J. Opt. Soc. Am. B, vol. 21, No. 6, Jun. 2004, pp. 1146-1155.
Leon-Saval, S. G., et al., "Supercontinuum generation in submicron fibre waveguides", Optics Express, vol. 12, No. 13, Jun. 28, 2004, pp. 2864-2869.
Nicholson, J. W., et al., "High power, single mode, all-fiber source of femtosecond pulses at 1550 nm and its use in supercontinuum generation", Optics Express, vol. 12, No. 13, Jun. 28, 2004, pp. 3025-3034.
Genty, G., et al., "Enhanced bandwidth of supercontinuum generated m microstructured fibers", Optics Express, vol. 12, No. 15, Jul. 26, 2004, pp. 3471-3480.
Champert, Pierre-Alain, et al., "White-light supercontinuum generation in normally dispersive optical fiber using original multi-wavelength pumping system", Optics Express, vol. 12, No. 19, Sep. 20, 2004, pp. 4366-4371.
Nicholson, J. W., "Supercontinuum generation in ultraviolet-irradiated fibers", Optics Letters, vol. 29, No. 20, Oct. 15, 2004, pp. 2363-2365.
Hori, Takashi, et al., "Experimental and numerical analysis of widely broadened supercontinuum generation in highly nonlinear dispersion-shifted fiber with a femtosecond pulse", J. Opt. Soc. Am. B, vol. 21, No. 11, Nov. 2004, pp. 1969-1980.
Demircan, Ayhan, et al., "Supercontinuum generation by the modulation instability", Optics Communications 244, 2005, pp. 181-185.
Papernyi, S.B., et al., "Sixth-Order Cascaded Raman Amplification", OFC/NFOEC, 2005, 3 pages.
Tanaka, Keiji, "Optical nonlinearity in photonic glasses", Journal of Materials Science: Materials in Electronics 16, 2005, pp. 633-643.
Westbrook, Paul S., "Improved Supercontinuum Generation Through UV Processing of Highly Nonlinear Fibers", Journal of Lightwave Technology, vol. 23, No. 1, Jan. 2005, pp. 13-18.
Abeeluck, Akheelesh K., et al., "Continuous-wave pumping in the anomalous- and normal dispersion regimes of nonlinear fibers for supercontinuum generatfon", Optics Letters, vol. 30, No. 1, Jan. 1, 2005, pp. 61-63.
Kutz, J. Nathan, et al., Enhanced Supercontinuum Generation through Dispersion-Management, Optics Express, vol. 13, No. 11, May 30, 2005, pp. 3989-3998.
Lee, Ju Han, et al., "Experimental performance comparison for various continuous-wave supercontinuum schemes: ring cavity and single pass structures", Optics Express, vol. 13, No. 13, Jun. 27, 2005, pp. 4848-4853.
Saliminia, A., et al., "Ultra-broad and coherent white light generation in silica glass by focused femtosecond pulses at 1.5pm", Optics Express, vol. 13, No. 15, Jul. 25, 2005, pp. 5731-5738.
Takushima, Yuichi, High average power, depolarized super-continuum generation using a 1.55-um ASE noise source, Optics Express, vol. 13, No. 15, Jul. 25, 2005, pp. 5871.-5877.
Travers, J. C., et al., "Extended continuous-wave supercontinuum generation in a low-water-loss holey fiber", Optics Letters, vol. 30, No. 15, Aug. 1, 2005, pp. 1938-1940.
Kobtsev, Serguei M., et al., "Modelling of high-power supercontinuum generation in highly nonlinear, dispersion shifted fibers at CW pump", Optics Express, vol. 13, No. 18, Sep. 5, 2005, pp. 6912-6918.
Falk, Peter, et al., "Supercontinuum generation in a photonic crystal fiber with two zero-dispersion wavelengths tapered to normal dispersion at all wavelengths", Optics Express, vol. 13, No. 19, Sep. 19, 2005, pp. 7535-7540.
Tombelaine, Vincent, et al., "Ultra wide band supercontinuum generation in air-silica holey fibers by SHG-induced modulation instabilities", Optics Express, vol. 13, No. 19, Sep. 19, 2005, pp. 7399-7404.
Lee, Ju Han, et al., "Continuous-wave supercontinuum laser based on an erbium-doped fiber ring cavity incorporating a highly nonlinear optical fiber", Optics Letters, vol. 30, No. 19, Oct. 1, 2005, pp. 2599-2601.
Genty, G., et al., "Supercontinuum generation in large mode-area microstructured fibers", Optics Express, vol. 13, No. 21, Oct. 17, 2005, pp. 8625-8633.

(56) **References Cited**

OTHER PUBLICATIONS

Schreiber, T., et al., "Supercontinuum generation by femtosecond single and dual wavelength pumping in photonic crystal fibers with zero dispersion wavelengths", Optics Express, vol. 13, No. 23, Nov. 14, 2005, pp. 9556-9569.

Travers, J. C., et al., "Extended blue supercontinuum generation in cascaded holey fibers", Optics Letters, vol. 30, No. 23, Dec. 1, 2005, pp. 3132-3134.

Hagen, C. L., et al., "Generation of a Continuum Extending to the Midinfrared by Pumping ZBLAN Fiber With an Ultrafast 1550-nm Source", IEEE Photonics Technology Letters, vol. 18, No. 1, Jan. 1, 2006, pp. 91-93.

Moon, Sucbei, et al., "Generation of octave-spanning supercontinuum with I550-nm amplified diode-laser pulses and a dispersion-shifted fiber", Optics Express, vol. 14, No. 1, Jan. 9, 2006, pp. 270-278.

Fedotova, O., et al., "Supercontinuum generation in planar rib waveguides enabled by anomalous dispersion", Optics Express, vol. 14, No. 4, Feb. 20, 2006, pp. 1512-1517.

Harrington, James A., "Infrared Fiber Optics", OSA Handbook, vol. III, white paper, to be published by McGraw Hill, Undated, 13 pages.

Aaviksoo, J., et al., "Observation of optical precursors at pulse propagation in GaAs", Physical Review A, vol. 44, No. 9, Nov. 1, 1991, pp. R5353-R5356.

Boppart, Stephen A., et al., "Imaging developing neural morphology using optical coherence tomography", Journal of Neuroscience Methods 70, 1996, pp. 65-72.

Boppart, Stephen A., et al., "Noninvasive assessment of the developing Xenopus cardiovascular system using optical coherence tomography", Prec. Natl. Acad. Sci. USA, vol. 94, Apr. 1997, pp. 4256-4261.

Tearney, Guillermo J., et al., "In vivo Endoscopic Optical Biopsy with Optical Coherence Tomography", Science, New Series, vol. 276, Jun. 27, 1997, pp. 2037-2039.

de Boer, Johannes F., et al., "Imaging thermally damaged tissue by polarization sensitive optical coherence tomography", Optics Express 212, vol. 3, No. 6, Sep. 14, 1998, pp. 212-218.

Roggan, Andre, et al., "Optical Properties of Circulating Human Blood in the Wavelength Range 400-2500 NM", Journal of Biomedical Optics, vol. 4, No. 1, Jan. 1999, pp. 36-46.

de Boer, Johannes F., et al., "Determination of the depth-resolved Stokes parameters of light backscattered from turbid media by use of polarization-sensitive optical coherence tomography", Optics Letters, vol. 24, No. 5; Mar. 1, 1999, pp. 300-302.

Rollins, Andrew M., et al., "Real-time in vivo imaging of human gastrointestinal ultrastructure by use of endoscopic optical coherence tomography with a novel efficient interferometer design", Optics Letters, vol. 24, No. 19, Oct. 1, 1999, pp. 1358-1360.

D'Amico, Anthony V., et al., "Optical Coherence Tomography As a Method for Identifying Benign and Malignant Microscopic Structures in the Prostate Gland", Basic Science, Urology 55 (5), 2000, pp. 783-787.

Li, Xingde, et al., "Imaging needle for optical coherence tomography", Optics Letters, vol. 25, No. 20, Oct. 15, 2000, pp. 1520-1522.

Oughstun, Kurt E., "Influence of precursor fields on ultrashort pulse autocorrelation measurements and pulse width evolution", Optics Express, vol. 8, No. 8, Apr. 9, 2001, pp. 481-491.

Kowalevicz, Andrew M., et al., "Ultrahigh resolution optical coherence tomography using a superluminescent light source" Optics Express 349, vol. 10, No. 7, Apr. 8, 2002, pp. 349-353.

Povazay, B., et al., "Submicrometer axial resolution optical coherence tomography", Optics Letters, vol. 27, No. 20, Oct. 15, 2002, pp. 1800-1802.

Xie, T.-Q., et al., "Detection of tumorigenesis in urinary bladder with optical coherence tomography: optical characterization of morphological changes", Optics Express, vol. 10, No. 24, Dec. 2, 2002, 2003, pp. 1431-1443.

Seefeldt, Michael, et al., "Compact white-light source with an average output power of 2.4 Wand 900 nm spectral bandwidth", Optics Communications 216, pp. 199-202.

Wang, Yimin, et al., "Ultrahigh-resolution optical coherence tomography by broadband continuum generation from a photonic crystal fiber", Optics Letters, vol. 28, No. 3, Feb. 1, 2003, pp. 182-184.

Bizheva, K, et al., "Compact, broad-bandwidth fiberlaserforsub-2-pm axial resolution optical coherence tomography in the 1300-nm wavelength region," Optics Letters, vol. 28, No. 9, May 1, 2003, pp. 707-709.

Hazen, K.H., M.A. Arnold, G.W. Small, "Measurement of glucose and other analytes in undiluted human serum with near-infrared transmission spectroscopy," Analytica Chimica Acta, vol. 371, pp. 255-267 (1998).

Malin, S.F., T.L. Ruchti, T.B. Blank, S.N. Thennadil, S.L. Monfre, "Noninvasive prediction of glucose by near-infrared diffuse reflectance spectroscopy," Clinical Chemistry, vol. 45, No. 9, pp. 1651-1658 (1999).

Thennadil, S.N., J.L. Rennert, B.J. Wenzel, K.H. Hazen, T.L. Ruchti, M.B. Block, "Comparison of glucose concentration in interstitial fluid, and capillary and venous blood during rapid changes in blood glucose levels," Diabetes Technology & Therapeutics, vol. 3, No. 3, pp. 357-365 (2001).

Troy, T.L., S.N. Thennadil, "Optical properties of human skin in the near infrared wavelength range of 1000 to 2200nm," Journal of Biomedical Optics, vol. 6, No. 2, pp. 167-176, (2001).

Blank, T.B., T.L. Ruchti, A.D. Lorenz, S.L. Monfre, M.R. Makarewicz, M. Mattu, K.H. Hazen, "Clinical results from a non-invasive blood glucose monitor," Optical Diagnostics and Sensing of Biological Fluids and Glucose and Cholesterol Monitoring II, A.V. Priezzhev and G.L. Cote, Editors, Proceedings of SPIE, vol. 4624, pp. 1019 (2002).

Yeh, S-J, C.F. Hanna, O.S. Khalil, "Monitoring blood glucose changes in cutaneous tissue by temperature-modulated localized reflectance measurements," Clinical Chemistry, vol. 49, No. 6, pp. 924-934 (2003).

Marbach, R., T. Koschinsky, E.A. Gries, H.M. Heise, "Noninvasive blood glucose assay by near-infrared diffuse reflectance spectroscopy of the human inner lip," Applied Spectroscopy, vol. 47, No. 7, pp. 875-881 (1993).

Enejder, A.M.K., T.G. Scecina, J. Oh, M. Hunter, W.C. Shih, S. Sasic, G.L. Horowitz, M.S. Feld, "Raman spectroscopy for noninvasive glucose measurements," Journal of Biomedical Optics, vol. 10, No. 3, 031114 (2005).

Olesberg, J.T., L. Liu, V.V. Zee, M.A. Arnold, "In vivo near-infrared spectroscopy of rat skin tissue with varying blood glucose levels," Analytic Chemistry, vol. 78, No. 1, pp. 215-223 (2006).

Olesberg, J.T., M.A. Arnold, C. Mermelstein, J. Schmitz, J. Wagner, "Tunable laser diode system for noninvasive blood glucose measurements," Applied Spectroscopy, vol. 59, No. 12, pp. 1480-1484 (2005).

Harman-Boehm, I. A. Gal, A.M. Raykhman, J.D. Zahn, E. Naidis, Y. Mayzel, "Noninvasive glucose monitoring: a novel approach," Journal of Diabetes Science and Technology, vol. 3, No. 2 pp. 253-260 (2009).

Kim-K.D. G.S. Son, S.S. Lim, S.S. Lee, "Measurement of glucose level exploiting a relative optical absorption at discrete probe wavelengths," Japanese Journal of Applied Physics, vol. 48, 077001 (2009).

Smith, J.L., "The Pursuit of Noninvasive Glucose: Hunting the Deceitful Turkey," 2nd Edition, pp. 1-141 (2011).

Pezzaniti, J.L., T.W. Jeng, L. McDowell, G.M. Costa, "Preliminary investigation of near-infrared spectroscopic measurements of urea, creatinine, glucose, protein and ketone in urine," Clinical Biochemistry, vol. 34, pp. 239-246 (2001).

Lussi, A., R. Hibst, R. Paulus, "Diagnodent: An optical method for caries detection," Journal of Dental Research, vol. 83, special issue C, pp. C80-C83 (2004).

Reese, E.L, E.E. Fisher, D.A. Horowitz, "Photoelectric densitometry of the circulation of the human dental pulp," The Journal of the Baltimore College of Dental Surgery, vol. 26, No. 1, pp. 6-18 (1971).

(56) **References Cited**

OTHER PUBLICATIONS

Zakian, C., I. Pretty, R. Ellwood, "Near-infrared hyperspectral imaging of teeth for dental caries detection," Journal of Biomedical Optics, vol. 16, No. 6, 064047 (2009).
Belikov, A.V., A.V. Skripnik, K.V. Shatilova, "Study of the dynamics of the absorption spectra of human tooth enamel and dentine under heating and ablation by submillisecond pulse radiation of an erbium laser with a generation wavelength of 2.79 um," Optics and Spectroscopy, vol. 109, No. 2, pp. 211-216 (2010).
Karlsson, L. "Caries detection methods based on changes in optical properties between healthy and carious tissue," International Journal of Dentistry, vol. 2010, Article ID 270729, 9 pages (2010).
Fried, D. M. Staninec, C.L. Darling, "Near-infrared imaging of dental decay at 1310nm," Journal of Laser Dentistry, vol. 18, No. 1, pp. 8-16 (2010).
Burmen, M. P. Usenik, A. Fidler, F. Pernus, B. Likar, "A construction of standardized near infrared hyper-spectral teeth database—a first step in the development of reliable diagnostic tool for quantification and early detection of caries," Lasers in Dentistry XVII, edited by P. Rechmann, D. Fried, Proceedings of SPIE, vol. 7884, Paper 78840E (2011).
Maia, A., L. Karlsson, W. Margulis, A. Gomes, "Evaluation of two imaging techniques: near-infrared transillumination and dental radiographs for the detection of early approximal enamel caries," Dentomaxillofacial Radiology, vol. 40, pp. 429-433 (2011).
Chung, S., D. Fried, M. Staninec, C.L. Darling, "Multispectral near-IR reflectance and transillumination imaging of teeth," Biomedical Optics Express, vol. 2, No. 10, pp. 2804-2814 (2011).
Chung, S., D. Fried, M. Staninec, C.L. Darling, "Near infrared imaging of teeth at wavelengths between 1200 and 1600nm," Proceedings of the Society of Photo Optical Instrument Engineering, paper 7884 (2011).
Staninec, M., S.M. Douglas, C.L. Darling, K. Chan, H. Kang, R. C. Lee, D. Fried, "Nondestructive clinical assessment of occlusal caries lesions using near-IR imaging methods," Lasers in Surgery and Medicine, vol. 43, No. 10, pp. 951-959 (2011).
Nishizawa, N., "Generation and application of high-quality supercontinuum sources," Optical Fiber Technology, vol. 18, pp. 394-402 (2012).
Sun, Y., C.F. Booker, S. Kumari, R.N. Day, M. Davidson, A. Periasamy, "Characterization of an orange acceptor fluorescent protein for sensitized spectral fluorescence resonant energy transfer microscopy using a white-light laser," Journal of Biomedical Optics, vol. 14, No. 5, paper 054009 (2009).
Borlinghaus, R., "Colours Count: how the challenge of fluorescence was solved in confocal microscopy," in Modern Research and Educational Topics in Microscopy, A. Mendez-Vilas and J. Diaz, eds, pp. 890-899, Formatex (2007).
Borlinghaus, R., "The White Confocal: Continuous Spectral Tuning in Excitation and Emission," in Optical Fluorescence Microscopy, A. Diaspro (Ed), Chapter 2, pp. 37-54, ISBN 978-3-642-15174-3, Springer-Verlag, Berlin (2011).
Borlinghaus, R.T., L. Kuschel, "White Light Laser: The Ultimate Source for Confocal Microscopy," http://www.leica-microsystems.com/science-lab/white-light-laser (Jun. 27, 2012).
Ziegler, U., A.G. Bittermann, M. Hoechli, "Introduction to Confocal Laser Scanning Microscopy (LEICA)," www.zmb.unizh.ch, May 29, 2013.
Pan, Yingtian, et al., "Hand-held arthroscopic optical coherence tomography for in vivo high-resolution imaging of articular cartilage", Journal of Biomedical Optics 8(4), Oct. 2003, pp. 648-654.
Xie, Tuqiang, et al., "Endoscopic optical coherence tomography with a modified microelectromechanical systems mirror for detection of bladder cancers", Applied Optics, vol. 42, No. 31, Nov. 1, 2003, pp. 6422-6426.
Dubois, A., et al., "Three-dimensional cellular-level imaging using full-field optical coherence tomography", Physics in Medicine and Biology, Phys. Med. Biol. 49, 2004, pp. 1227-1234.
Park, Jesung, et al., "Analysis of birefringent image in the retinal nerve fiber layer by polarization sensitive optical coherence tomography", Ophthalmic Technologies XIV, Proceedings of SPIE, vol. 5314, 2004, pp. 188-194.
Unterhuber, A., et al., "Advances in broad bandwidth light sources for ultrahigh resolution optical coherence tomography", Physics in Medicine and Biology, Phys. Med. Biol. 49, 2004, pp. 1235-1246.
Drexler, Wolfgang, "Ultrahigh-resolution optical coherence tomography", Journal of Biomedical Optics, vol. 9, No. 1, Jan./Feb. 2004, pp. 47-74.
Schmitt, Joseph, et al., "Intravascular Optical Coherence Tomography Opens a Window Onto Coronary Artery Disease", Optics & Photonics News, Feb. 2004, pp. 20-25.
Nassif, N.A., et al., "In vivo high-resolution video-rate spectral-domain optical coherence tomography of the human retina and optic nerve", Optics Express, vol. 12, No. 3, Feb. 9, 2004, pp. 367-376.
Choi, Seung-Ho, et al., "Observation of Optical Precursors in Water", Physical Review Letters, vol. 92, No. 19, May 14, 2004, pp. 193903-1-193903-.3.
Pierce, Mark C., et al., "Advances in Optical Coherence Tomography imaging for Dermatology", Optical Coherence Tomography Advances, The Journal of Investigative Dermatology, Sep. 3, 2004, pp. 458-463.
"State-Specific Trends in Chronic Kidney Failure—United States, 1990-2001", Morbidity and Mortality Weekly Report, Department of Health and Human Services Centers for Disease Control and Prevention, vol. 53, No. 39, from internet: file://C:\Documentsand Settings\eturlo\Desktop\State-Speciflc Trends in Chronic Kidney . . . Feb. 12, 2010, Oct. 8, 2004, pp. 918-920.
I.B. Ads, A.A.E. Wagie, N.B. Mariun, A.B.E. Jammal, "An Internet-based blood pressure monitoring system for patients," Journal of Telemedicine and Telecare, 2001, pp. 51-53.
R.H. Istepanian, B. Woodward, P.A. Bales, S. Chen, B. Luk, "The comparative performance of mobile telemediCal systems based on the IS-54 and GSM cellular telephone standards," Journal of Telemedicine and Telecare, 1999, pp. 97-104.
Shaw, et al, IR Supercontinuum Generation in As—Se Photonic Crystal Fiber, Optical Society of America, Copyright 2005, 3 pages.
PCT/US06/44451, Notification of Transmittal of the International Search Report and the Written Opinion of the International Searching Authority, or the Declaration, Nov. 29, 2007, 12 pages.
G.S. Edwards et al., "Free-electron-laser-based biophysical and biomedical instrumentation," American Institute of Physics, vol. 74, No. 7, Jul. 2003, pp. 3207-3245.
Computer Motion, Inc., "501(k) Summary—ZEUS® MicroWrist™ Surgical System and Accessories," Sep. 24, 2002, 6 pages.
Computer Motion, Inc. "HERMES™ O.R. Control Center—510(k) Summary of Safety and Effectiveness," Oct. 11, 2002, 5 pages.
K.M. Joos, et al. "Optic Nerve Sheath Fenestration with a Novel Wavelength Produced by the Free Electron Laser (FEL)," Lasers in Surgery and Medicine, 27: 2000,191-205.
J. Sanghera, I. Aggarwal, "IR Fiber Optics at NRL," undated, 10 pages.
J. Sanghera, L.B. Shaw, I.D. Aggarwal, "Applications of chalcogenide glass optical fibers," Academic of Science, 2003, pp. 1-11.
B. Rigas, P.T.T. Wong, "Human Colon Adenocarcinoma Cell Lines Display Infrared Spectroscopic Features," Cancer Research, Jan. 1, 1992, pp. 84-88.
G. Edwards, et al., "Comparison of OPA and Mark-III FEL for Tissue Ablation at 6.45 Microns," Department of Physics and Free Electron Laser Laboratory, Duke University, 2002, 7 pages.
Glenn Edwards, "Biomedical and potential clinical applications for pulsed lasers operating near 6.45 um," Society of Photo-Optical Instrumentation Engineers, 1995, 2 pages.
PASSAT, "Solid-State Lasers and Optical Components," Jul. 14, 2003, 5 pages.
P.A. Thielen and L.B. Shaw, et al., "Small-core As—Se fiber for Raman amplification," Optics LETI-ERS, vol. 28, No. 16, Aug. 15, 2003, 3 pages.

(56) **References Cited**

OTHER PUBLICATIONS

R.Rox Anderson, et al., "Selective Photothermolysis: Precise Microsurgery by Selective Absorption of Pulsed Radiation," Department of Dermatology, Harvard Medical School, Science, vol. 220, Apr. 29, 1983, 4 pages.

U.S. Appl. No. 10/652,276, "System and Method for Voice Control of Medical devices," by Mohammed N. Islam, abandoned filed Aug. 29, 2003.

U.S. Appl. No. 10/757,341, "System and Method for Voice Control of Medical devices," by Mohammed N. Islam, issued filed Jan. 13, 2004.

U.S. Appl. No. 12/206,432, "System and Method for Voice Control of Medical Devices," by Mohammed N. Islam, pending filed Sep. 8, 2008.

U.S. Patent and Trademark Office, Office Action for U.S. Appl. No. 12/206,432, filed Sep. 8, 2008, Mohammed N, Islam, Date filed: Mar. 12, 2009.

U.S. Patent and Trademark Office, Notice of Allowance and Fee(s) Due for U.S. Appl. No. 12/206,432, filed Sep. 8, 2008, Mohammed N. Islam, Date filed: Aug. 28, 2009.

Islam, M. N., et al., "Broad bandwidths from frequency-shifting solitons in fibers", Optics Letters, vol. 14, No. 7, Apr. 1, 1989, pp. 370-372.

Islam, M. N., et al., "Femtosecond distributed soliton spectrum in fibers", J. Opt. Soc. Am. B, vol. 6, No. 6, Jun. 1989, pp. 1149-1158.

Busse, Lynda E., et al., "Design Parameters for Fluoride Multimode Fibers", Journal of Lightwave Technology, vol. 9, No. 7, Jul. 1991, pp. 828-831.

Wuthrich, Stefan, et al., "Optical damage thresholds at 2.94 um in fluoride glass fibers", Applied Optics, vol. 31, No. 27, Sep. 20, 1992, pp. 5833-5837.

Inoue, H., et al., "Computer simulation of the vibrational spectra and properties of fluoride glasses based on ZrF4", Journal of Non-Crystalline Solids, vol. 161, 1993, pp. 118-122.

Mizunami, Toru, et al., "Gain saturation characteristics of Raman amplification in silica and fluoride glass optical fibers", Optics Communications 97, 1993, pp. 74-78.

Desthieux, B., et al., "111 kW (0. 5 mJ) pulse amplification at 1.5 um using a gated cascade of three erbium-doped fiber amplifiers," Appl. Phys. Lett. vol. 63, Aug. 2, 1993, pp. 586-588.

Edwards, Glenn, et al., Tissue ablation by a free-electron laser tuned to the amide II band, Nature, vol. 371, Sep. 29, 1994, pp. 416-419.

Borrelli, N. F., et al., "Resonant and non-resonant effects in photonic glasses", Journal of Non-Crystalline Solids 185, 1995, pp. 109-122.

Asobe, Masaki, et al., "Third-order nonlinear spectroscopy in As2S3 chalcogenide glass fibers", J. Appl. Phys. 77 (11), Jun. 1, 1995, pp. 5518-5523.

Jarman, Richard H., "Novel optical fiber lasers", Current Opinion in Solid State and Materials Science, 1996, pp. 199-203.

Iatridis, James C., et al., "Is the Nucleus Pulposus a Solid or a Fluid? Mechanical Behaviors of the Nucleus Pulposus of the Human Intervertebral Disc", Spine, vol. 21(10), May 15, 1996, pp. 1174-1184.

Asobe, Masaki, "Nonlinear Optical Properties of Chalcogenide Glass Fibers and Their Application to All-Optical Switching", Optical Fiber Technology, vol. 3, Article No. OF970214, 1997, pp. 142-148.

Smektala, F., et al., "Chalcogenide glasses with large non-linear refractive indices", Journal of Non-Crystalline Solids 239, 1998, pp. 139-142.

Hamilton, James D., et al., "High Frequency Ultrasound Imaging with Optical Arrays", IEEE Transactions on Ultrasonics, Ferroelectrics, and Frequency Control, vol. 45, No. 1, Jan. 1998, pp. 216-235.

Hamilton, James D., et al., "High Frequency Ultrasound Imaging Using an Active Optical Detector", IEEE Transactions on Ultrasonics, Ferroelectrics, and Frequency Control, vol. 45, No. 3, May 1998, pp. 719-727.

Nowak, G. A., et al., "Low-power high-efficiency wavelength conversion based on modulational instability in high-nonlinearity fiber," Optics Letters, vol. 23, No. 12, Jun. 15, 1998, pp. 936-938.

Cardinal, T., et al., "Non-linear optical properties of chalcogenide glasses in the system As—S—Se", Journal of Non-Crystalline Solids 256 & 257, 1999, pp. 353-360.

Lucas, Jacques, "Infrared glasses", Current Opinion in Solid State & Materials Science 4, 1999. pp. 181-187.

Sanghera, J. S., et al., Active and passive chalcogenide glass optical fibers for IR applications: a review, Journal of Non-Crystalline Solids 256 & 257, 1999, pp. 6-16.

Nishida, Yoshiki, et al., "Reliability of Fluoride Fiber Module for Optical Amplifier Use", IEEE Photonics Technology Letters, vol. 11, No. 12, Dec. 1999, pp. 1596-1598.

Nowak, George A., et al., "Stable supercontinuum generation in short lengths of conventional dispersion-shifted fiber", Applied Optics, vol. 38, No. 36, Dec. 20, 1999, pp. 7364-7369.

Urban, J. P. G., et al., "The Nucleus of the Intervertebral Disc from Development to Degeneration" Amer. Zool., vol. 40, 2000, pp. 53-61.

Hamilton, James D., et al., "High Frequency Optoacoustic Arrays Using Etalon Detection", IEEE Transactions on Ultrasonics, Ferroelectrics, and Frequency Control, vol. 47, No. 1, Jan. 2000, pp. 160-169.

Ranka, Jinendra K., et al., "Visible continuum generation in air-silica microstructure optical fibers with anomalous dispersion at 800 nm", Optics Letters, vol. 25, No. 1, Jan. 1, 2000, pp. 25-27.

Boult, Maggi, et al., "Systematic Review of Percutaneous Endoscopic Laser Discectomy: Update and Re-appraisal", Australian Safety and Efficacy Register of New Interventional Procedures—Surgical Report No. 5, Feb. 2000, 49 pages.

Boult, Maggi, et al., "Percutaneous Endoscopic Laser Discectomy", Systematic Review, Aust. N.Z.J. Surg., vol. 70, Apr. 7, 2000, pp. 475-479.

Camacho, Nancy P., et al., "FTIR Microscopic Imaging of Collagen and Proteoglycan in Bovine Cartilage," Biopolymers (Biospectroscopy), vol. 62, 2001, pp. 1-8.

Choi, Joon Y., et al, "Thermal, Mechanical, Optical, and Morphologic Changes in Bovine Nucleus Pulposus Induced by Nd:YAG (•=1.32 um) Laser Irradiation", Lasers in Surgery and Medicine, vol. 28, 2001, pp. 248-254.

Hafez, M. I., et al., "The Effect of Irrigation on Peak Temperatures in Nerve Root, Dura, and Intervertebral Disc During Laser-Assisted Foraminoplasty", Lasers in Surgery and Medicine, vol. 29, 2001, pp. 33-37.

Jackson, Stuart D., et al., "Theory and numerical simulation of nth-order cascaded Raman fiber lasers", J. Opt. Soc. Am. B, vol. 18, No. 9, Sep. 2001, pp. 1297-1306.

Werle, Peter, et a!., "Near- and mid-infrared laser-optical sensors for gas analysis", Optics and Lasers in Engineering 37, 2002, pp. 101-114.

Beck, Mattias, et al., "Continuous Wave Operation of a Mid-Infrared Semiconductor Laser at Room Temperature," Science vol. 295, www.sciencemag.org, Jan. 11, 2002, pp. 301-305.

Harbold, J. M., et al., "Highly nonlinear As—S—Se glasses for all-optical switching", Optics Letters, vol. 27, No. 2, Jan. 15, 2002, pp. 119-121.

Coen, Stephane, et al., "Supercontinuum generation by stimulated Raman scattering and parametric four-wave mixing in photonic crystal fibers", J. Opt. Soc. Am. B, vol. 19, No. 4, Apr. 2002, pp. 753-764.

Dudley, John M., et al., "Supercontinuum generation in air-silica microstructured fibers with nanosecond and femtosecond pulse pumping", J. Opt. Soc. Am. B, vol. 19, No. 4, Apr. 2002, pp. 765-771.

Harbold, Jeffrey M., et al., "Highly Nonlinear Ge—As'Se and.Ge—As—S—Se Glasses for All-Optical Switching", IEEE Photonics Technology Letters, vol. 14, No. 6, Jun. 2002, pp. 822-824.

Husakou, Anton V., et al, "Supercontinuum generation, four-wave mixing, and fission of higher-order solitons in photonic-crystal fibers", J. Opt. Soc. Am. B, vol. 19, No. 9, Sep. 2002, pp. 2171-2182.

(56) **References Cited**

OTHER PUBLICATIONS

Wadsworth, William J., et al., "Supercontinuum generation in photonic crystal fibers and optical fiber tapers: a novel light source", J. Opt. Soc. Am. B, vol. 19, No. 9, Sep. 2002, pp. 2148-2155.
Kumar, V.V. Ravi Kanth, et al, "Extruded soft glass photonic crystal fiber for ultrabroad supercontinuum generation", Optics Express, vol. 10, No. 25, Dec. 16, 2002, pp. 1520-1525.
Edwards, Glenn S., et al., "Advantage of the Mark-III FEL for biophysical research and biomedical applications", J. Synchrotron Rad. vol. 10, 2003, pp. 354-357.
Nicholson, J. W., et al., "Pulsed and continuous-wave supercontinuum generation in highly nonlinear, dispersion-shifted fibers", Applied Physics B 77, 2003, pp. 211-218.
Sobol, Emil, et al., "Time-resolved, light scattering measurements of cartilage and cornea denaturation due to free electron laser radiation", Journal of Biomedical Optics, vol. 8, No. 2, Apr. 2003, pp. 216-222.
Nicholson, J. W., et al., "All-fiber, octave-spanning supercontinuum", Optics Letters, vol. 28, No. 8, Apr. 15, 2003, pp. 643-645.
Faralli, S., et al., "Impact of Double Rayleigh Scattering Noise in Distributed Higher Order Raman Pumping Schemes", IEEE Photonics Technology Letters, vol. 15, No. 6, Jun. 2003, pp. 804-806.
"New and Emerging Techniques—Surgical, Rapid Review, Laser Discectomy", Australian Safety and Efficacy Register of New Interventional Procedures—Surgical, Jun. 2003, 12 pages.
Avdokhin, A. V., et al, "Continuous-wave, high-power, Raman continuum generation in holey fibers", Optics Letters, vol. 28, No. 15, Aug. 1, 2003, pp. 1353-1355.
Mussot, Arnaud, et al., "Generation of a broadband single-mode supercontinuum in a conventional dispersion-shifted fiber by use of a subnanosecond microchip laser", Optics Letters, vol. 28, No. 19, Oct. 1, 2003, pp. 1820-1822.
Slusher, Richard, et al., "Highly nonlinear composite chalcogenide/polymer fibers", OSA 2004, 1 page.
Thongtrangan, Issada, et al., "Minimally invasive spinal surgery: a historical perspective", Neurosurg. Focus, vol. 16, Article 13, Jan. 2004, pp. 1-10.
U.S. Appl. No. 61/350,673; titled: Opticoustic Sensor; Inventor: Massi Joe E. Kiani, filed Jun. 2, 2010.
International Search Report and Written Opinion for International Application No. PCT/US2013/075700 dated Apr. 24, 2014.
International Preliminary Report on Patentability for International Application No. PCT/US2013/075700 dated Jul. 9, 2015.
Ooi ET, Zhang XQ, Chen JH, Soh PH, Ng K, Yeo JH, "Non-invasive glucose measurement using multiple laser diodes," Optical Diagnostic and Sensing VII, edited by Gerard L. Cote, Alexander V. Priezzhev, Proc. of SPIE vol. 6445, 64450K , (2007).
Schulz, I., J. Putzger, A. Niklas, M. Brandt, A. Jager, A. Hardt, S. Knorzer, K.A. Hiller, S. Loffler, G. Schmalz, S.N. Danilov, S. Giglberger, M. Hirmer, S.D. Ganichev, G. Monkman, "PPG signal acquisition and analysis on in vitro tooth model for dental pulp vitality assessment," ARC Submission 16, (2012).
Drexler, C., Hirmer, M., Danilov, S., Giglberger, S., Putzger, J., Niklas, A., Jager, A., Hiller, K., Loffler, S., Schmalz, G., Redlich, B., Schulz, I., Monkman, G., Ganichev, S. "Infrared spectroscopy for clinical diagnosis of dental pulp vitality." Infrared, Millimeter, and Terahertz Waves (IRMMW-THz), 2012 37th International Conference on. IEEE (2012).
Hirmer, Marion, Danilov, Sergey, Giglberger, Stephan, Putzger, Jurgen, Niklas, Andreas, Jager, Andreas, Hiller, Karl-Anton, Loffler, Susanne, Schmalz, Gotffried, Redlich, Britta, Schulz, Irene, Monkman, Gareth, Ganichev, Sergey. "Spectroscopic Study of Human Teeth and Blood from Visible to Terahertz Frequencies for Clinical Diagnosis of Dental Pulp Vitality." Journal of Infrared, Millimeter, and Terahertz Waves 33.3 (2012): 366-375.
Na, J, J.H. Baek, S.Y. Ryu, C. Lee, B.H. Lee, "Tomographic imaging of incipient dental-caries using optical coherence tomography and comparison with various modalities," Optical Review, vol. 16, No. 4, pp. 426-431 (2009).
Vinay V. Alexander et al.; Modulation Instability High Power All-Fiber Supercontinuum Lasers and Their Applications; Optical Fiber Technology 18; 2012; pp. 349-374.
Robert S. Jones et al.; Near-Infrared Transillumination At 1310-nm for the Imaging of Early Dental Decay; vol. 11, No. 18; Optics Express 2259; Sep. 8, 2003.
Extended European Search Report for European Application No. 13867874.3 dated Jul. 15, 2016.
Extended European Search Report for European Application No. 13867892.5 dated Jul. 22, 2016.
Extended European Search Report for European Application No. 17156625.0 dated Mar. 20, 2017.

* cited by examiner

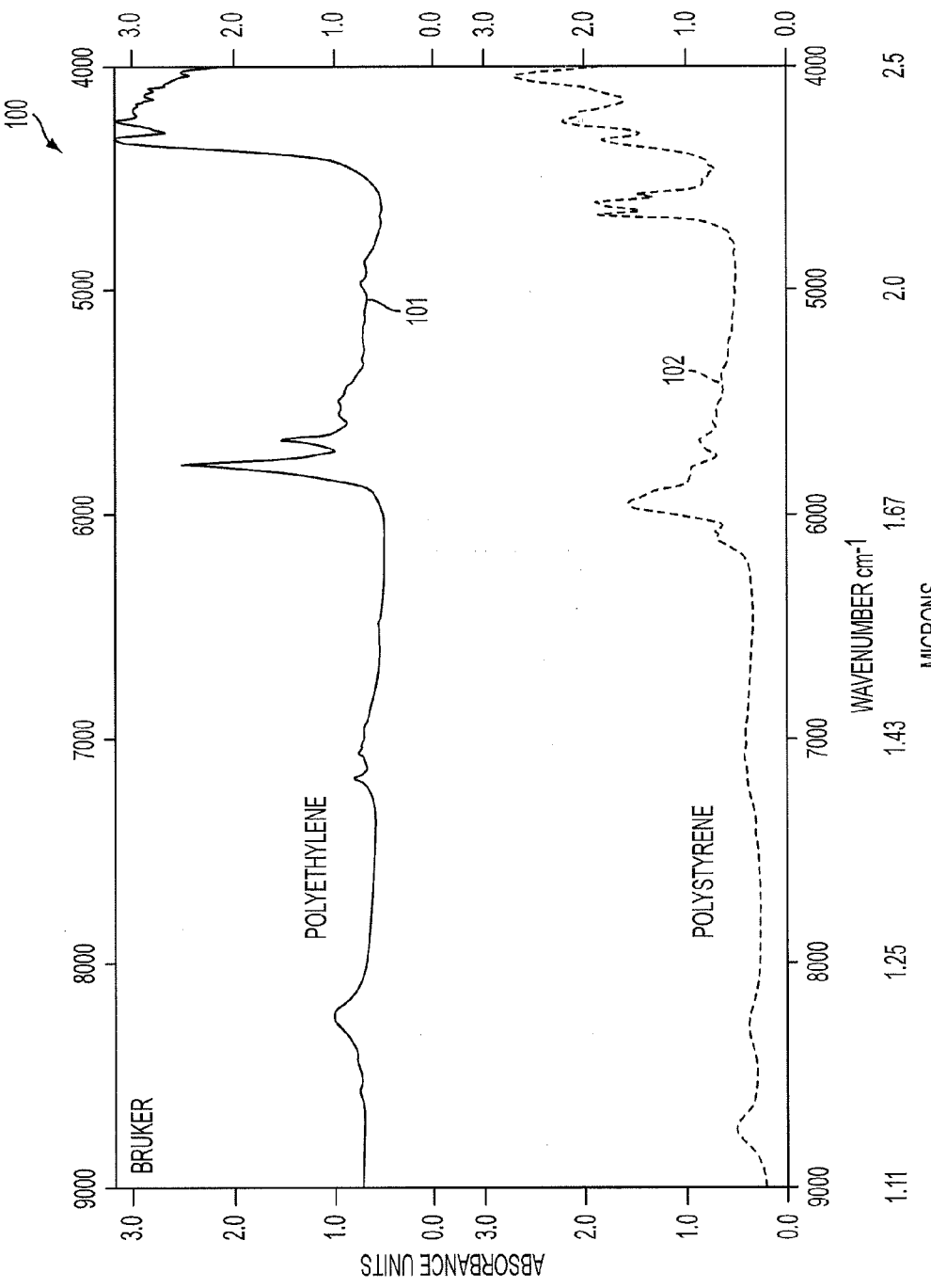

100
BRUKER
POLYETHYLENE
POLYSTYRENE
101
102
ABSORBANCE UNITS
WAVENUMBER cm-1
MICRONS
4000
5000
6000
7000
8000
9000
2.5
2.0
1.67
1.43
1.25
1.11
3.0
2.0
1.0
0.0

FIG. 1

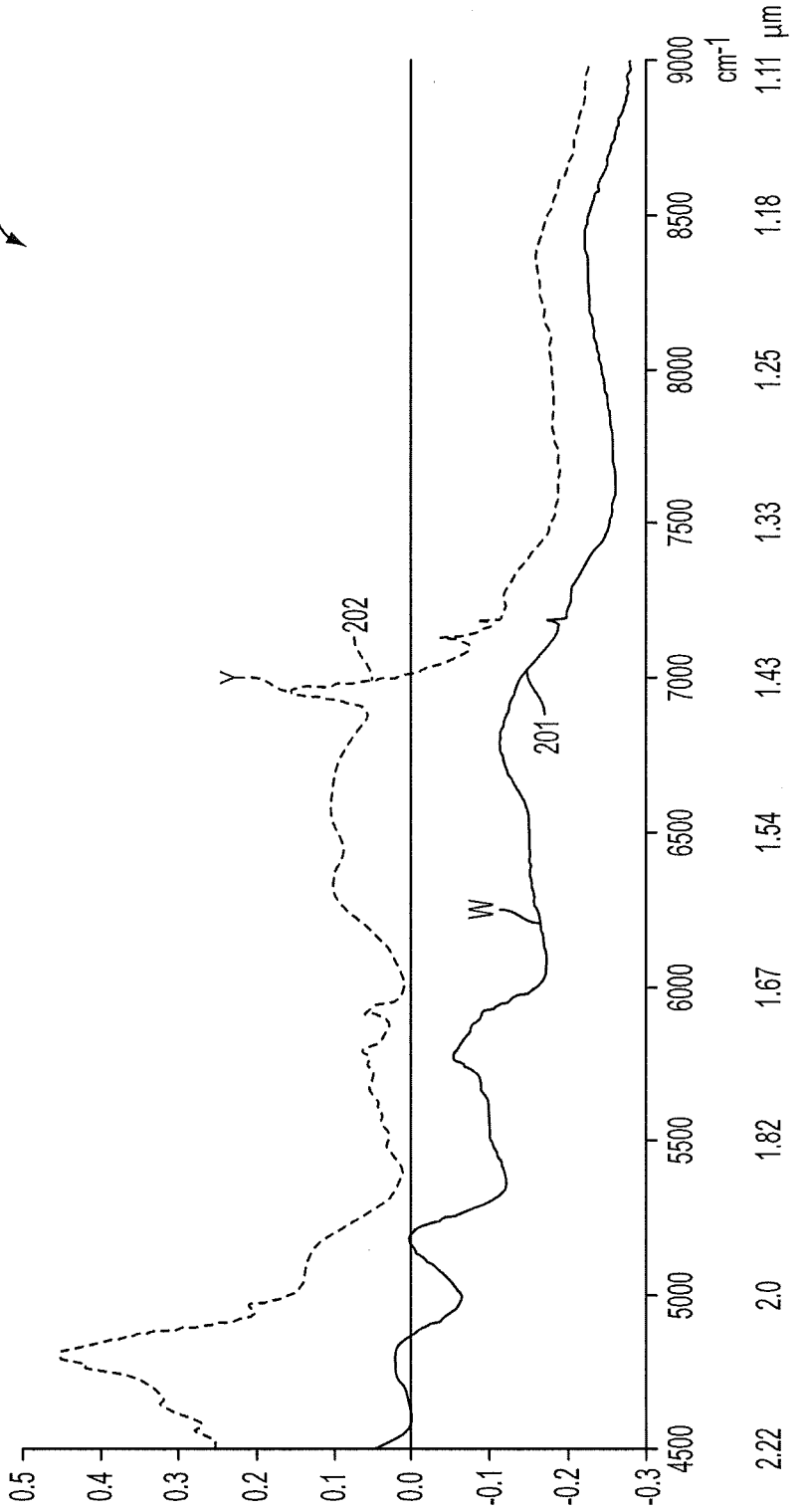

200
202
Y
W
201
0.5
0.4
0.3
0.2
0.1
0.0
-0.1
-0.2
-0.3
4500
5000
5500
6000
6500
7000
7500
8000
8500
9000
cm-1
2.22
2.0
1.82
1.67
1.54
1.43
1.33
1.25
1.18
1.11 µm

FIG. 2

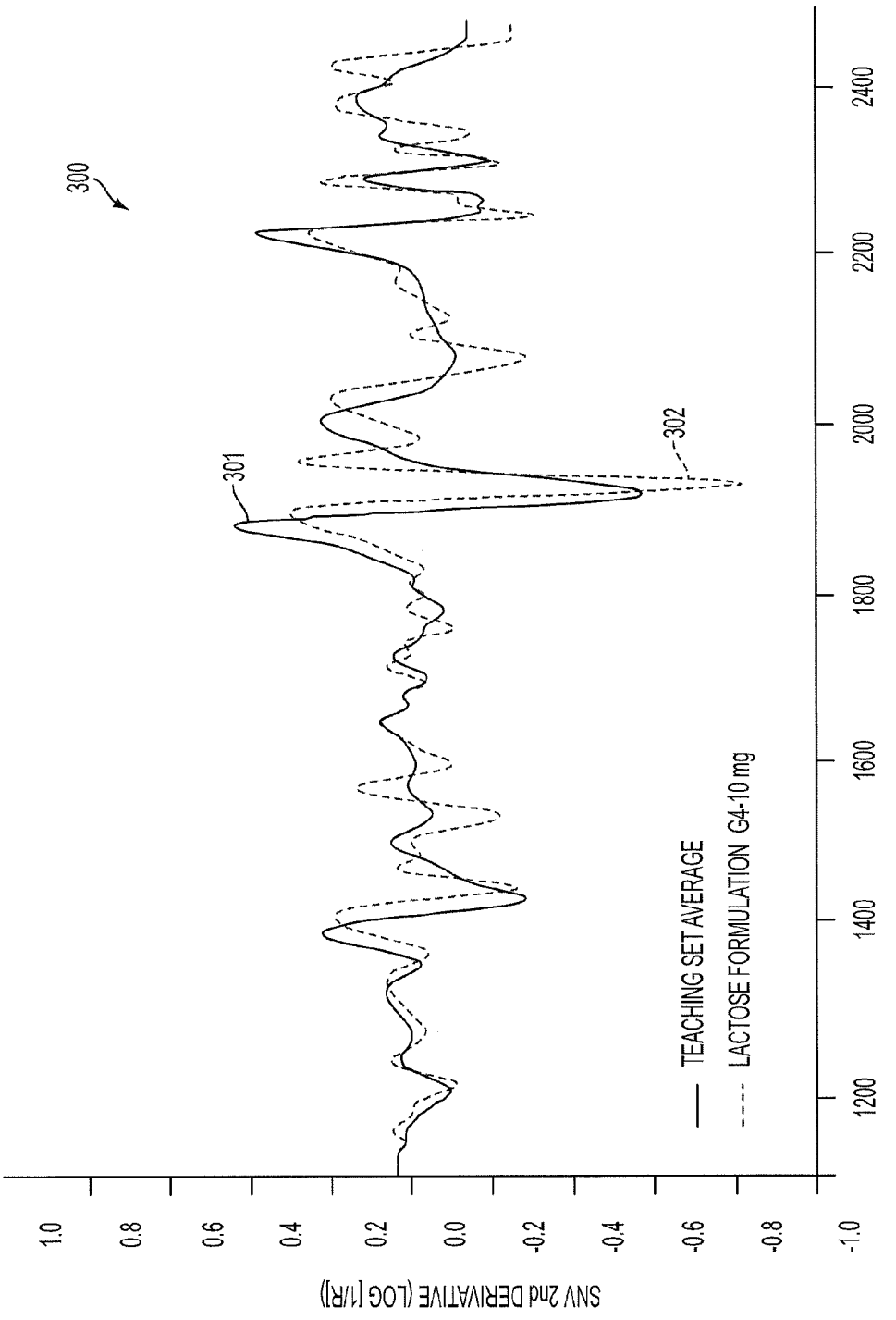

300
301
302
TEACHING SET AVERAGE
LACTOSE FORMULATION G4-10 mg
SNV 2nd DERIVATIVE (LOG [1/R])
1.0
0.8
0.6
0.4
0.2
0.0
-0.2
-0.4
-0.6
-0.8
-1.0
1200
1400
1600
1800
2000
2200
2400
WAVELENGTH (nm)

FIG. 3

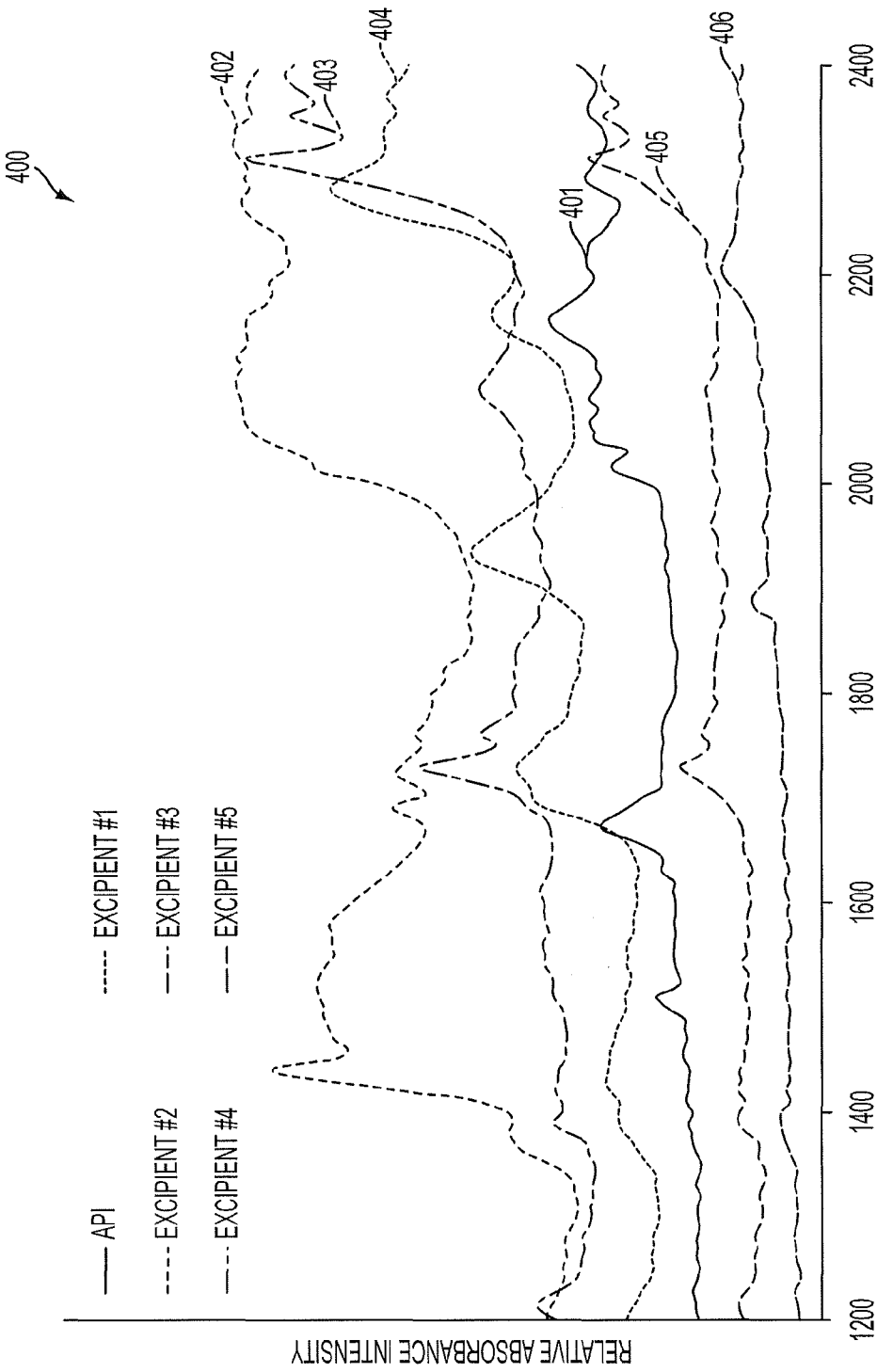

400
API
EXCIPIENT #1
EXCIPIENT #2
EXCIPIENT #3
EXCIPIENT #4
EXCIPIENT #5
401
402
403
404
405
406
RELATIVE ABSORBANCE INTENSITY
1200
1400
1600
1800
2000
2200
2400
WAVELENGTH (nm)

FIG. 4

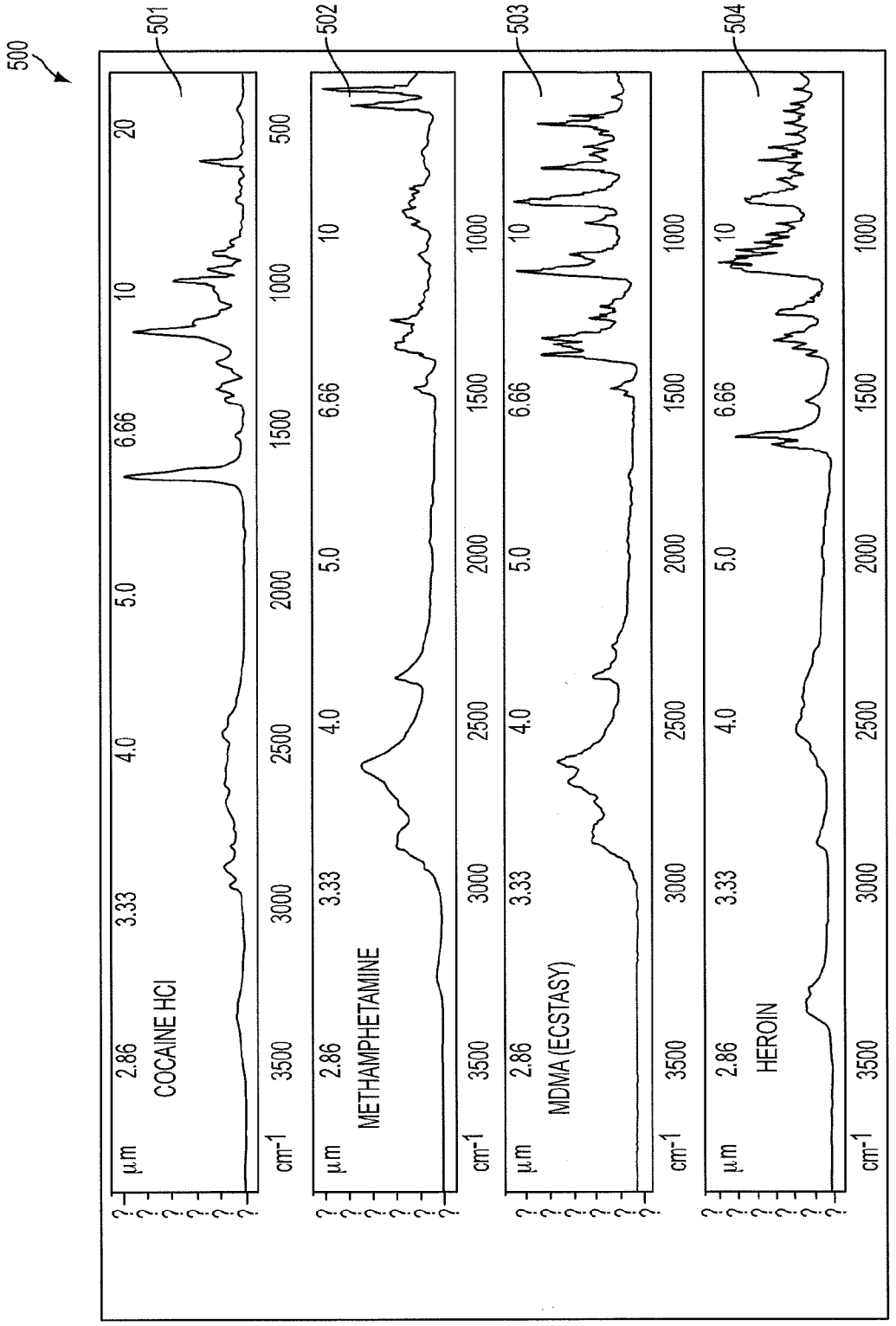

500
501
502
503
504
COCAINE HCl
METHAMPHETAMINE
MDMA (ECSTASY)
HEROIN
µm
cm-1
2.86
3.33
4.0
5.0
6.66
10
20
500
1000
1500
2000
2500
3000
3500

FIG. 5

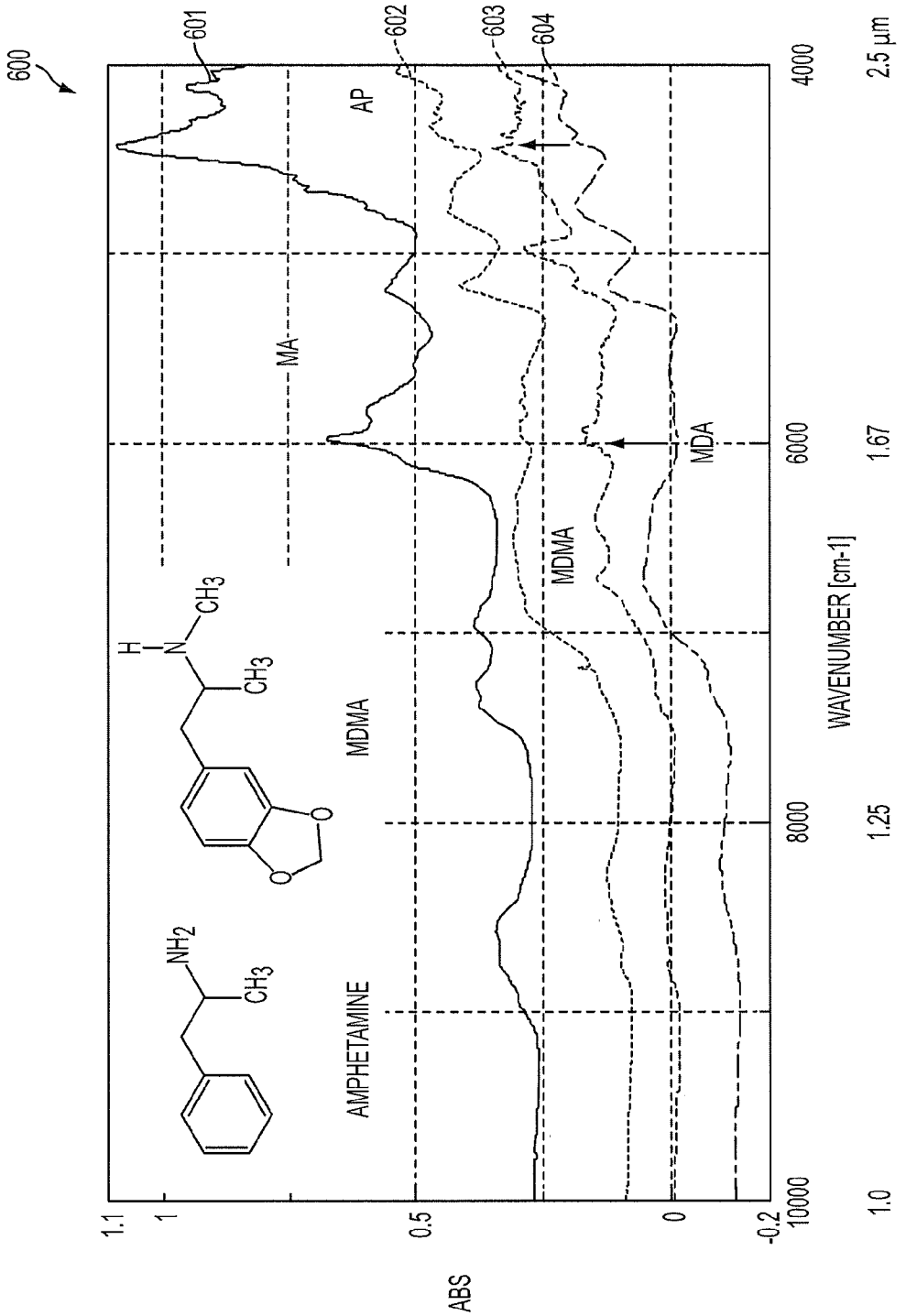

600
601
602
603
604
AP
MA
MDMA
MDA
AMPHETAMINE
MDMA
NH2
CH3
CH3
H
N
CH3
CH3
O
O
O
1.1
1
0.5
0
-0.2
ABS
10000
8000
6000
4000
WAVENUMBER [cm-1]
1.0
1.25
1.67
2.5 µm

FIG. 6

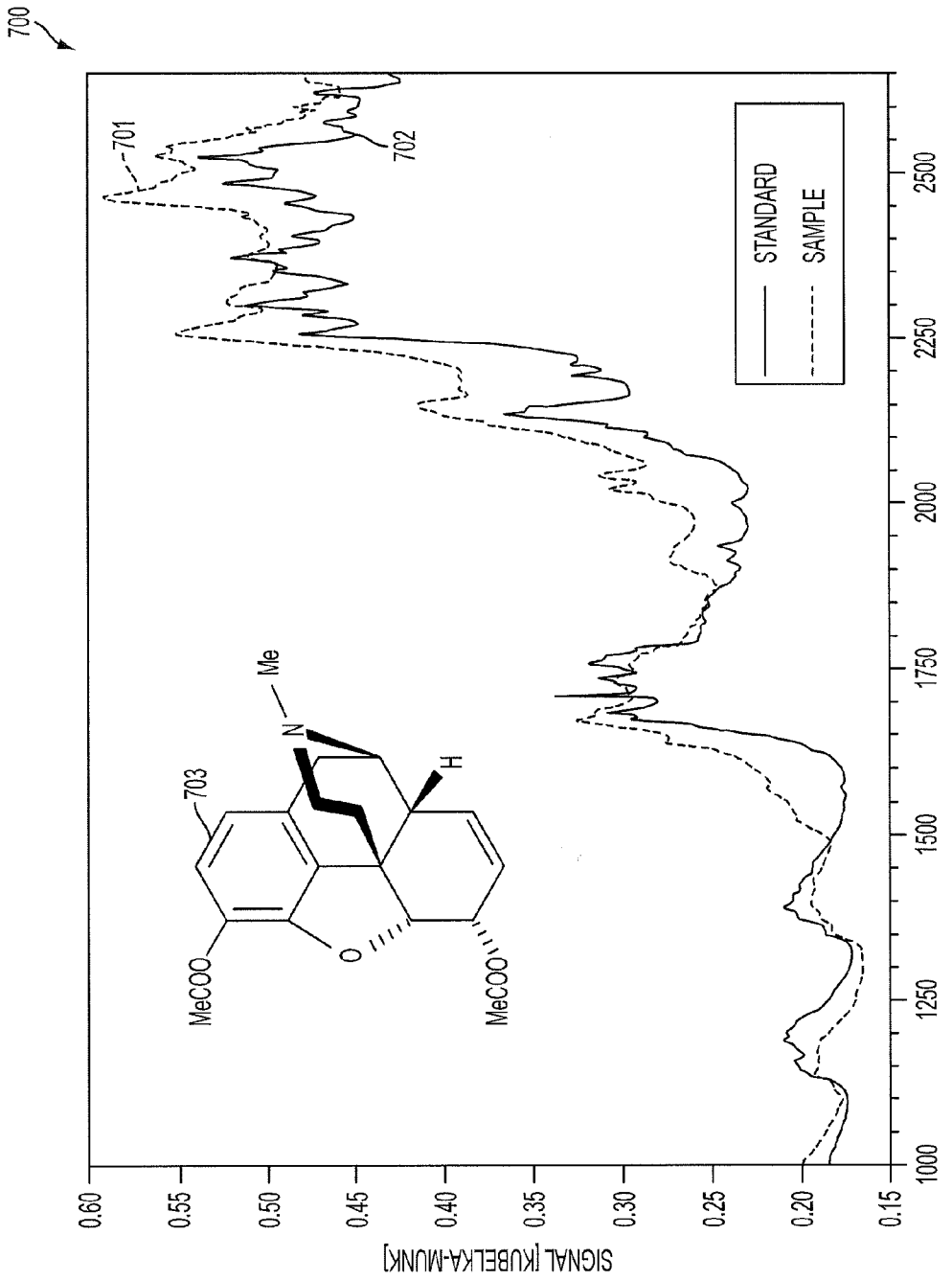

700
701
702
703
STANDARD
SAMPLE
Me
N
H
O
MeCOO
MeCOO
SIGNAL [KUBELKA-MUNK]
0.60
0.55
0.50
0.45
0.40
0.35
0.30
0.25
0.20
0.15
1000
1250
1500
1750
2000
2250
2500
FREQUENCY [nm]

FIG. 7

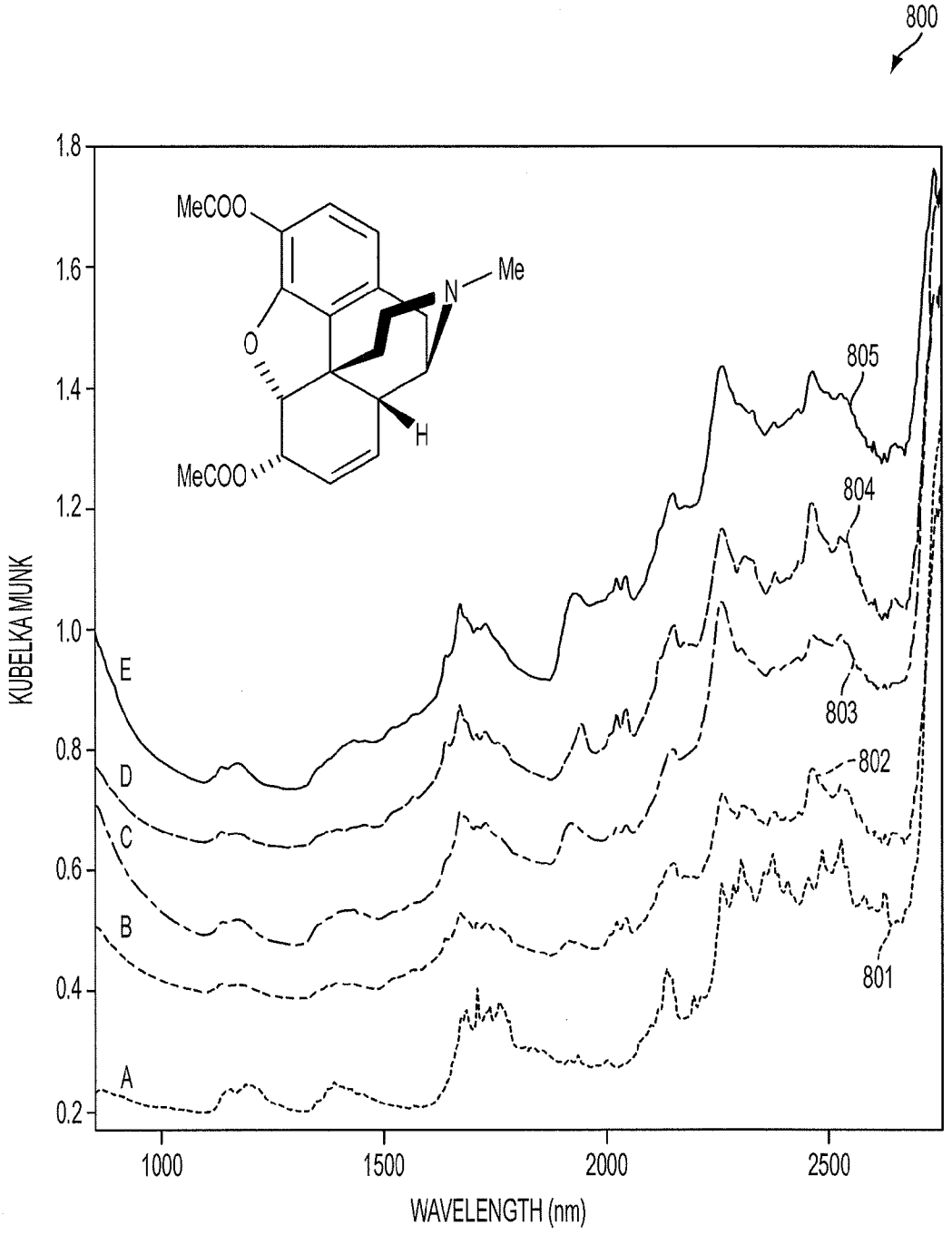

800
1.8
1.6
1.4
1.2
1.0
0.8
0.6
0.4
0.2
KUBELKA MUNK
MeCOO
MeCOO
O
N
Me
H
805
804
803
802
801
E
D
C
B
A
1000
1500
2000
2500
WAVELENGTH (nm)

FIG. 8

900

TENTATIVE FREQUENCIES OF HEROIN BANDS (nm)	ACTUALLY MEASURED PEAK FREQUENCIES (nm)	FORMS OF MODES OF VIBRATION ASSIGNMENT
1160	1157	C—O STRETCH FOURTH OVERTONE
1195	1190	C—H SECOND OVERTONE
	1200	C—H SECOND OVERTONE
1360	1357	C—H COMBINATION
1395	1391	C—H COMBINATION
1420	1425	O—H FIRST OVERTONE
1570	1570	N—H STRETCH FIRST OVERTONE
1685	1684	C—H STRETCH FIRST OVERTONE
1705	1709	C—H STRETCH FIRST OVERTONE
1725	1727	C—H STRETCH FIRST OVERTONE
1765	1767	C—H STRETCH FIRST OVERTONE
1780	1780	C—H STRETCH FIRST OVERTONE
1920	1914	C—O STRETCH SECOND OVERTONE
1950	1936	C—O STRETCH SECOND OVERTONE
1990	2000	N—H STRETCH/N—H BEND COMBINATION
2070	2074	N—H DEFORMATION OVERTONE
2090	2100	C—H COMBINATION
2140	2135	C—H STRETCH/C—O STRETCH COMBINATION OR SYM C—H DEFORMATION
	2144	C—H STRETCH/C—O STRETCH COMBINATION OR SYM C—H DEFORMATION

TO FIG. 9B

FIG. 9A

FROM FIG. 9A

2170	2172	ASYMMETRIC C—H STRETCH/C—H DEFORMATION COMBINATION
2180	2178	N—H BEND SECOND OVERTONE OR C—H STRETCH/C—O STRETCH COMBINATION, OR C—O STRETCH C—N STRETCH; N—H IN-PLANE BEND.
2200	2194	CH STRETCH/C—O STRETCH COMBINATION
2280	2284	C—H STRETCH/CH_2 DEFORMATION
2300	2300	C—H BEND SECOND OVERTONE
2325	2320	CH STRETCH/CH_2 DEFORMATION COMBINATION
2352	2352	CH_2 BEND SECOND OVERTONE
2380	2384	C—H STRETCH/C—C STRETCH COMBINATION
2470	2454	C—H COMBINATION OR SYM C—N—C STRETCH OVERTONE
2488	2485	C—H STRETCH/C—C STRETCH COMBINATION
2530	2524	ASYMMETRIC C—N—C STRETCH FIRST OVERTONE
2530	2537	ASYMMETRIC C—N—C STRETCH FIRST OVERTONE

FIG. 9B

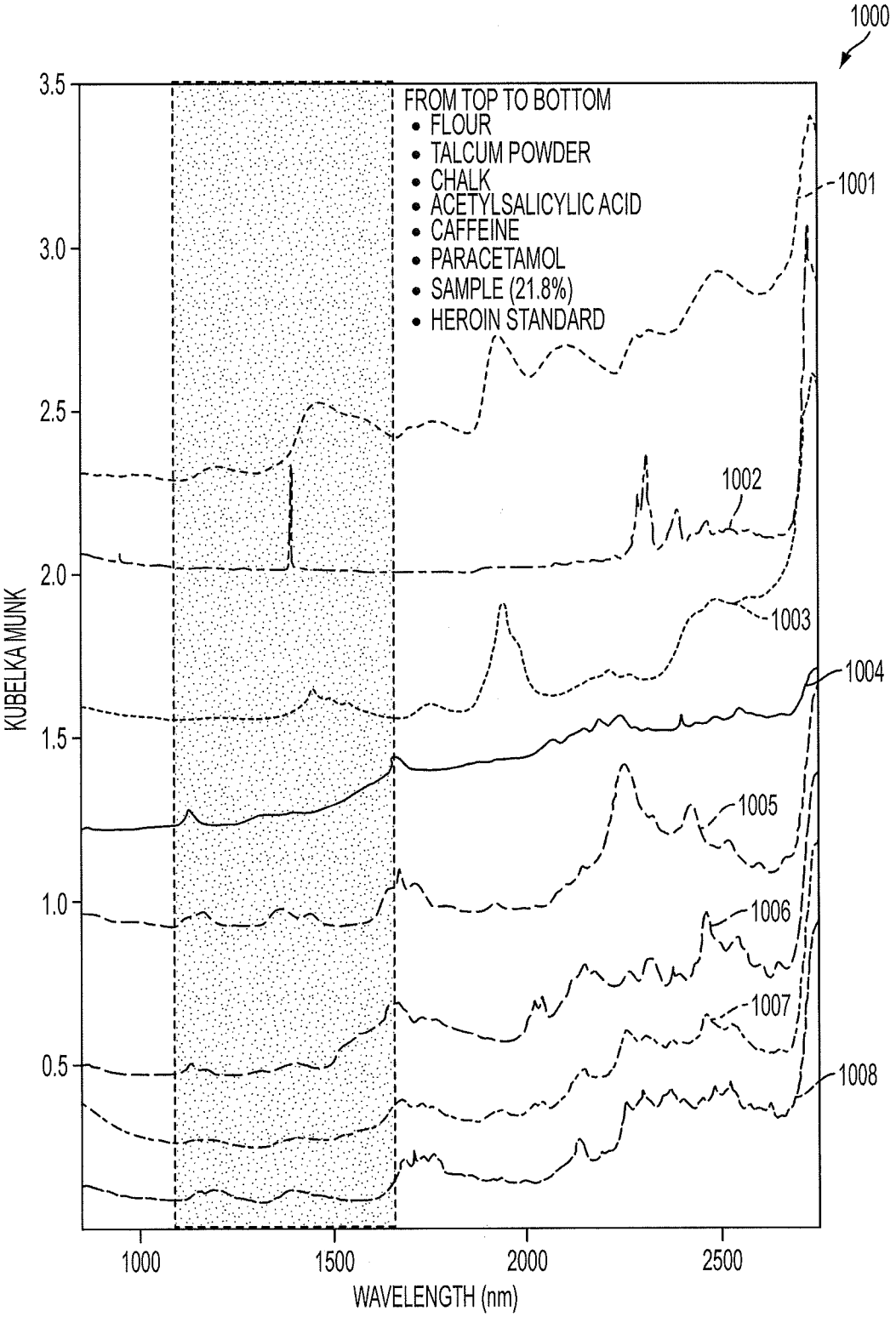

1000
FROM TOP TO BOTTOM
• FLOUR
• TALCUM POWDER
• CHALK
• ACETYLSALICYLIC ACID
• CAFFEINE
• PARACETAMOL
• SAMPLE (21.8%)
• HEROIN STANDARD
1001
1002
1003
1004
1005
1006
1007
1008
KUBELKA MUNK
3.5
3.0
2.5
2.0
1.5
1.0
0.5
1000
1500
2000
2500
WAVELENGTH (nm)

FIG. 10

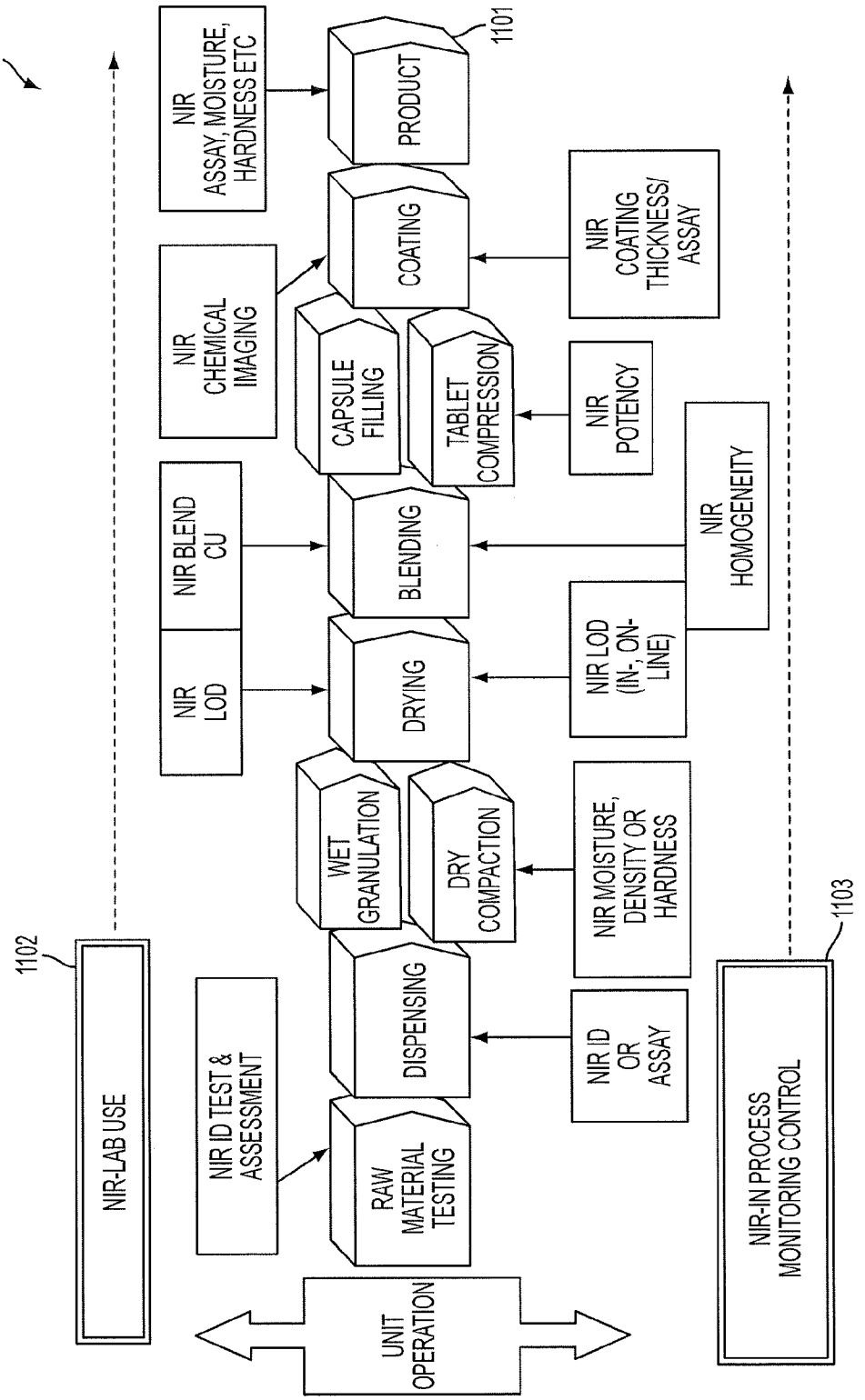

1100
1101
1102
1103
NIR-LAB USE
NIR ID TEST & ASSESSMENT
RAW MATERIAL TESTING
DISPENSING
WET GRANULATION
DRY COMPACTION
DRYING
BLENDING
CAPSULE FILLING
TABLET COMPRESSION
COATING
PRODUCT
NIR LOD
NIR BLEND CU
NIR CHEMICAL IMAGING
NIR ASSAY, MOISTURE, HARDNESS ETC
UNIT OPERATION
NIR ID OR ASSAY
NIR MOISTURE, DENSITY OR HARDNESS
NIR LOD (IN-, ON-LINE)
NIR POTENCY
NIR COATING THICKNESS/ ASSAY
NIR HOMOGENEITY
NIR-IN PROCESS MONITORING CONTROL

FIG. 11

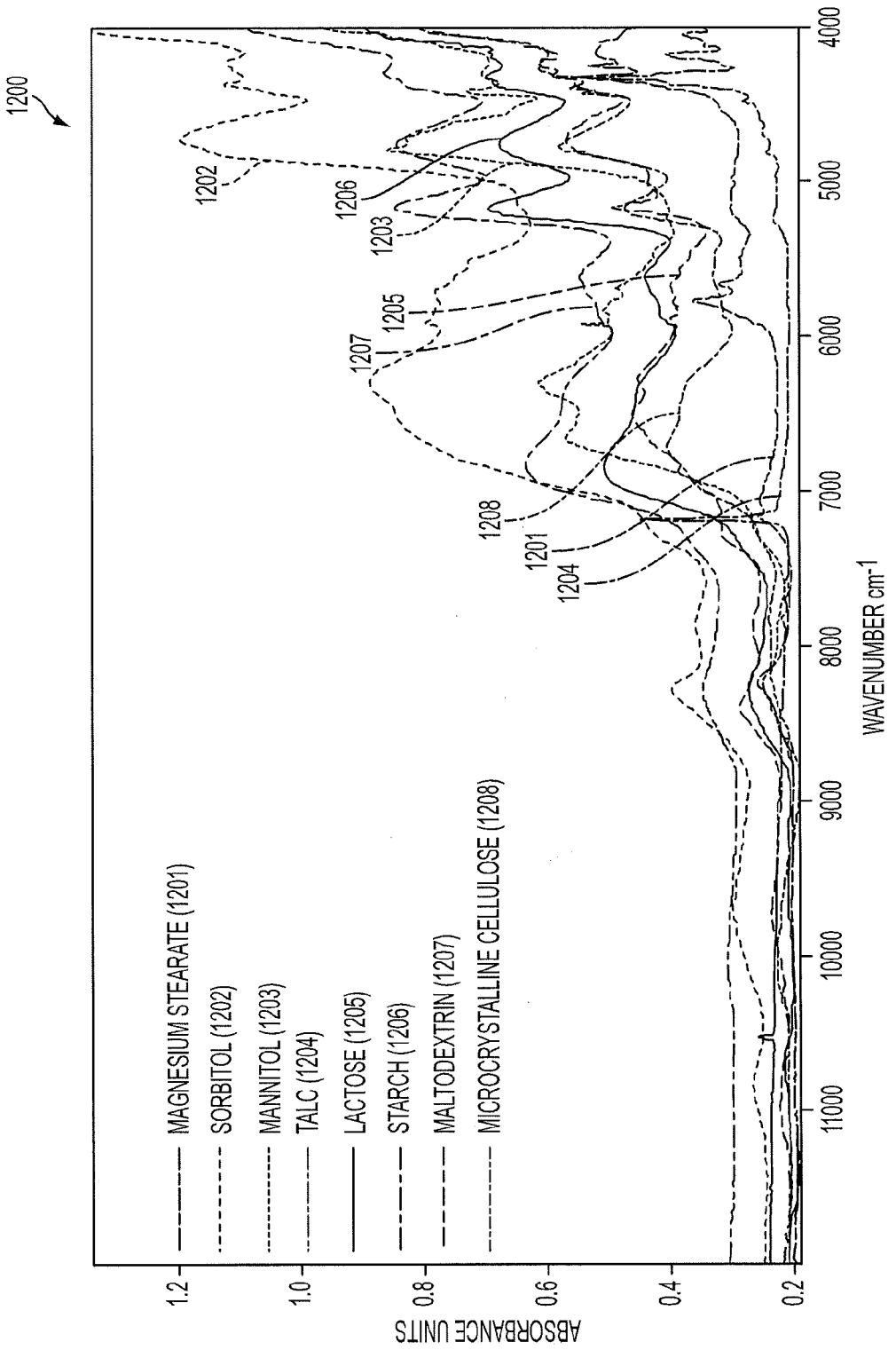

1200
1202
1206
1203
1205
1207
1208
1201
1204
MAGNESIUM STEARATE (1201)
SORBITOL (1202)
MANNITOL (1203)
TALC (1204)
LACTOSE (1205)
STARCH (1206)
MALTODEXTRIN (1207)
MICROCRYSTALLINE CELLULOSE (1208)
ABSORBANCE UNITS
1.2
1.0
0.8
0.6
0.4
0.2
WAVENUMBER cm-1
11000
10000
9000
8000
7000
6000
5000
4000

FIG. 12

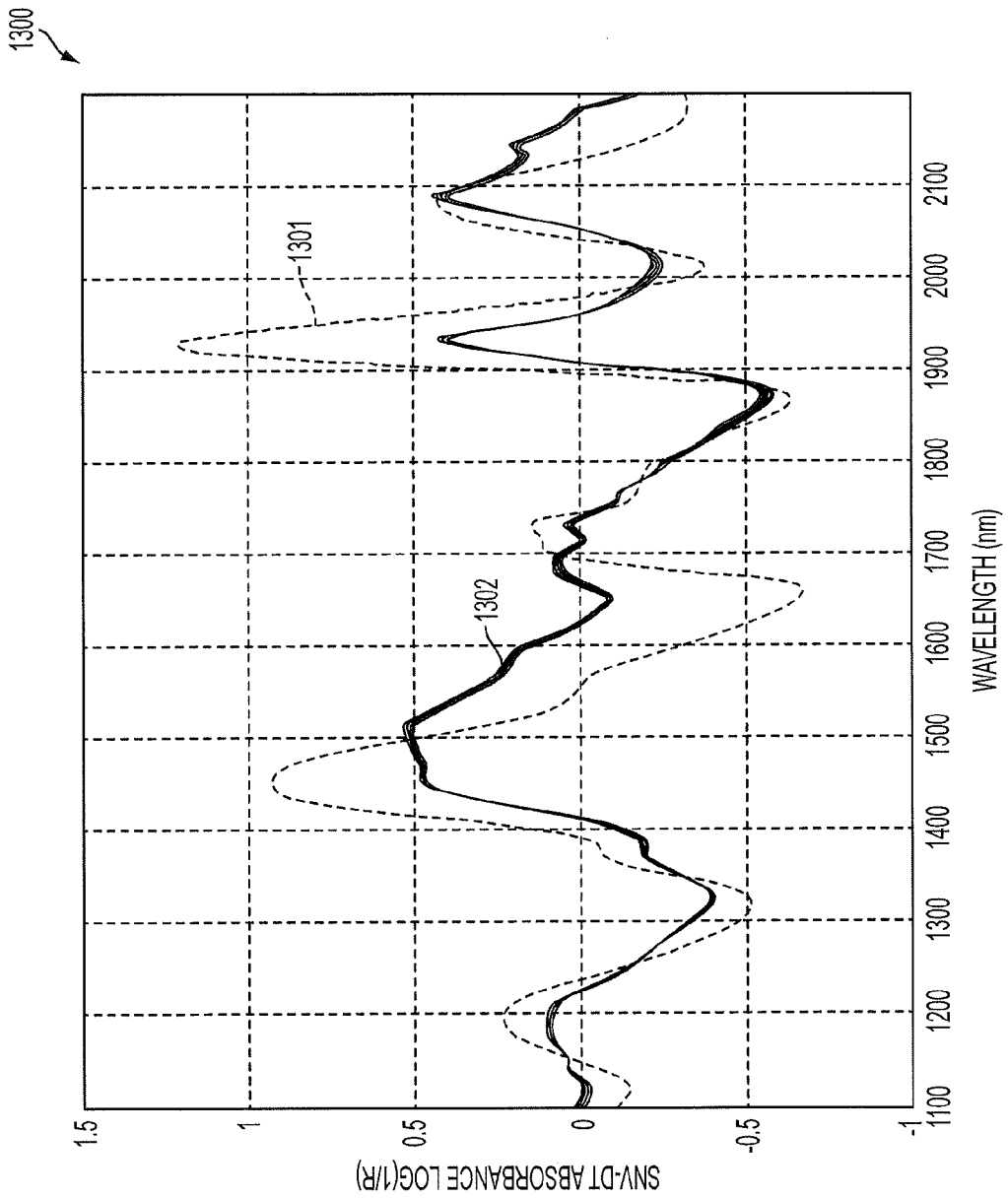

1300
1301
1302
SNV-DT ABSORBANCE LOG(1/R)
1.5
1
0.5
0
-0.5
-1
1100
1200
1300
1400
1500
1600
1700
1800
1900
2000
2100
WAVELENGTH (nm)

FIG. 13

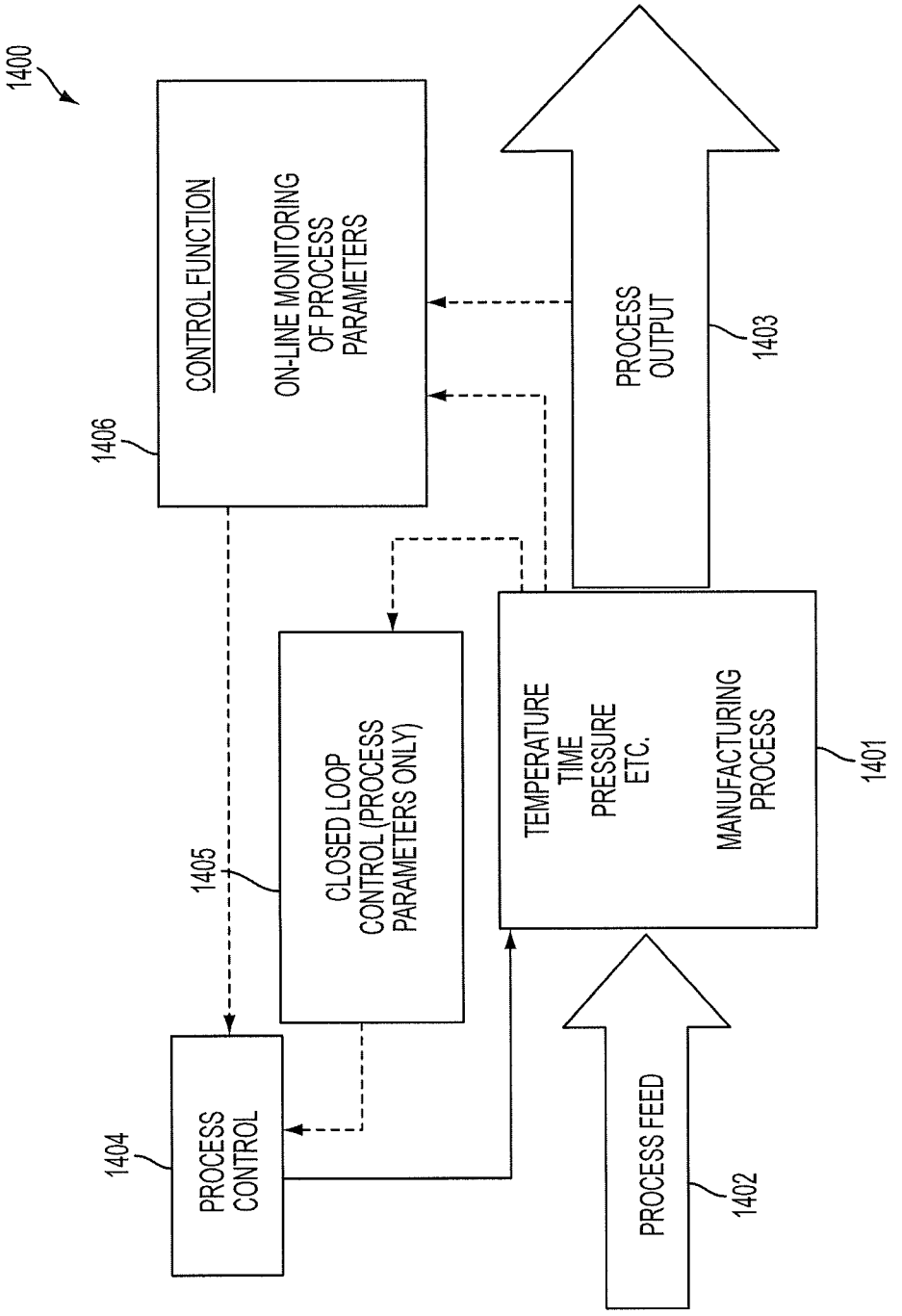

1400
CONTROL FUNCTION
ON-LINE MONITORING OF PROCESS PARAMETERS
1406
PROCESS OUTPUT
1403
CLOSED LOOP CONTROL (PROCESS PARAMETERS ONLY)
1405
TEMPERATURE TIME PRESSURE ETC.
MANUFACTURING PROCESS
1401
PROCESS CONTROL
1404
PROCESS FEED
1402

FIG. 14

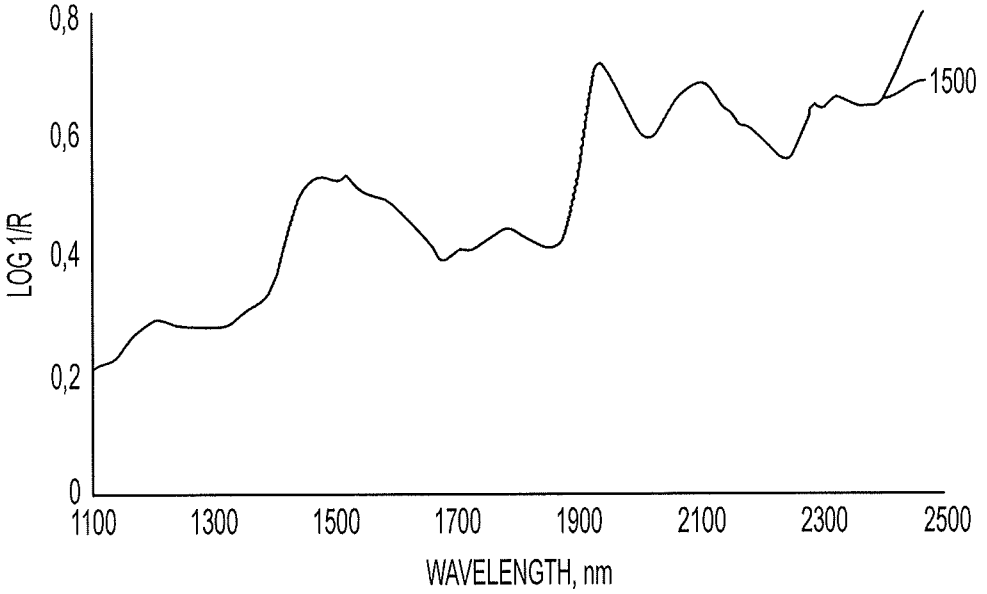


FIG. 15A

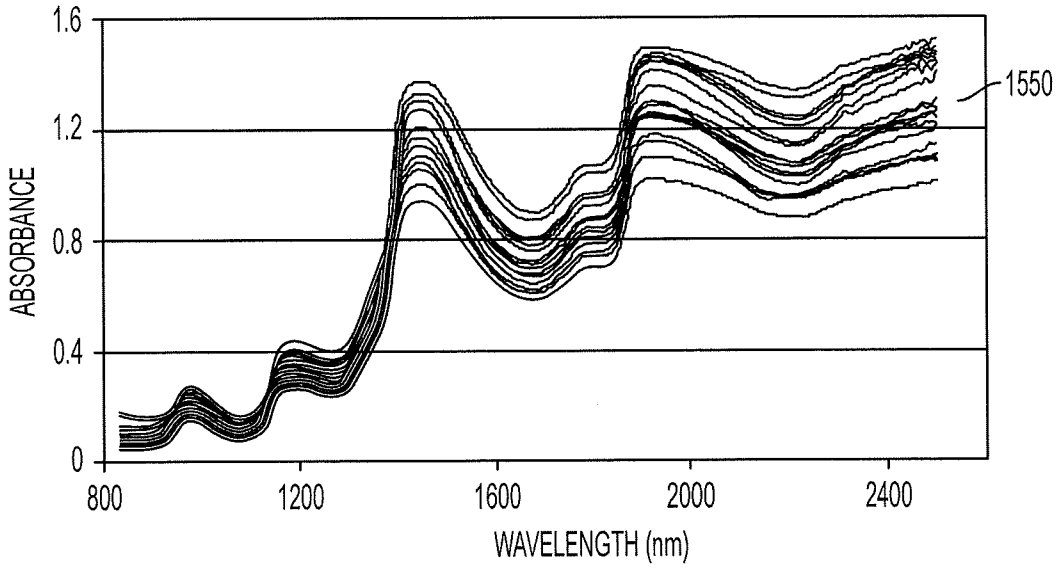


FIG. 15B

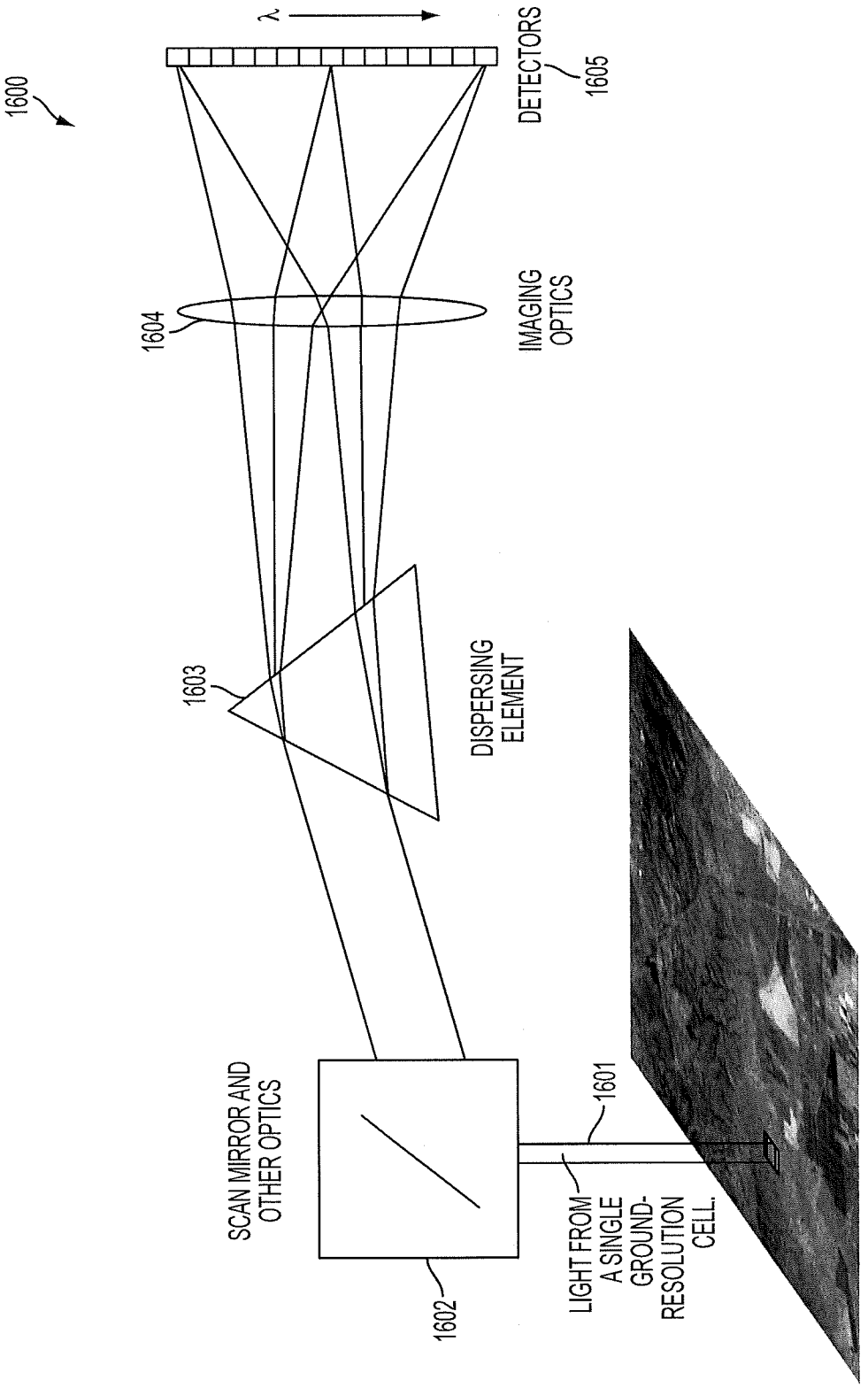

1600
λ
DETECTORS
1605
IMAGING OPTICS
1604
DISPERSING ELEMENT
1603
SCAN MIRROR AND OTHER OPTICS
1602
1601
LIGHT FROM A SINGLE GROUND-RESOLUTION CELL

FIG. 16A

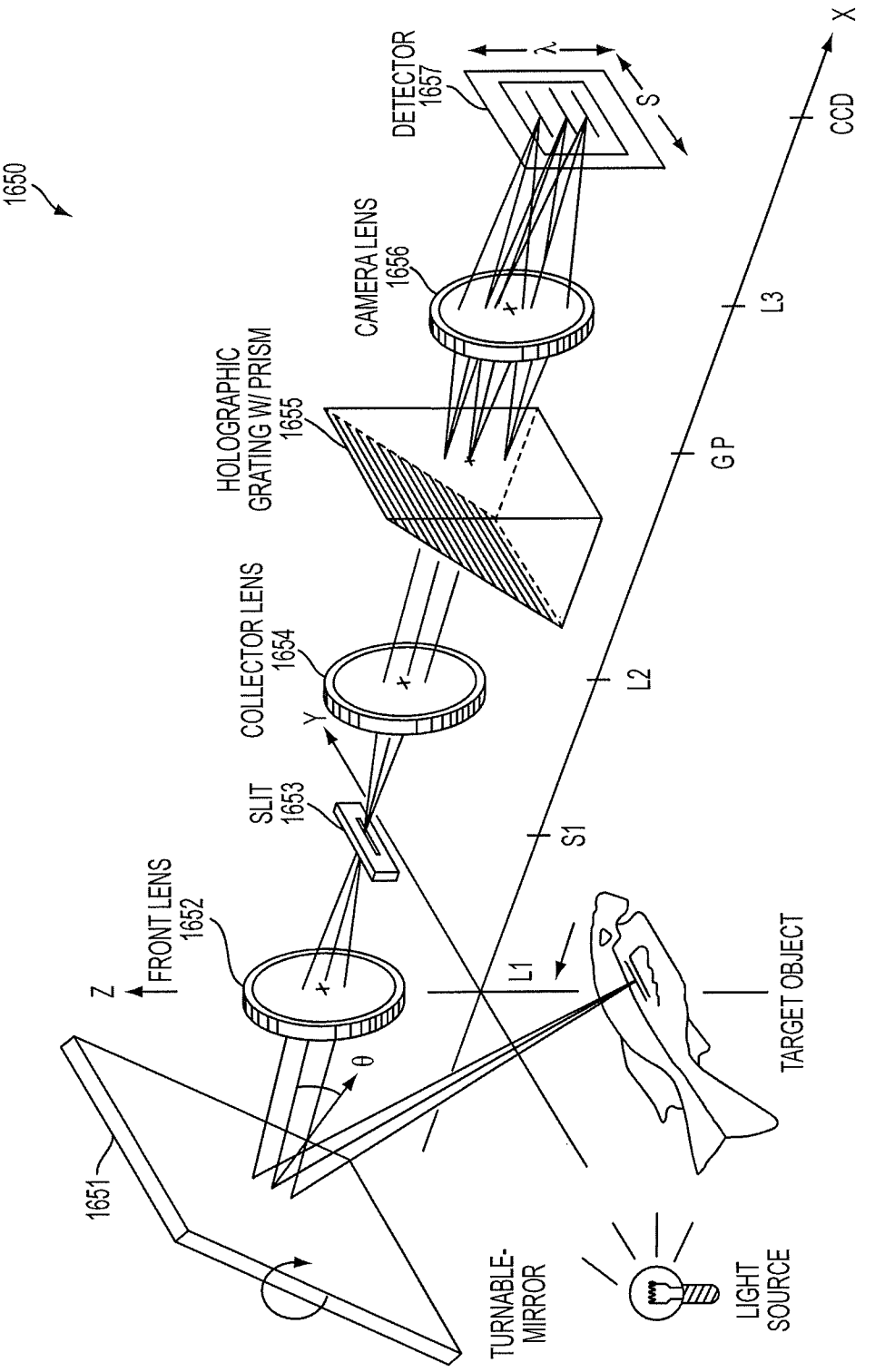

1650
1651
TURNABLE-MIRROR
LIGHT SOURCE
TARGET OBJECT
FRONT LENS 1652
SLIT 1653
COLLECTOR LENS 1654
HOLOGRAPHIC GRATING W/ PRISM 1655
CAMERA LENS 1656
DETECTOR 1657
Z
Y
X
θ
L1
S1
L2
G P
L3
CCD
S
λ

FIG. 16B

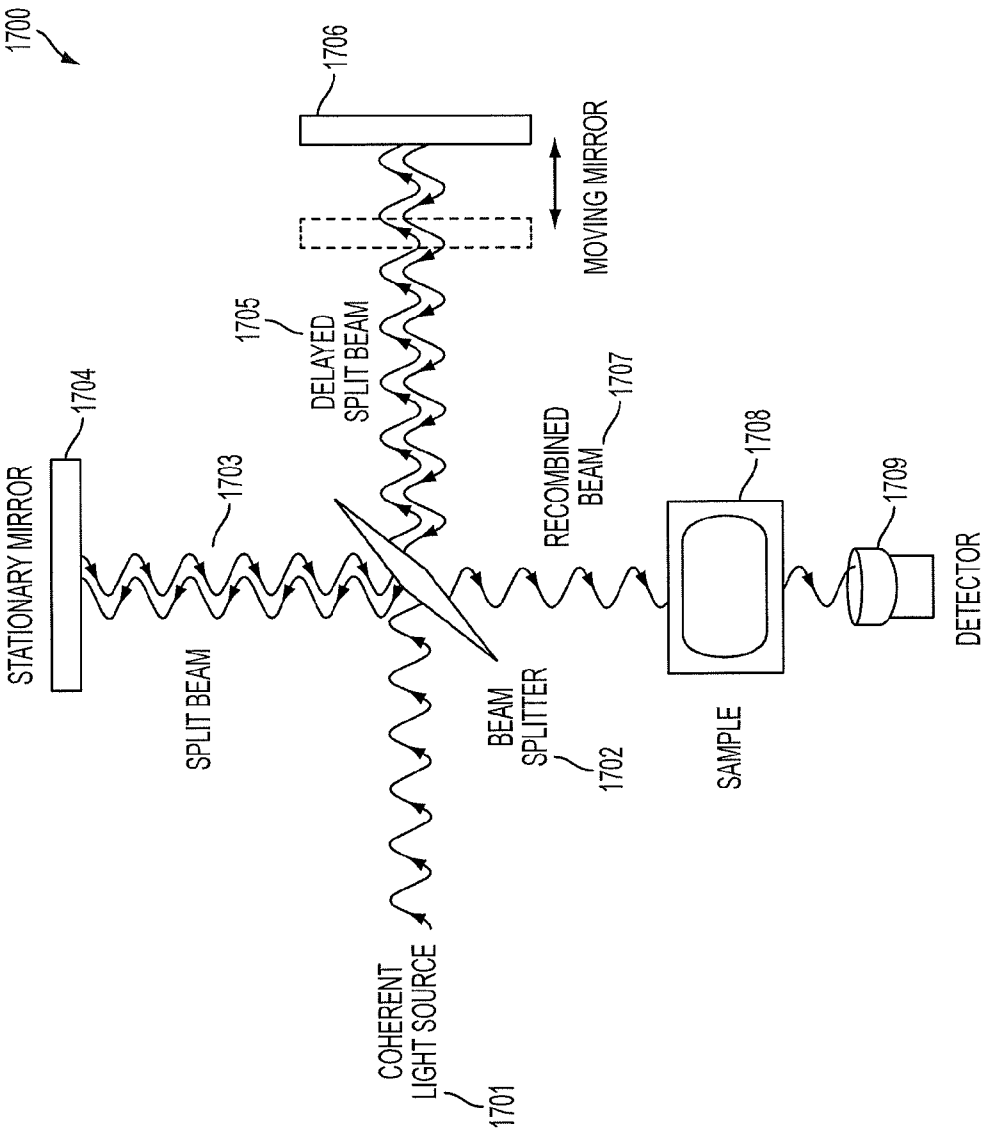

1700
1706
MOVING MIRROR
1705
DELAYED SPLIT BEAM
1704
STATIONARY MIRROR
1703
SPLIT BEAM
RECOMBINED BEAM
1707
1708
1709
DETECTOR
BEAM SPLITTER
1702
SAMPLE
COHERENT LIGHT SOURCE
1701

FIG. 17

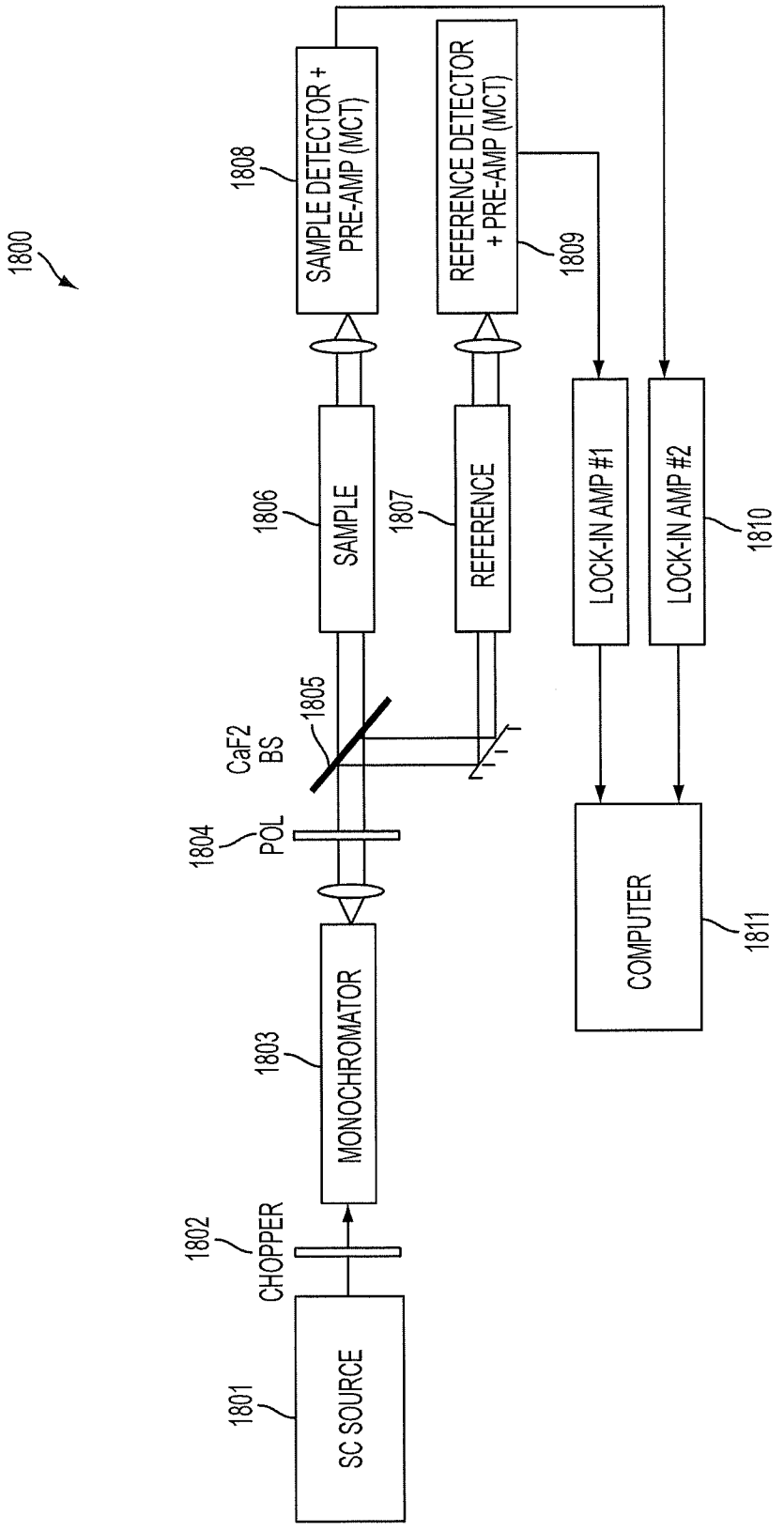

1800
1801
SC SOURCE
1802
CHOPPER
1803
MONOCHROMATOR
1804
POL
1805
CaF2
BS
1806
SAMPLE
1807
REFERENCE
1808
SAMPLE DETECTOR + PRE-AMP (MCT)
1809
REFERENCE DETECTOR + PRE-AMP (MCT)
1810
LOCK-IN AMP #1
LOCK-IN AMP #2
1811
COMPUTER

FIG. 18

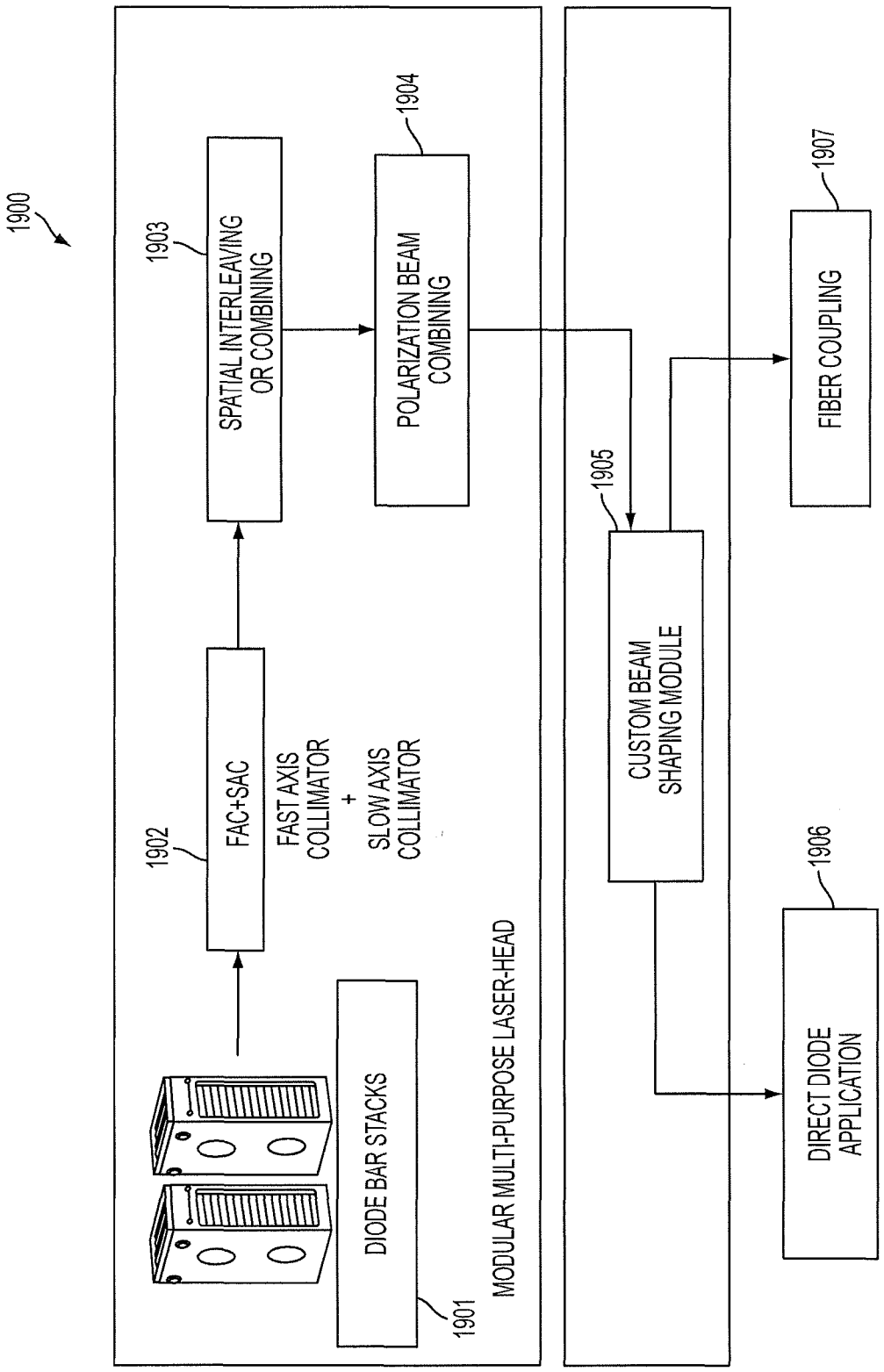

1900
MODULAR MULTI-PURPOSE LASER-HEAD
1901
DIODE BAR STACKS
1902
FAC+SAC
FAST AXIS COLLIMATOR
+
SLOW AXIS COLLIMATOR
1903
SPATIAL INTERLEAVING OR COMBINING
1904
POLARIZATION BEAM COMBINING
1905
CUSTOM BEAM SHAPING MODULE
1906
DIRECT DIODE APPLICATION
1907
FIBER COUPLING

FIG. 19

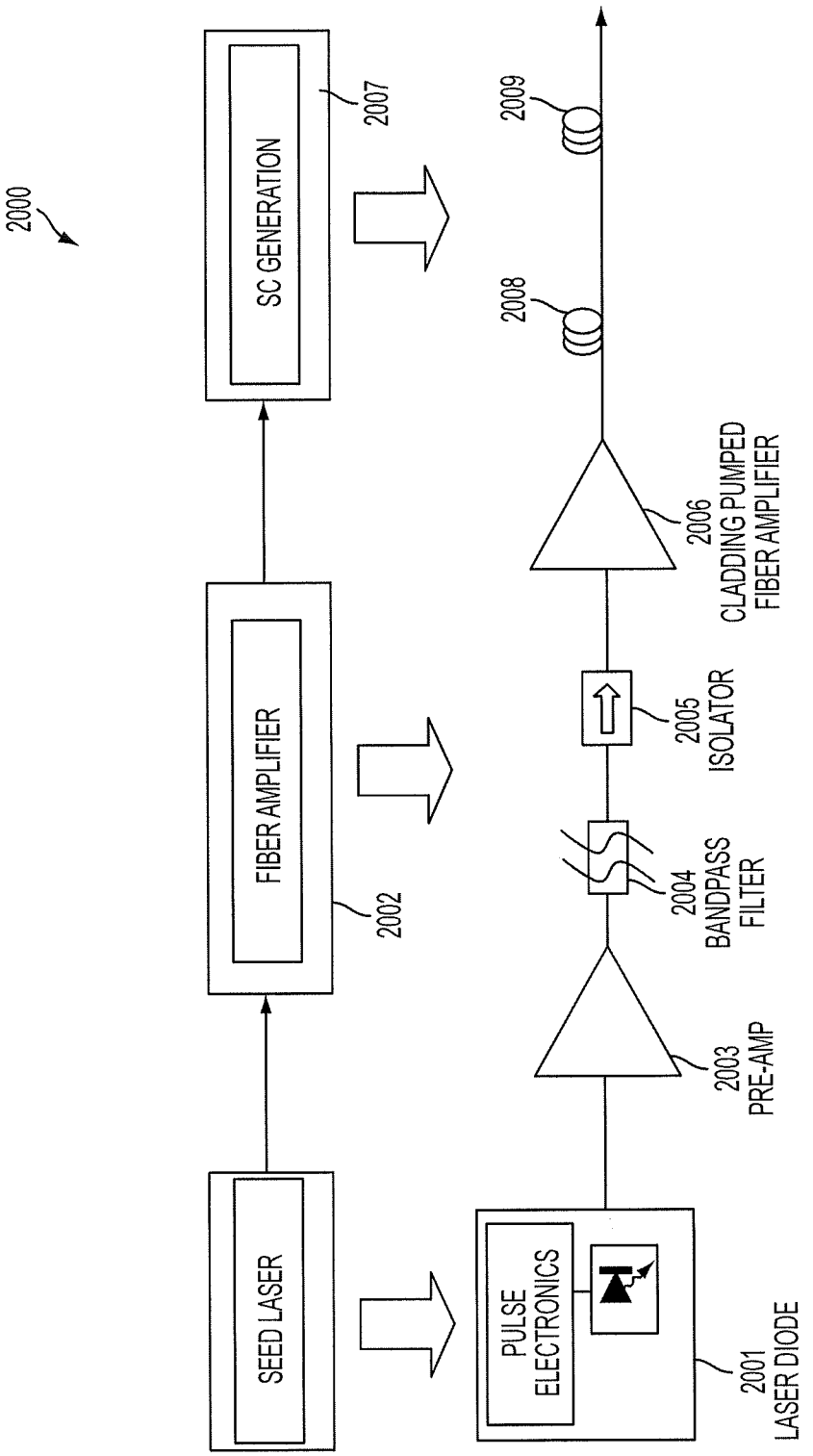

2000
SEED LASER
FIBER AMPLIFIER
2002
SC GENERATION
2007
PULSE ELECTRONICS
2001 LASER DIODE
2003 PRE-AMP
2004 BANDPASS FILTER
2005 ISOLATOR
2006 CLADDING PUMPED FIBER AMPLIFIER
2008
2009

FIG. 20

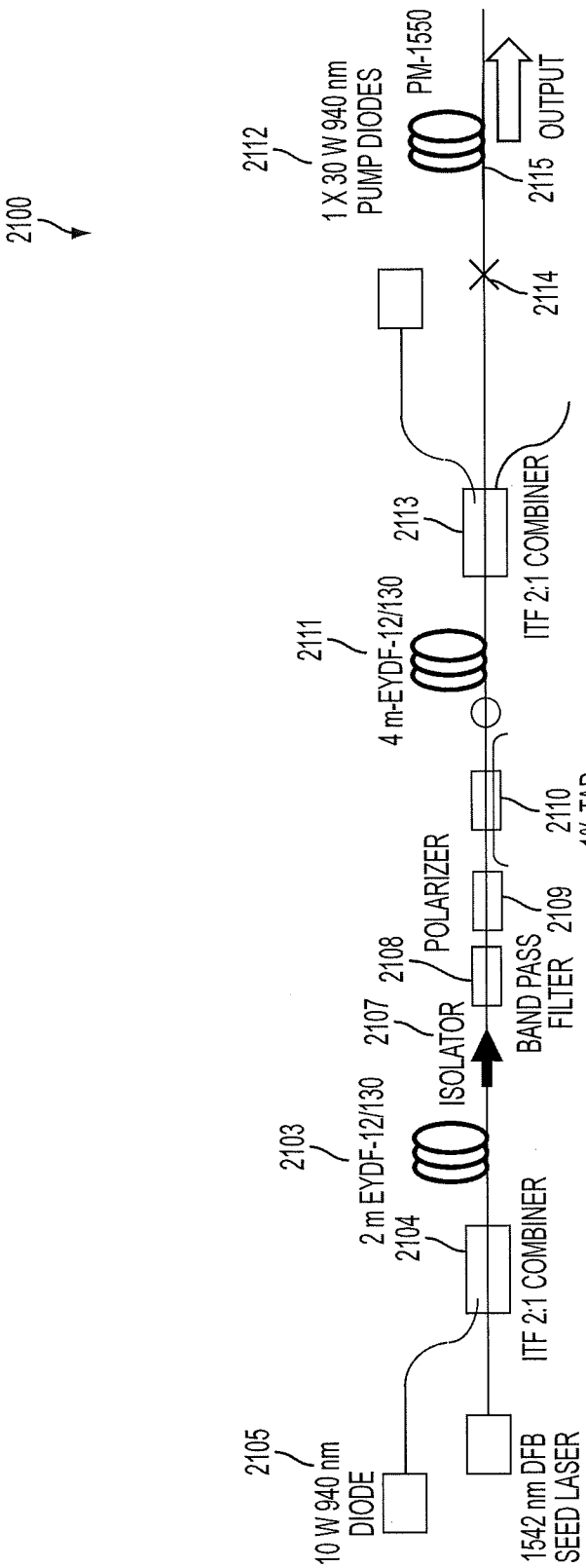

2100
2112
1 X 30 W 940 nm PUMP DIODES
PM-1550
2115 OUTPUT
2114
2113
ITF 2:1 COMBINER
2111
4 m-EYDF-12/130
2110 1% TAP
POLARIZER 2109
2108
2107 ISOLATOR
BAND PASS FILTER
2103
2 m EYDF-12/130
2104
ITF 2:1 COMBINER
2105
10 W 940 nm DIODE
1542 nm DFB SEED LASER
2101
PRE-AMP
2102
POWER-AMP
2106

FIG. 21

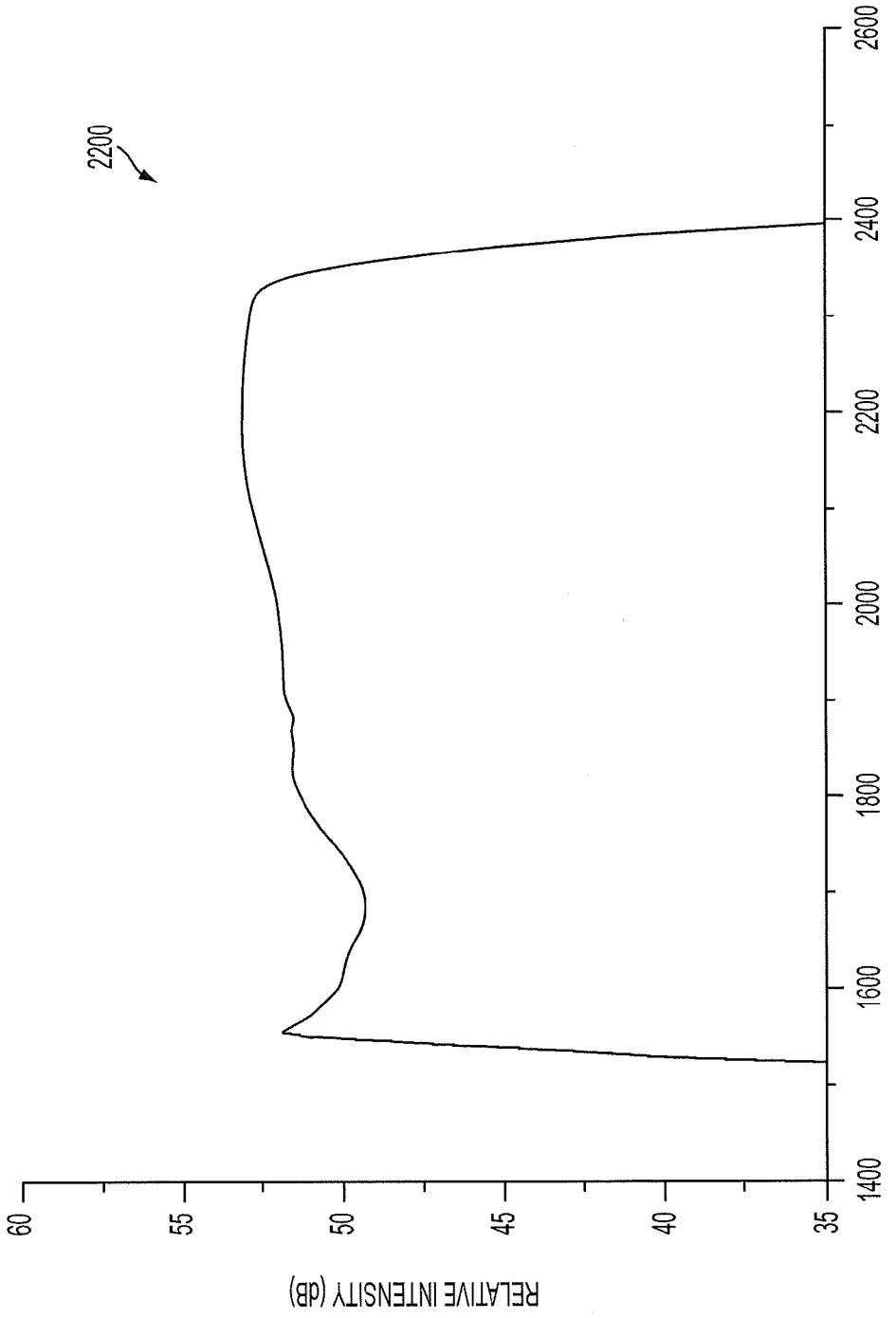

2200
RELATIVE INTENSITY (dB)
60
55
50
45
40
35
1400
1600
1800
2000
2200
2400
2600
WAVELENGTH (nm)

FIG. 22

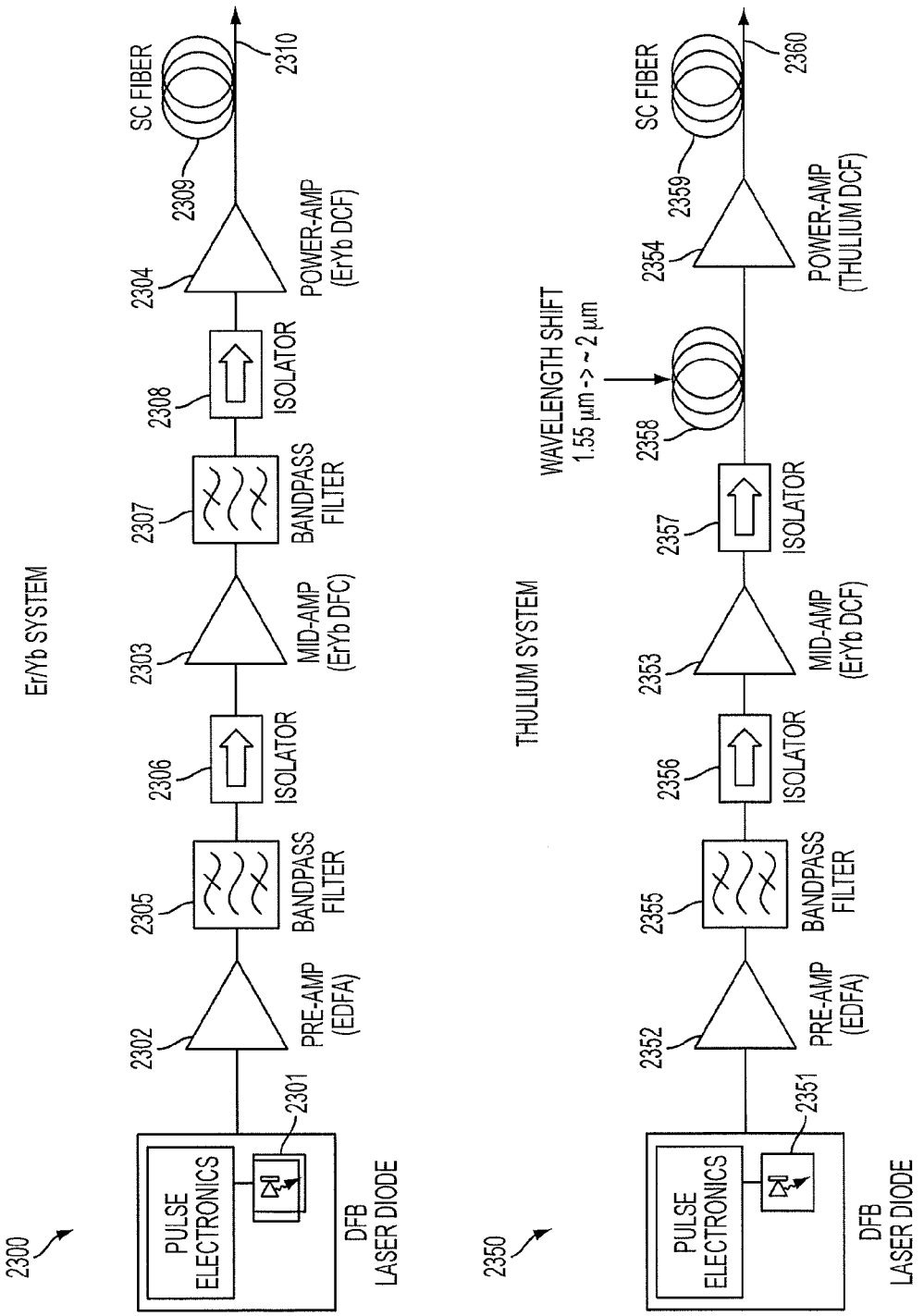

Er/Yb SYSTEM
2300
PULSE ELECTRONICS
2301
DFB LASER DIODE
2302
PRE-AMP (EDFA)
2305
BANDPASS FILTER
2306
ISOLATOR
2303
MID-AMP (ErYb DFC)
2307
BANDPASS FILTER
2308
ISOLATOR
2304
POWER-AMP (ErYb DCF)
2309
SC FIBER
2310
THULIUM SYSTEM
2350
PULSE ELECTRONICS
2351
DFB LASER DIODE
2352
PRE-AMP (EDFA)
2355
BANDPASS FILTER
2356
ISOLATOR
2353
MID-AMP (ErYb DCF)
2357
ISOLATOR
WAVELENGTH SHIFT
1.55 µm -> ~ 2 µm
2358
2354
POWER-AMP (THULIUM DCF)
2359
SC FIBER
2360

FIG. 23

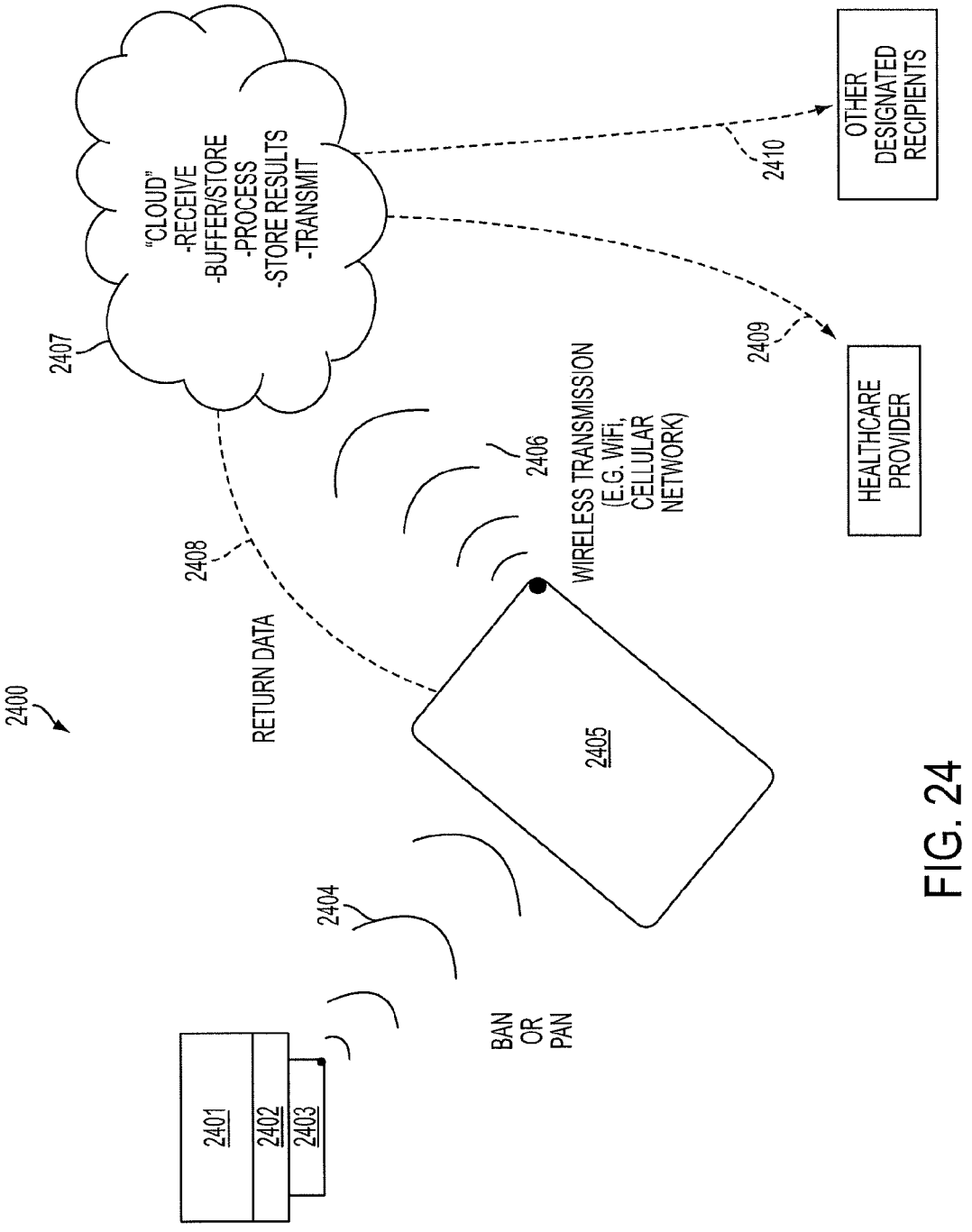

2400
"CLOUD"
-RECEIVE
-BUFFER/STORE
-PROCESS
-STORE RESULTS
-TRANSMIT
2407
OTHER DESIGNATED RECIPIENTS
2410
2409
HEALTHCARE PROVIDER
2406
WIRELESS TRANSMISSION (E.G. WiFi, CELLULAR NETWORK)
2408
RETURN DATA
2405
2404
BAN OR PAN
2401
2402
2403

FIG. 24

SHORT-WAVE INFRARED SUPER-CONTINUUM LASERS FOR DETECTING COUNTERFEIT OR ILLICIT DRUGS AND PHARMACEUTICAL PROCESS CONTROL

CROSS-REFERENCE TO RELATED APPLICATIONS

This application is a continuation of U.S. application Ser. No. 14/108,986 filed Dec. 17, 2013, which claims the benefit of U.S. provisional application Ser. No. 61/747,487 filed Dec. 31, 2012, the disclosures of which are hereby incorporated in their entirety by reference herein.

This application is related to U.S. provisional applications Ser. Nos. 61/747,477 filed Dec. 31, 2012; Ser. No. 61/747,481 filed Dec. 31, 2012; Ser. No. 61/747,485 filed Dec. 31, 2012; Ser. No. 61/747,472 filed Dec. 31, 2012; Ser. No. 61/747,492 filed Dec. 31, 2012; Ser. No. 61/747,553 filed Dec. 31, 2012; and Ser. No. 61/754,698 filed Jan. 21, 2013, the disclosures of which are hereby incorporated in their entirety by reference herein.

This application is also related to International Application No. PCT/US2013/075700 (Publication No. WO/2014/105520) entitled Near-Infrared Lasers For Non-Invasive Monitoring Of Glucose, Ketones, HBA1C, And Other Blood Constituents; International Application PCT/US2013/075736 (Publication No. WO/2014/105521) entitled Short-Wave Infrared Super-Continuum Lasers For Early Detection Of Dental Caries; U.S. application Ser. No. 14/108,995 (Publication No. 2014/0188092) entitled Focused Near-Infrared Lasers For Non-Invasive Vasectomy And Other Thermal Coagulation Or Occlusion Procedures; International Application PCT/US2013/075767 (Publication No. WO/2014/143276) entitled Short-Wave Infrared Super-Continuum Lasers For Natural Gas Leak Detection, Exploration, And Other Active Remote Sensing Applications; U.S. application Ser. No. 14/108,974 (Publication No. 2014/0188094) entitled Non-Invasive Treatment Of Varicose Veins; and U.S. application Ser. No. 14/109,007 (Publication No. 2014/0236021) entitled Near-Infrared Super-Continuum Lasers For Early Detection Of Breast And Other Cancers, the disclosures of which are hereby incorporated in their entirety by reference herein.

BACKGROUND AND SUMMARY

Counterfeiting of pharmaceuticals is a significant issue in the healthcare community as well as for the pharmaceutical industry worldwide. For example, according to the World Health Organization, in 2006 the market for counterfeit drugs worldwide was estimated at around $43 Billion. Moreover, the use of counterfeit medicines may result in treatment failure or even death. For instance, in 1995 dozens of children in Haiti and Nigeria died after taking counterfeit medicinal syrups that contained diethylene glycol, an industrial solvent. As another example, in Asia one report estimated that 90% of Viagra sold in Shanghai, China, was counterfeit. With more pharmaceuticals being purchased through the internet, the problem of counterfeit drugs coming from across the borders into the United States has been growing rapidly.

A rapid, non-destructive, non-contact optical method for screening or identification of counterfeit pharmaceuticals is needed. Spectroscopy using near-infrared or short-wave infrared (SWIR) light may provide such a method, because most pharmaceuticals comprise organic compounds that have overtone or combination absorption bands in this wavelength range (e.g., between approximately 1-2.5 microns). Moreover, most drug packaging materials are at least partially transparent in the near-infrared or SWIR, so that drug compositions may be detected and identified through the packaging non-destructively. Also, using a near-infrared or SWIR light source with a spatially coherent beam permits screening at stand-off or remote distances. Beyond identifying counterfeit drugs, the near-infrared or SWIR spectroscopy may have many other beneficial applications. For example, spectroscopy may be used for rapid screening of illicit drugs or to implement process analytical technology in pharmaceutical manufacturing. There are also a wide array of applications in assessment of quality in the food industry, including screening of fruit, vegetables, grains and meats.

In one embodiment, a near-infrared or SWIR super-continuum (SC) source may be used as the light source for spectroscopy, active remote sensing, or hyper-spectral imaging. One embodiment of the SWIR light source may be an all-fiber integrated SWIR SC source, which leverages the mature technologies from the telecommunications and fiber optics industry. Exemplary fiber-based super-continuum sources may emit light in the near-infrared or SWIR between approximately 1.4-1.8 microns, 2-2.5 microns, 1.4-2.4 microns, 1-1.8 microns, or any number of other bands. In particular embodiments, the detection system may be a dispersive spectrometer, a Fourier transform infrared spectrometer, or a hyper-spectral imaging detector or camera. In addition, reflection or diffuse reflection light spectroscopy may be implemented using the SWIR light source, where the spectral reflectance can be the ratio of reflected energy to incident energy as a function of wavelength.

In one embodiment, a measurement system includes a light source configured to generate an output optical beam comprising one or more semiconductor sources configured to generate an input beam, one or more optical amplifiers configured to receive at least a portion of the input beam and to deliver an intermediate beam to an output end of the one or more optical amplifiers, and one or more optical fibers configured to receive at least a portion of the intermediate beam and to deliver at least the portion of the intermediate beam to a distal end of the one or more optical fibers to form a first optical beam. A nonlinear element is configured to receive at least a portion of the first optical beam and to broaden a spectrum associated with the at least a portion of the first optical beam to at least 10 nm through a nonlinear effect in the nonlinear element to form the output optical beam with an output beam broadened spectrum, wherein at least a portion of the output beam broadened spectrum comprises a short-wave infrared wavelength between approximately 1400 nanometers and approximately 2500 nanometers, and wherein at least a portion of the one or more fibers is a fused silica fiber with a core diameter less than approximately 400 microns. A measurement apparatus is configured to receive a received portion of the output optical beam and to deliver a delivered portion of the output optical beam to a sample for a non-destructive and non-contact measurement, wherein the delivered portion of the output optical beam is configured to generate a spectroscopy output beam from the sample. A receiver is configured to receive at least a portion of the spectroscopy output beam having a bandwidth of at least 10 nanometers and to process the portion of the spectroscopy output beam to generate an output signal, and wherein at least a part of the delivered portion of the output optical beam is at least partially transmitting through a packaging material covering at least

a part of the sample, and wherein the output signal is based on a chemical composition of the sample.

In another embodiment, a measurement system includes a light source configured to generate an output optical beam comprising a plurality of semiconductor sources configured to generate an input optical beam, a multiplexer configured to receive at least a portion of the input optical beam and to form an intermediate optical beam, and one or more fibers configured to receive at least a portion of the intermediate optical beam and to form the output optical beam, wherein the output optical beam comprises one or more optical wavelengths. A measurement apparatus is configured to receive a received portion of the output optical beam and to deliver a delivered portion of the output optical beam to a sample, wherein the delivered portion of the output optical beam is configured to generate a spectroscopy output beam from the sample. A receiver is configured to receive at least a portion of the spectroscopy output beam and to process the portion of the spectroscopy output beam to generate an output signal, wherein the receiver comprises a Fourier transform infrared (FTIR) spectrometer or a dispersive spectrometer, and wherein at least a part of the delivered portion of the output optical beam is at least partially transmitting through a packaging material covering at least a part of the sample.

In yet another embodiment, a method of measuring includes generating an output optical beam comprising generating an input optical beam from a plurality of semiconductor sources, multiplexing at least a portion of the input optical beam and forming an intermediate optical beam, and guiding at least a portion of the intermediate optical beam and forming the output optical beam, wherein the output optical beam comprises one or more optical wavelengths. The method may also include receiving a received portion of the output optical beam and delivering a delivered portion of the output optical beam to a sample, wherein the sample comprises an organic compound with an overtone or combinational absorption band in the wavelength range between approximately 1 micron and approximately 2.5 microns. The method may further include generating a spectroscopy output beam having a bandwidth of at least 10 nanometers from the sample using a Fourier transform infrared (FTIR) spectrometer or a dispersive spectrometer, receiving at least a portion of the spectroscopy output beam, and processing the portion of the spectroscopy output beam and generating an output signal.

With the growing obesity epidemic, the number of individuals with diabetes is increasing dramatically. For example, there are over 200 million people who have diabetes. Diabetes control requires monitoring of the glucose level, and most glucose measuring systems available commercially require drawing of blood. Depending on the severity of the diabetes, a patient may have to draw blood and measure glucose four to six times a day. This may be extremely painful and inconvenient for many people. In addition, for some groups, such as soldiers in the battlefield, it may be dangerous to have to measure periodically their glucose level with finger pricks.

Thus, there is an unmet need for non-invasive glucose monitoring (e.g., monitoring glucose without drawing blood). The challenge has been that a non-invasive system requires adequate sensitivity and selectivity, along with repeatability of the results. Yet, this is a very large market, with an estimated annual market of over $10B in 2011 for self-monitoring of glucose levels.

One approach to non-invasive monitoring of blood constituents or blood analytes is to use near-infrared spectroscopy, such as absorption spectroscopy or near-infrared diffuse reflection or transmission spectroscopy. Some attempts have been made to use broadband light sources, such as tungsten lamps, to perform the spectroscopy. However, several challenges have arisen in these efforts. First, many other constituents in the blood also have signatures in the near-infrared, so spectroscopy and pattern matching, often called spectral fingerprinting, is required to distinguish the glucose with sufficient confidence. Second, the non-invasive procedures have often transmitted or reflected light through the skin, but skin has many spectral artifacts in the near-infrared that may mask the glucose signatures. Moreover, the skin may have significant water and blood content. These difficulties become particularly complicated when a weak light source is used, such as a lamp. More light intensity can help to increase the signal levels, and, hence, the signal-to-noise ratio.

As described in this disclosure, by using brighter light sources, such as fiber-based supercontinuum lasers, superluminescent laser diodes, light-emitting diodes or a number of laser diodes, the near-infrared signal level from blood constituents may be increased. By shining light through the teeth, which have fewer spectral artifacts than skin in the near-infrared, the blood constituents may be measured with less interfering artifacts. Also, by using pattern matching in spectral fingerprinting and various software techniques, the signatures from different constituents in the blood may be identified. Moreover, value-add services may be provided by wirelessly communicating the monitored data to a handheld device such as a smart phone, and then wirelessly communicating the processed data to the cloud for storing, processing, and transmitting to several locations.

In various embodiments, a measurement system includes a light source configured to generate an output optical beam that includes one or more semiconductor sources configured to generate an input beam, one or more optical amplifiers configured to receive at least a portion of the input beam and to output an intermediate beam from at least one of the one or more optical amplifiers; and one or more optical fibers configured to receive at least a portion of the intermediate beam and to communicate at least part of the portion of the intermediate beam to a distal end of the one or more optical fibers to form a first optical beam. The light source may also include a nonlinear element configured to receive at least a portion of the first optical beam and to broaden a spectrum associated with the at least a portion of the first optical beam to at least 10 nm through a nonlinear effect in the nonlinear element to form the output optical beam with an output beam broadened spectrum. The at least a portion of the output beam broadened spectrum comprises a near-infrared wavelength between approximately 700 nm and approximately 2500 nm, and at least a portion of the one or more fibers is a fused silica fiber with a core diameter less than approximately 400 microns. The system may also include a measurement apparatus configured to receive a received portion of the output optical beam and to deliver to a sample an analysis output beam, which is a delivered portion of the output optical beam and wherein the delivered portion of the output optical beam is a spatially coherent beam, and a receiver configured to receive and process at least a portion of the analysis output beam reflected or transmitted from the sample having a bandwidth of at least 10 nanometers and to generate an output signal. In addition, a personal device comprising a wireless receiver, a wireless transmitter, a display, a microphone, a speaker, one or more buttons or knobs, a microprocessor and a touch screen may be configured to receive and process at least a portion of the output

signal, wherein the personal device is configured to store and display the processed output signal, wherein at least a portion of the processed output signal is configured to be transmitted over a wireless transmission link.

In another embodiment, a measurement system includes a light source comprising a plurality of semiconductor sources that are light emitting diodes, the light emitting diodes configured to generate an output optical beam with one or more optical wavelengths, wherein at least a portion of the one or more optical wavelengths is a near-infrared wavelength between 700 nanometers and 2500 nanometers. The light source is configured to increase signal-to-noise ratio by increasing a light intensity from at least one of the plurality of semiconductor sources and by increasing a pulse rate of at least one of the plurality of semiconductor sources. An apparatus comprising a plurality of lenses is configured to receive a portion of the output optical beam and to deliver an analysis output beam to a sample. A receiver is configured to receive and process at least a portion of the analysis output beam reflected or transmitted from the sample and to generate an output signal. The system includes a personal device comprising a wireless receiver, a wireless transmitter, a display, a microphone, a speaker, one or more buttons or knobs, a microprocessor and a touch screen, the personal device configured to receive and process at least a portion of the output signal, wherein the personal device is configured to store and display the processed output signal, and wherein at least a portion of the processed output signal is configured to be transmitted over a wireless transmission link, and a remote device configured to receive over the wireless transmission link a received output status comprising the at least a portion of the processed output signal, to process the received output status to generate processed data and to store the processed data.

Other embodiments may include a measurement system comprising a wearable measurement device for measuring one or more physiological parameters, including a light source comprising a plurality of semiconductor sources that are light emitting diodes, the light emitting diodes configured to generate an output optical beam with one or more optical wavelengths, wherein at least a portion of the one or more optical wavelengths is a near-infrared wavelength between 700 nanometers and 2500 nanometers. The light source is configured to increase signal-to-noise ratio by increasing a light intensity from at least one of the plurality of semiconductor sources and by increasing a pulse rate of at least one of the plurality of semiconductor sources. The wearable measurement device comprises a plurality of lenses configured to receive a portion of the output optical beam and to deliver an analysis output beam to a sample. The wearable measurement device further comprises a receiver configured to receive and process at least a portion of the analysis output beam reflected or transmitted from the sample and to generate an output signal. The system also includes a personal device comprising a wireless receiver, a wireless transmitter, a display, a microphone, a speaker, one or more buttons or knobs, a microprocessor and a touch screen, the personal device configured to receive and process at least a portion of the output signal, wherein the personal device is configured to store and display the processed output signal, and wherein at least a portion of the processed output signal is configured to be transmitted over a wireless transmission link. The system also includes remote device configured to receive over the wireless transmission link a received output status comprising the at least a portion of the processed output signal, to process the received output status to generate processed data and to store the processed data, wherein the remote device is capable of storing a history of at least a portion of the received output status over a specified period of time.

BRIEF DESCRIPTION OF THE DRAWINGS

For a more complete understanding of the present disclosure, and for further features and advantages thereof, reference is now made to the following description taken in conjunction with the accompanying drawings, in which:

FIG. **1** shows the absorbance for two common plastics, polyethylene and polystyrene.

FIG. **2** illustrates one example of the difference in near-infrared spectrum between an authentic tablet and a counterfeit tablet.

FIG. **3** shows the second derivative of the spectral comparison of Prozac and a similarly formulated generic.

FIG. **4** illustrates an example of the near infrared spectra for different pure components of a studied drug.

FIG. **5** shows the mid-wave infrared and long-wave infrared absorption spectra for various illicit drugs.

FIG. **6** shows the absorbance versus wavelength in the near-infrared region for four classes of illegal drugs.

FIG. **7** illustrates the diffuse reflectance near-infrared spectrum of heroin samples.

FIG. **8** illustrates the diffuse reflectance near-infrared spectra of different seized illicit drugs containing heroin of different concentrations, along with the spectrum for pure heroin.

FIGS. **9**A and **9**B list possible band assignments for the various spectral features in pure heroin.

FIG. **10** shows the diffuse reflectance near-infrared spectra of different compounds that may be frequently employed as cutting agents.

FIG. **11** provides one example of a flow-chart in the process analytical technology for the pharmaceutical industry.

FIG. **12** illustrates the typical near-infrared spectra of a variety of excipients.

FIG. **13** exemplifies the absorbance from the blending process of a pharmaceutical compound.

FIG. **14** shows what might be an eventual flow-chart of a smart manufacturing process.

FIG. **15**A illustrates the near-infrared reflectance spectrum of wheat flour.

FIG. **15**B shows the near-infrared absorbance spectra obtained in diffusion reflectance mode for a series of whole 'Hass' avocado fruit.

FIG. **16**A is a schematic diagram of the basic elements of an imaging spectrometer.

FIG. **16**B illustrates one example of a typical imaging spectrometer used in hyper-spectral imaging systems.

FIG. **17** shows one example of the Fourier transform infrared spectrometer.

FIG. **18** exemplifies a dual-beam experimental set-up that may be used to subtract out (or at least minimize the adverse effects of) light source fluctuations.

FIG. **19** illustrates a block diagram or building blocks for constructing high power laser diode assemblies.

FIG. **20** shows a platform architecture for different wavelength ranges for an all-fiber-integrated, high powered, super-continuum light source.

FIG. **21** illustrates one embodiment for a short-wave infrared super-continuum light source.

FIG. **22** shows the output spectrum from the SWIR SC laser of FIG. **21** when about a 10 m length of fiber for SC

generation is used. This fiber is a single-mode, non-dispersion shifted fiber that is optimized for operation near 1550 nm.

FIG. **23** illustrates high power SWIR-SC lasers that may generate light between approximately 1.4-1.8 microns (top) or approximately 2-2.5 microns (bottom).

FIG. **24** schematically shows a medical measurement device as part of a personal or body area network that communicates with another device (e.g., smart phone or tablet) that communicates with the cloud. The cloud may in turn communicate information with the user, healthcare providers, or other designated recipients.

DETAILED DESCRIPTION

As required, detailed embodiments of the present disclosure are described herein; however, it is to be understood that the disclosed embodiments are merely exemplary of the disclosure that may be embodied in various and alternative forms. The figures are not necessarily to scale; some features may be exaggerated or minimized to show details of particular components. Therefore, specific structural and functional details disclosed herein are not to be interpreted as limiting, but merely as a representative basis for teaching one skilled in the art to variously employ the present disclosure.

One advantage of optical systems is that they can perform non-contact, stand-off or remote sensing distance spectroscopy of various materials. As an example, optical systems can be used for identification of counterfeit drugs, detection of illicit drugs, or process control in the pharmaceutical industry, especially when the sensing is to be done at remote or stand-off distances in a non-contact, rapid manner. In general, the near-infrared region of the electromagnetic spectrum covers between approximately 0.7 microns (700 nm) to about 2.5 microns (2500 nm). However, it may also be advantageous to use just the short-wave infrared (SWIR) between approximately 1.4 microns (1400 nm) and about 2.5 microns (2500 nm). One reason for preferring the SWIR over the entire NIR may be to operate in the so-called "eye safe" window, which corresponds to wavelengths longer than about 1400 nm. Therefore, for the remainder of the disclosure the SWIR will be used for illustrative purposes. However, it should be clear that the discussion that follows could also apply to using the near infrared—NIR—wavelength range, or other wavelength bands.

In particular, wavelengths in the eye safe window may not transmit down to the retina of the eye, and therefore, these wavelengths may be less likely to create permanent eye damage from inadvertent exposure. The near-infrared wavelengths have the potential to be dangerous, because the eye cannot see the wavelengths (as it can in the visible), yet they can penetrate and cause damage to the eye. Even if a practitioner is not looking directly at the laser beam, the practitioner's eyes may receive stray light from a reflection or scattering some surface. Hence, it can always be a good practice to use eye protection when working around lasers. Since wavelengths longer than about 1400 nm are substantially not transmitted to the retina or substantially absorbed in the retina, this wavelength range is known as the eye safe window. For wavelengths longer than 1400 nm, in general only the cornea of the eye may receive or absorb the light radiation.

The SWIR wavelength range may be particularly valuable for identifying materials based on their chemical composition because the wavelength range comprises overtones and combination bands for numerous chemical bonds. For example, in the SWIR numerous hydro-carbon chemical compounds have overtone and combinational bands, along with oxygen-hydrogen and carbon-oxygen compounds. Thus, gases, liquids and solids that comprise these chemical compounds may exhibit spectral features in the SWIR wavelength range. In a particular embodiment, the spectra of organic compounds may be dominated by the C—H stretch. The C—H stretch fundamental occurs near 3.4 microns, the first overtone is near 1.7 microns, and a combination band occurs near 2.3 microns.

One embodiment of remote sensing that is used to identify and classify various materials is so-called "hyper-spectral imaging." Hyper-spectral sensors may collect information as a set of images, where each image represents a range of wavelengths over a spectral band. Hyper-spectral imaging may deal with imaging narrow spectral bands over an approximately continuous spectral range. As an example, in hyper-spectral imaging a lamp may be used as the light source. However, the incoherent light from a lamp may spatially diffract rapidly, thereby making it difficult to perform spectroscopy at stand-off distances or remote distances. Therefore, it would be advantageous to have a broadband light source covering the SWIR that may be used in place of a lamp to identify or classify materials in remote sensing or stand-off detection applications.

As used throughout this document, the term "couple" and or "coupled" refers to any direct or indirect communication between two or more elements, whether or not those elements are physically connected to one another. As used throughout this disclosure, the term "spectroscopy" means that a tissue or sample is inspected by comparing different features, such as wavelength (or frequency), spatial location, transmission, absorption, reflectivity, scattering, fluorescence, refractive index, or opacity. In one embodiment, "spectroscopy" may mean that the wavelength of the light source is varied, and the transmission, absorption, fluorescence, or reflectivity of the tissue or sample is measured as a function of wavelength. In another embodiment, "spectroscopy" may mean that the wavelength dependence of the transmission, absorption, fluorescence or reflectivity is compared between different spatial locations on a tissue or sample. As an illustration, the "spectroscopy" may be performed by varying the wavelength of the light source, or by using a broadband light source and analyzing the signal using a spectrometer, wavemeter, or optical spectrum analyzer.

As used throughout this document, the term "fiber laser" refers to a laser or oscillator that has as an output light or an optical beam, wherein at least a part of the laser comprises an optical fiber. For instance, the fiber in the "fiber laser" may comprise one of or a combination of a single mode fiber, a multi-mode fiber, a mid-infrared fiber, a photonic crystal fiber, a doped fiber, a gain fiber, or, more generally, an approximately cylindrically shaped waveguide or light-pipe. In one embodiment, the gain fiber may be doped with rare earth material, such as ytterbium, erbium, and/or thulium. In another embodiment, the mid-infrared fiber may comprise one or a combination of fluoride fiber, ZBLAN fiber, chalcogenide fiber, tellurite fiber, or germanium doped fiber. In yet another embodiment, the single mode fiber may include standard single-mode fiber, dispersion shifted fiber, non-zero dispersion shifted fiber, high-nonlinearity fiber, and small core size fibers.

As used throughout this disclosure, the term "pump laser" refers to a laser or oscillator that has as an output light or an optical beam, wherein the output light or optical beam is coupled to a gain medium to excite the gain medium, which

in turn may amplify another input optical signal or beam. In one particular example, the gain medium may be a doped fiber, such as a fiber doped with ytterbium, erbium and/or thulium. In one embodiment, the "pump laser" may be a fiber laser, a solid state laser, a laser involving a nonlinear crystal, an optical parametric oscillator, a semiconductor laser, or a plurality of semiconductor lasers that may be multiplexed together. In another embodiment, the "pump laser" may be coupled to the gain medium by using a fiber coupler, a dichroic minor, a multiplexer, a wavelength division multiplexer, a grating, or a fused fiber coupler.

As used throughout this document, the term "super-continuum" and or "supercontinuum" and or "SC" refers to a broadband light beam or output that comprises a plurality of wavelengths. In a particular example, the plurality of wavelengths may be adjacent to one-another, so that the spectrum of the light beam or output appears as a continuous band when measured with a spectrometer. In one embodiment, the broadband light beam may have a bandwidth of at least 10 nm. In another embodiment, the "super-continuum" may be generated through nonlinear optical interactions in a medium, such as an optical fiber or nonlinear crystal. For example, the "super-continuum" may be generated through one or a combination of nonlinear activities such as four-wave mixing, parametric amplification, the Raman effect, modulational instability, and self-phase modulation.

As used throughout this disclosure, the terms "optical light" and or "optical beam" and or "light beam" refer to photons or light transmitted to a particular location in space. The "optical light" and or "optical beam" and or "light beam" may be modulated or unmodulated, which also means that they may or may not contain information. In one embodiment, the "optical light" and or "optical beam" and or "light beam" may originate from a fiber, a fiber laser, a laser, a light emitting diode, a lamp, a pump laser, or a light source.

As used throughout this disclosure, the term "remote sensing" may include the measuring of properties of an object from a distance, without physically sampling the object, for example by detection of the interactions of the object with an electromagnetic field. In one embodiment, the electromagnetic field may be in the optical wavelength range, including the infrared or SWIR. One particular form of remote sensing may be stand-off detection, which may range exemplary from non-contact up to hundreds of meters away.

Identification of Counterfeit Drugs

Pharmaceutical counterfeiting is a growing and significant issue for the healthcare community as well as the pharmaceutical industry worldwide. As a result of counterfeiting, users may be threatened by substandard drug quality or harmful ingredients, and legitimate companies may lose significant revenues. The definition for "counterfeit drug" by the World Health Organization was as follows: "A counterfeit medicine is one which is deliberately and fraudulently mislabeled with respect to identity and/or source. Counterfeiting can apply to both branded and generic products and counterfeit products may include products with the correct ingredients or with the wrong ingredients, without active ingredients, with insufficient active ingredient or with fake packaging." Later this definition was slightly modified, "Counterfeiting in relation to medicinal products means the deliberate and fraudulent mislabeling with respect to the identity, composition and/or source of a finished medicinal product, or ingredient for the preparation of a medicinal product."

A rapid screening technique such as near-infrared or SWIR spectroscopy could aid in the search for and identification of counterfeit drugs. In particular, using a non-lamp based light source could lead to contact-free control and analysis of drugs. In a particular embodiment, remote sensing, stand-off detection, or hyper-spectral imaging may be used for process control or counterfeit drug identification in a factory or manufacturing setting, or in a retail, wholesale, or warehouse setting. In one embodiment, the light source for remote sensing may direct the light beam toward the region of interest (e.g., conveyor belt, stocking shelves, boxes or cartons, etc), and the diffuse reflected light may then be measured using a detection system. Various kinds of SWIR light sources will be discussed later in this disclosure. The detection system may comprise, in one embodiment, a spectrometer followed by one or more detectors. In another embodiment, the detection system may be a dispersive element (examples include prisms, gratings, or other wavelength separators) followed by one or more detectors or detector arrays. In yet another embodiment, the detection system may comprise a Fourier transform infrared spectrometer. These are merely specific examples of the detection system, but combinations of these or other detection systems may also be used and are contemplated within the scope of this disclosure.

For monitoring drugs, the SWIR light source and the detection system could be used in transmission, reflection, fluorescence, or diffuse reflection. Also, different system configurations may also be used and are included in the scope of this disclosure. For example, the light source and detection system may be placed in a fixed location, and for reflection the light source and detectors may be close to one another, while for transmission the light source and detectors may be at different locations. The region of interest may be surveyed, and the light beam may also be scanned to cover an area larger than the light source beam. In yet another embodiment, the system could be placed on a vehicle such as an automobile or a truck, or the light source could be placed on one vehicle, while the detection system is on another vehicle. If the light source and detection system are compact and lightweight, they might even be carried by a person in the field, either in their hands or in a backpack.

Another advantage of using the near-infrared or SWIR is that most drug packaging materials are at least partially transparent in this wavelength range, so that drug compositions may be detected and identified through the packaging non-destructively. As an example, SWIR light could be used to see through plastics, since the signature for plastics can be subtracted off and there are large wavelength windows where the plastics are transparent. FIG. **1** illustrates the absorbance **100** for two common plastics: polyethylene **101** and polystyrene **102**. Because of the hydro-carbon bonds, there are absorption features near 1.7 microns and 2.2-2.5 microns. In general, the absorption bands in the near infrared are due to overtones and combination bands for various functional group vibrations, including signals from C—H, O—H, C═O, N—H, —COOH, and aromatic C—H groups. It may be difficult to assign an absorption band to a specific functional group due to overlapping of several combinations and overtones. However, with advancements in computational power and chemometrics or multivariate analysis methods, complex systems may be better analyzed. In one embodiment, using software analysis tools the absorption spectrum may be converted to its second derivative equiva-

lent. The spectral differences may permit a fast, accurate, non-destructive and reliable identification of materials. Although particular derivatives are discussed, other mathematical manipulations may be used in the analysis, and these other techniques are also intended to be covered by this disclosure.

Spectroscopy in the near-infrared or SWIR may be sensitive to both the chemical and physical nature of the sample composition and may be performed rapidly with minimal sample preparation. For example, near-infrared or SWIR spectroscopy may be used to study the homogeneity of powder samples, particle size determinations, product composition, the determination of the concentrations and distribution of components in solid tablets and content uniformity, among other applications. In yet other embodiments, applications include tablet identification, determination of moisture, residual solvents, active ingredient potency, the study of blending operations, and the detection of capsule tampering.

FIG. **2** illustrates one example of the difference in near-infrared spectrum **200** between an authentic tablet and a counterfeit tablet. Two grades of film coated tablets comprising drugs were investigated: curve **201** is the genuine drug, while **202** is a counterfeit drug. These two grades of capsules have noticeably different contents, and the differences are apparent in the near-infrared or SWIR spectra. In some cases the differences may not be as distinct. For these cases, more signal processing may be necessary to distinguish between samples.

In another embodiment, it may be advantageous to take a first, second or higher order derivative to elucidate the difference between real and counterfeit drugs. For example, FIG. **3** shows the second derivative **300** of the spectral comparison of Prozac **301** and a similarly formulated generic **302**, which had a fluoxetine hydrochloride (10 mg). Although the reflectance curves from the two samples are close and, therefore, difficult to distinguish, the second derivative of the data helps to bring out the differences more clearly. Although a second derivative is used in this example, any number of signal processing algorithms and methods may be used, and these are also intended to be covered by this disclosure. For example, partial least square algorithms, multivariate data analysis, principal component analysis, or chemometric software may be implemented without departing from the scope of this disclosure.

In yet another embodiment, near-infrared or SWIR spectroscopy may be used to measure and calibrate various pharmaceutical formulations based on the active pharmaceutical ingredients and excipients. An excipient may be a pharmacologically inactive substance used as a carrier for the active ingredients of a medication. In some cases, the active substance may not be easily administered and/or absorbed by the human body; in such cases the active ingredient may be dissolved into or mixed with an excipient. Also, excipients are also sometimes used to bulk up formulations that contain very potent active ingredients, to allow for convenient and accurate dosage. In addition to their use in the single-dosage quantity, excipients can be used in the manufacturing process to aid in the handling of the active substance concerned.

FIG. **4** shows an example of the near-infrared spectra **400** for different pure components of a studied drug. The spectrum for the active pharmaceutical ingredient (API) **401** is plotted, along with the spectra for five different excipients **402**, **403**, **404**, **405** and **406**. Each spectrum has been baseline shifted to avoid overlapping. The near-infrared spectra have been obtained by averaging the spectra of each pixel of an area of a hyper-spectral image. As FIG. **4** shows, each of the chemical compositions have a distinct spectrum, and the composition of a drug may be decomposed into its constitutive ingredients. These are just some examples of how near-infrared or SWIR spectroscopy may be applied to counterfeit drug detection, but other methods and analysis techniques may also be used without departing from the scope of this disclosure. As one other example, once the active pharmaceutical ingredient and the excipients spectral distribution of a drug formulation are understood, feedback may be provided of this information to the drug development stages.

Rapid Screening for Illicit Drugs

Thus, FIGS. **2-4** show that near-infrared or SWIR spectroscopy may be used to identify counterfeit drugs. More generally, various materials including illicit drugs, explosives, fertilizers, vegetation, and paints have features in the near-infrared and SWIR that can be used to identify the various samples, and these applications are also intended to be within the scope of this disclosure. Although stronger features may be found in the mid-infrared, the near-infrared may be easier to measure due to higher quality detection systems, more mature fiber optics and light sources, and transmission through atmospheric transmission windows. Because of these distinct spectral signatures, these materials could also be detected using active remote sensing, hyper-spectral imaging, or near-infrared or SWIR spectroscopy. As just another example, illicit drugs may be detectable using remote sensing, hyper-spectral imaging, or near-infrared spectroscopy. FIG. **5** shows the mid-wave infrared and long-wave infrared absorption spectra **500** for various illicit drugs. The absorbance for cocaine **501**, methamphetamine **502**, MDMA (ecstasy) **503**, and heroin **504** are plotted versus wavelength from approximately 2.5-20 microns. Although the fundamental resonances for these drugs may lie in the longer wavelength regions, there are corresponding overtones and combination bands in the SWIR and near-infrared wavelength range. Therefore, the active remote sensing, hyper-spectral imaging, or near-infrared or SWIR spectroscopy techniques described herein may also be applicable to detecting illicit drugs from aircraft, vehicles, or hand held devices.

The diffuse reflectance technique may be useful with near-infrared or SWIR spectroscopy for rapid identification of illegal drugs due to simple handling and simple use of a search data library created using near-infrared diffuse reflectance. For instance, FIG. **6** illustrates the absorbance **600** versus wavelength in the near-infrared region for four classes of illegal drugs. In particular, the spectra are shown for methamphetamine (MA) **601**, amphetamine (AP) **602**, MDMA (street name: ecstasy) **603**, and MDA (street name: the love drug) **604**. Each of the illegal drugs have unique spectral features in the near-infrared and SWIR. Also, comparing the mid-infrared spectrum for MDMA (**503** in FIG. **5**) with the near-infrared spectrum for MDMA (**603** in FIG. **6**), it seems clear that the near-infrared region shows overtones and combination bands that should be discernible. Referring to FIG. **6**, sample identification may be accomplished by using the region (indicated by the arrows) where the spectral absorptions may provide specific peaks depending on the drug component.

In another embodiment, FIG. **7** shows the diffuse reflectance near-infrared spectrum **700** of heroin samples. Heroin, the 3,6-diacetyl derivative of morphine (hence diacetylmorphine) is an opiate drug synthesized from morphine,

which is usually a naturally occurring substance extracted from the seedpod of certain varieties of poppy plants. In particular, **701** is the near-infrared spectrum for an illicit street drug sample, while **702** is the spectra for a pure heroin standard. The difference between the spectra may arise at least in part from cutting agents. The inset **703** shows the molecular structure for heroin. As in the other examples, the absorption in the near-infrared range is caused by overtone and combination vibrations of O—H, C—H, N—H and C═O groups, which exhibit their fundamental molecular stretching and bending absorption in the mid-infrared range (c.f., the mid-infrared spectrum for heroin is shown **504** in FIG. **5**). These overtone and combination bands do not behave in a simple way, making the near-infrared spectra complex and harder to directly interpret. Also, although the near-infrared signatures may be weaker in magnitude, they are probably easier to detect in the near-infrared, and the sample preparation may also be much simpler in the near-infrared. Moreover, for remote sensing, the near-infrared may be preferable because of atmospheric transmission windows between approximately 1.4-1.8 microns and 2-2.5 microns.

Pure heroin may be a white powder with a bitter taste that is rarely sold on the streets, while illicit heroin may be a powder varying in color from white to dark brown due to impurities left from the manufacturing process or the presence of additives. The purity of street heroin may also vary widely, as the drug can be mixed with other white powders. The impurity of the drug may often make it difficult to gauge the strength of the dosage, which runs the risk of overdose. One nice feature of near-infrared or SWIR spectroscopy is that the technique may be used in a non-destructive, non-contact manner to determine rapidly the concentration of compounds present in complex samples at percentage levels with very little sample preparation. In a particular embodiment, FIG. **8** illustrates the diffuse reflectance near-infrared spectra **800** of different seized illicit drugs containing heroin (between 10.7 and 21.8%) compared with the spectrum of pure heroin **801**. Curve **802** is for 21.8% by weight, curve **803** is 13.2% by weight, curve **804** is 17% by weight, and curve **805** is 10.7% by weight of heroin. The spectra have been shifted along the vertical axis to better illustrate the differences.

Although quite complex in the near-infrared, it may be possible to identify from the pure heroin near-infrared spectrum (**801** in FIG. **8** or **702** in FIG. **7**) the main wavelengths related to the most common functional groups in heroin. For example, FIG. **9** lists possible band assignments **900** for the various spectral features in pure heroin. As can be seen from FIG. **9**, the absorption in the near-infrared may be mainly due to overtone and combination bands associated with O—H, C—H, N—H and C═O groups.

As can be appreciated from FIG. **8**, there may be significant differences between the spectrum of pure heroin and sample spectra. These differences may be due to the presence of different compounds used as cutting agents, which can affect the shape and intensity of the near-infrared signals. FIG. **10** illustrates the diffuse reflectance near-infrared spectra **1000** of different compounds that may be frequently employed as cutting agents. In the bottom of FIG. **10** are shown the spectra **1008** for pure heroin and the spectra **1007** for a seized illicit street drug sample comprising 21.8% of heroin. The spectra for various cutting agents include: **1001** for flour, **1002** for talcum powder, **1003** for chalk, **1004** for acetylsalicylic acid, **1005** for caffeine, and **1006** for paracetamol. Thus, near-infrared or SWIR spectroscopy may be used to work back to the composition of an unknown drug. Although particular examples of counterfeit and illicit drugs have been described, the near-infrared or SWIR spectroscopy (including diffuse reflectance, reflectance, fluorescence or transmission) may also be applied to the identification of other drugs and substances without departing from the scope of this disclosure. This spectroscopy may be used non-destructively and non-contact over stand-off distances or in remote sensing distances, whether from an airborne, vehicle, hand-held, or stationary platform.

Process Analytical Technology (PAT)

One definition of process analytical technology, PAT, is "a system for designing, analyzing and controlling manufacturing through timely evaluations (i.e., during processing) of significant quality and performance attributes of raw and in-process materials and processes, with the goal of ensuring final product quality." Near-infrared or SWIR spectroscopy may have applications in the PAT of the pharmaceutical industry by providing, for example, quantitative analysis of multiple components in a sample and in pack quantification of drugs in formulation, as well as quality of a drug and quality control of complex excipients used in formulation. The PAT process may benefit from near-infrared or SWIR spectroscopy for some steps, such as: raw material identification, active pharmaceutical ingredient applications, drying, granulation, blend uniformity and content uniformity. Some of the strengths of near-infrared or SWIR spectroscopy include: radiation has good penetration properties, and, thus, minimal sample preparation may be required; measurement results may be obtained rapidly, and simultaneous measurements may be obtained for several parameters; non-destructive methods with little or no chemical waste; and organic chemicals that comprise most pharmaceutical products have unique spectra in the near-infrared and SWIR ranges, for example.

FIG. **11** shows one example of a flow-chart **1100** in the PAT for the pharmaceutical industry. While the center shows the steps of the manufacturing process **1101**, the top and bottom sides show where near-infrared spectroscopy could be applicable for lab use **1102** (top) or in process monitoring control **1103** (bottom). Indeed, near-infrared or SWIR spectroscopy has the potential to benefit almost every step in the manufacturing process. Just to provide a few examples of using near-infrared or SWIR spectroscopy in the PAT process, the raw material testing and blending process will be examined briefly.

At the commencement of manufacture of a drug product, it may be required to identify the correct material and grade of the pharmaceutical excipients to be used in the formulation. FIG. **12** illustrates the typical near-infrared spectra **1200** for a variety of excipients. Included in the graph **1200** are spectra for: magnesium stearate **1201**, sorbitol **1202**, mannitol **1203**, talc **1204**, lactose **1205**, starch **1206**, maltodextrin **1207**, and microcrystalline cellulose **1208**. A suitable spectral database may be used to rapidly identify and qualify excipients. One nice aspect of the spectroscopy is that the near-infrared and SWIR are sensitive to both the physical and chemical characteristics of the samples.

One of the next steps in the manufacture of a dosage form is the blending together of the active component with the excipients to produce a homogeneous blend. In one embodiment, the near-infrared or SWIR spectroscopy apparatus may comprise a fiber-optic probe, which may, for example, interface with the blending vessel. For such a fiber-optic probe, near infrared or SWIR spectra may be collected in real-time from a blending process. FIG. **13** exemplifies the

absorbance **1300** from the blending process. Although the initial spectra **1301** shows differences from the eventual spectra, as the process continues the blend converges to the final spectra **1302** and continues to overlap that spectra. Similar converging or overlapping spectra may also be used to check the product uniformity at the end of the process. The near-infrared spectra may be acquired in real-time; and, using appropriate data pre-processing and chemometric analysis, blend homogeneity plots may be derived, such as **1300**.

One goal of the manufacturing process and PAT may be the concept of a "smart" manufacturing process, which may be a system or manufacturing operation responding to analytical data generated in real-time. Such a system may also have an in-built "artificial intelligence" as decisions may be made whether to continue a manufacturing operation. For example, with respect to the raw materials, integration of the quality measurement into smart manufacturing processes could be used to improve manufacturing operations by ensuring that the correct materials of the appropriate quality are used in the manufacture. Similarly, a smart blender would be under software control and would respond to the real-time spectral data collected.

FIG. **14** illustrates what might be an eventual flow-chart **1400** of a smart manufacturing process. The manufacturing process **1401** may have as input the process feed **1402** and result in a process output **1403**. A process controller **1404** may at least partially control the manufacturing process **1401**, and the controller **1404** may receive inputs from the closed loop control (process parameters) **1405** as well as the on-line monitoring of process parameters **1406**. The feedback loops in the process could refine the manufacturing process **1401** and improve the quality of the process output **1403**. These are particular embodiments of the use of near-infrared or SWIR spectroscopy in the PAT of the pharmaceutical industry, but other variations, combinations, and methods may also be used and are intended to be covered by this disclosure.

The discussion thus far has centered on use of near-infrared or SWIR spectroscopy in applications such as identification of counterfeit drugs, detection of illicit drugs, and pharmaceutical process control. Although drugs and pharmaceuticals are one example, many other fields and applications may also benefit from the use of near infrared or SWIR spectroscopy, and these may also be implemented without departing from the scope of this disclosure. As just another example, near-infrared or SWIR spectroscopy may also be used as an analytic tool for food quality and safety control. Applications in food safety and quality assessment include contaminant detection, defect identification, constituent analysis, and quality evaluation. The techniques described in this disclosure are particularly valuable when non-destructive testing is desired at stand-off or remote distances.

In one example, near-infrared or SWIR spectroscopy may be used in cereal breeding. The breeding purposes may require knowledge on both composition and functional properties of grain, while the functionality of wheat grain is an issue for wheat breeders. Most of the wheat functionality parameters depend on the protein-proteinase complex of wheat grain, as well as the condition of the carbohydrate complex. FIG. **15**A illustrates the near-infrared reflectance spectrum **1500** of wheat flour. Since these samples are complex in composition, several organic bonds involving hydrogen vibrate to produce overlapped spectral bands. Thus, the resulting spectrum **1500** appears like a wavy line without clearly defined features. Analytical methods based on this type of spectroscopy may have the potential to improve the quality of final cereal products by testing the products through the entire production process in the processing industry.

In yet another embodiment, near-infrared or SWIR spectroscopy may be used for the assessment of fruit and vegetable quality. Most commercial quality classification systems for fruit and vegetables are based on external features of the product, such as shape, color, size, weight and blemishes. However, the external appearance of most fruit is generally not an accurate guide to the internal eating quality of the fruit. As an example, for avocado fruit the external color is not a maturity characteristic, and its smell is too weak and appears later in its maturity stage. Analysis of the near-infrared or SWIR absorption spectra may provide qualitative and quantitative determination of many constituents and properties of horticulture produce, including oil, water, protein, pH, acidity, firmness, and soluble solids content or total soluble solids of fresh fruits. FIG. **15**B shows the near-infrared absorbance spectra **1550** obtained in diffusion reflectance mode for a series of whole 'Hass' avocado fruit. Four oil absorption bands are near 2200-2400 nm (CH_2 stretch bend and combinations), with weaker absorption around 750 nm, 1200 nm, and 900-930 nm ranges. On the other hand, near 1300-1750 nm range may be useful for determining the protein and oil content. The 900-920 nm absorbance band may be useful for sugar determination. Although described in the context of grains, fruits, and vegetables, the near-infrared or SWIR spectroscopy may also be valuable for other food quality control and assessment, such as measuring the properties of meats. These and other applications also fall within the scope of this disclosure.

Detection Systems

The near-infrared or SWIR spectroscopy system, remote sensing system or hyper-spectral imaging system may be on an airborne platform, mounted on a vehicle, a stationary transmission or reflection set-up, or even held by a human for a compact system. For such a system, there are fundamentally two hardware parts: the transmitter or light source and the detection system. Between the two, perhaps in a transmission or reflection setting, may be the sample being tested or measured. Moreover, the output from the detection system may go to a computational system, comprising computers or other processing equipment. The output from the computational system may be displayed graphically as well as with numerical tables and perhaps an identification of the material composition. These are just some of the parts of the systems, but other elements may be added or be eliminated, and these modified configurations are also intended to be covered by this disclosure.

By use of an active illuminator, a number of advantages may be achieved. First, stand-off or remote distances may be achieved if a non-lamp system is used—i.e., if the beam does not rapidly diffract. Also, higher signal-to-noise ratios may be achieved. For example, one way to improve the signal-to-noise ratio would be to use modulation and lock-in techniques. In one embodiment, the light source may be modulated, and then the detection system would be synchronized with the light source. In a particular embodiment, the techniques from lock-in detection may be used, where narrow band filtering around the modulation frequency may be used to reject noise outside the modulation frequency. In another embodiment, change detection schemes may be used, where the detection system captures the signal with the

light source on and with the light source off. Again, for this system the light source may be modulated. Then, the signal with and without the light source is differenced. Change detection may help to identify objects that change in the field of view. In the following some exemplary detection systems are described.

In one embodiment, a SWIR camera or infrared camera system may be used to capture the images. The camera may include one or more lenses on the input, which may be adjustable. The focal plane assemblies may be made from mercury cadmium telluride material (HgCdTe), and the detectors may also include thermo-electric coolers. Alternately, the image sensors may be made from indium gallium arsenide (InGaAs), and CMOS transistors may be connected to each pixel of the InGaAs photodiode array. The camera may interface wirelessly or with a cable (e.g., USB, Ethernet cable, or fiber optics cable) to a computer or tablet or smart phone, where the images may be captured and processed. These are a few examples of infrared cameras, but other SWIR or infrared cameras may be used and are intended to be covered by this disclosure.

In another embodiment, an imaging spectrometer may be used to detect the light received from the sample. For example, FIG. **16**A shows a schematic diagram **1600** of the basic elements of an imaging spectrometer. The input light **1601** from the sample may first be directed by a scanning minor and/or other optics **1602**. An optical dispersing element **1603**, such as a grating or prism, in the spectrometer may split the light into many narrow, adjacent wavelength bands, which may then be passed through imaging optics **1604** onto one or more detectors or detector arrays **1605**. Some sensors may use multiple detector arrays to measure hundreds of narrow wavelength bands.

An example of a typical imaging spectrometer **1650** used in hyper-spectral imaging systems is illustrated in FIG. **16**B. In this particular embodiment, the input light may be directed first by a tunable minor **1651**. A front lens **1652** may be placed before the entrance slit **1653** and the collector lens **1654**. In this embodiment, the dispersing element is a holographic grating with a prism **1655**, which separates the different wavelength bands. Then, a camera lens **1656** may be used to image the wavelengths onto a detector or camera **1657**.

FIG. **16** provide particular examples, but some of the elements may not be used, or other elements may be added, and these are also intended to be covered by this disclosure. For instance, a scanning spectrometer may be used before the detector, where a grating or dispersive element is scanned to vary the wavelength being measured by the detector. In yet another embodiment, filters may be used before one or more detectors to select the wavelengths or wavelength bands to be measured. This may be particularly useful if only a few bands or wavelengths are to be measured. The filters may be dielectric filters, Fabry-Perot filters, absorption or reflection filters, fiber gratings, or any other wavelength selective filter. In one embodiment, a wavelength division multiplexer, WDM, may be used followed by one or more detectors or detector arrays. One example of a planar wavelength division multiplexer may be a waveguide grating router or an arrayed waveguide grating. The WDM may be fiber coupled, and detectors may be placed directly at the output or the detectors may be coupled through fibers to the WDM. Some of these components may also be combined with the configurations in FIG. **16**.

While the above detection systems could be categorized as single path detection systems, it may be advantageous in some cases to use multi-path detection systems. In one embodiment, a detection system from a Fourier transform infrared spectrometer, FTIR, may be used. The received light may be incident on a particular configuration of mirrors, called a Michelson interferometer, that allows some wavelengths to pass through but blocks others due to wave interference. The beam may be modified for each new data point by moving one of the minors, which changes the set of wavelengths that pass through. This collected data is called an interferogram. The interferogram is then processed, typically on a computing system, using an algorithm called the Fourier transform. One advantageous feature of FTIR is that it may simultaneously collect spectral data in a wide spectral range.

FIG. **17** illustrates one example of the FTIR spectrometer **1700**. Light from the near-infrared or SWIR light source **1701** may be collimated and directed to a beam splitter **1702**. In one embodiment, the beam splitter **1702** may be a 50:50 beam splitter. One portion of the beam **1703** may be reflected toward a stationary mirror **1704**, while the other portion of the beam **1705** may be transmitted towards a moving mirror **1706**. Light may be reflected from the two minors **1704**, **1706** back to the beam splitter **1702**, and then a portion of the recombined beam **1707** may be directed toward the sample **1708**. The recombined beam **1707** may be focused onto the sample **1708**, in one embodiment. On leaving the sample **1708**, the light may be refocused or at least collected at a detector **1709**. A background interferogram may be obtained by using the set-up **1700** without a sample in the chamber **1708**. When a sample is inserted into **1708**, the background interferogram may be modulated by the presence of absorption bands in the sample. The FTIR spectrometer may have several advantages compared to a scanning (dispersive) spectrometer. Since all the wavelengths may be collected simultaneously, the FTIR may result in a higher signal-to-noise ratio for a given scan time or a shorter scan time for a given resolution. Moreover, unlike a spectrometer where a slit may limit the amount of the beam detected, the FTIR may accommodate the entire diameter of the beam coming from the light source **1701**. The configuration **1700** is one example of an FTIR, but other configurations may also be used, and these are also intended to be covered by this disclosure.

In yet another example of multi-beam detection systems, a dual-beam set-up **1800** such as in FIG. **18** may be used to subtract out (or at least minimize the adverse effects of) light source fluctuations. In one embodiment, the output from an SC source **1801** may be collimated using a CaF_2 lens **1802** and then focused into the entrance slit of the monochromator **1803**. At the exit slit, light at the selected wavelength is collimated again and may be passed through a polarizer **1804** before being incident on a calcium fluoride beam splitter **1805**. After passing through the beam splitter **1805**, the light is split into a sample **1806** and reference **1807** arm to enable ratiometric detection that may cancel out effects of intensity fluctuations in the SC source **1801**. The light in the sample arm **1806** passes through the sample of interest and is then focused onto a HgCdTe detector **1808** connected to a pre-amp. A chopper **1802** and lock-in amplifier **1810** setup enable low noise detection of the sample arm signal. The light in the reference arm **1807** passes through an empty container (cuvette, gas cell etc.) of the same kind as used in the sample arm. A substantially identical detector **1809**, pre-amp and lock-in amplifier **1810** is used for detection of the reference arm signal. The signal may then be analyzed using a computer system **1811**. This is one particular example of a method to remove fluctuations from the light source, but other components may be added and other

configurations may be used, and these are also intended to be covered by this disclosure.

Although particular examples of detection systems have been described, combinations of these systems or other systems may also be used, and these are also within the scope of this disclosure. As one example, environmental fluctuations (such as turbulence or winds) may lead to fluctuations in the beam for active remote sensing or hyperspectral imaging. A configuration such as FIG. **18** may be able to remove the effect of environmental fluctuations. Yet another technique may be to "wobble" the light beam after the light source using a vibrating mirror. The motion may lead to the beam moving enough to wash out spatial fluctuations within the beam waist at the sample or detection system. If the vibrating mirror is scanned faster than the integration time of the detectors, then the spatial fluctuations in the beam may be integrated out. Alternately, some sort of synchronous detection system may be used, where the detection is synchronized to the vibrating frequency.

Light Sources for SWIR and Near Infrared

There are a number of light sources that may be used in the near infrared. To be more specific, the discussion below will consider light sources operating in the short wave infrared (SWIR), which may cover the wavelength range of approximately 1400 nm to 2500 nm. Other wavelength ranges may also be used for the applications described in this disclosure, so the discussion below is merely provided for exemplary types of light sources. The SWIR wavelength range may be valuable for a number of reasons. The SWIR corresponds to a transmission window through water and the atmosphere. Also, the so-called "eye-safe" wavelengths are wavelengths longer than approximately 1400 nm as previously described.

Different light sources may be selected for the SWIR based on the needs of the application. Some of the features for selecting a particular light source include power or intensity, wavelength range or bandwidth, spatial or temporal coherence, spatial beam quality for focusing or transmission over long distance, and pulse width or pulse repetition rate. Depending on the application, lamps, light emitting diodes (LEDs), laser diodes (LD's), tunable LD's, super-luminescent laser diodes (SLDs), fiber lasers or supercontinuum sources (SC) may be advantageously used. Also, different fibers may be used for transporting the light, such as fused silica fibers, plastic fibers, mid-infrared fibers (e.g., tellurite, chalcogenides, fluorides, ZBLAN, etc), or a hybrid of these fibers.

Lamps may be used if low power or intensity of light is required in the SWIR, and if an incoherent beam is suitable. In one embodiment, in the SWIR an incandescent lamp that can be used is based on tungsten and halogen, which have an emission wavelength between approximately 500 nm to 2500 nm. For low intensity applications, it may also be possible to use thermal sources, where the SWIR radiation is based on the black body radiation from the hot object. Although the thermal and lamp based sources are broadband and have low intensity fluctuations, it may be difficult to achieve a high signal-to-noise ratio due to the low power levels. Also, the lamp based sources tend to be energy inefficient.

In another embodiment, LED's can be used that have a higher power level in the SWIR wavelength range. LED's also produce an incoherent beam, but the power level can be higher than a lamp and with higher energy efficiency. Also, the LED output may more easily be modulated, and the LED provides the option of continuous wave or pulsed mode of operation. LED's are solid state components that emit a wavelength band that is of moderate width, typically between about 20 nm to 40 nm. There are also so-called super-luminescent LEDs that may even emit over a much wider wavelength range. In another embodiment, a wide band light source may be constructed by combining different LEDs that emit in different wavelength bands, some of which could preferably overlap in spectrum. One advantage of LEDs as well as other solid state components is the compact size that they may be packaged into.

In yet another embodiment, various types of laser diodes may be used in the SWIR wavelength range. Just as LEDs may be higher in power but narrower in wavelength emission than lamps and thermal sources, the LDs may be yet higher in power but yet narrower in wavelength emission than LEDs. Different kinds of LDs may be used, including Fabry-Perot LDs, distributed feedback (DFB (LDs, distributed Bragg reflector (DBR) LDs. Since the LDs have relatively narrow wavelength range (typically under 10 nm), in one embodiment a plurality of LDs may be used that are at different wavelengths in the SWIR. The various LDs may be spatially multiplexed, polarization multiplexed, wavelength multiplexed, or a combination of these multiplexing methods. Also, the LDs may be fiber pig-tailed or have one or more lenses on the output to collimate or focus the light. Another advantage of LDs is that they may be packaged compactly and may have a spatially coherent beam output. Moreover, tunable LDs that can tune over a range of wavelengths are also available. The tuning may be done by varying the temperature, or electrical current may be used in particular structures such as distributed Bragg reflector LDs. In another embodiment, external cavity LDs may be used that have a tuning element, such as a fiber grating or a bulk grating, in the external cavity.

In another embodiment, super-luminescent laser diodes may provide higher power as well as broad bandwidth. An SLD is typically an edge emitting semiconductor light source based on super-luminescence (e.g., this could be amplified spontaneous emission). SLDs combine the higher power and brightness of LDs with the low coherence of conventional LEDs, and the emission band for SLD's may be 5 nm to 100 nm wide, preferably in the 60 nm to 100 nm range. Although currently SLDs are commercially available in the wavelength range of approximately 400 nm to 1700 nm, SLDs could and may in the future be made that cover a broader region of the SWIR.

In yet another embodiment, high power LDs for either direct excitation or to pump fiber lasers and SC light sources may be constructed using one or more laser diode bar stacks. FIG. **19** shows an example block diagram **1900** with building blocks for constructing the high power LDs. In this embodiment, one or more diode bar stacks **1901** may be used, where the diode bar stack may be an array of several single emitter LDs. Since the fast axis (e.g., vertical direction) may be nearly diffraction limited while the slow-axis (e.g., horizontal axis) may be far from diffraction limited, different collimators **1902** may be used for the two axes.

The brightness may be increased by spatially combining the beams from multiple stacks **1903**. The combiner may include spatial interleaving, wavelength multiplexing, or a combination of the two. Different spatial interleaving schemes may be used, such as using an array of prisms or mirrors with spacers to bend one array of beams into the beam path of the other. In another embodiment, segmented mirrors with alternate high-reflection and anti-reflection coatings may be used. Moreover, the brightness may be

increased by polarization beam combining **1904** the two orthogonal polarizations, such as by using a polarization beam splitter. In a particular embodiment, the output may then be focused or coupled into a large diameter core fiber. As an example, typical dimensions for the large diameter core fiber range from diameters of approximately 100 microns to 400 microns or more. Alternatively or in addition, a custom beam shaping module **1905** may be used, depending on the particular application. For example, the output of the high power LD may be used directly **1906**, or it may be fiber coupled **1907** to combine, integrate, or transport the high power LD energy. These high power LDs may grow in importance because the LD powers can rapidly scale up. For example, instead of the power being limited by the power available from a single emitter, the power may increase in multiples depending on the number of diodes multiplexed and the size of the large diameter fiber. Although FIG. **19** is shown as one embodiment, some or all of the elements may be used in a high power LD, or additional elements may also be used.

SWIR Super-Continuum Lasers

Each of the light sources described above have particular strengths, but they also may have limitations. For example, there is typically a trade-off between wavelength range and power output. Also, sources such as lamps, thermal sources, and LEDs produce incoherent beams that may be difficult to focus to a small area and may have difficulty propagating for long distances. An alternative source that may overcome some of these limitations is an SC light source. Some of the advantages of the SC source may include high power and intensity, wide bandwidth, spatially coherent beam that can propagate nearly transform limited over long distances, and easy compatibility with fiber delivery.

Supercontinuum lasers may combine the broadband attributes of lamps with the spatial coherence and high brightness of lasers. By exploiting a modulational instability initiated supercontinuum (SC) mechanism, an all-fiber-integrated SC laser with no moving parts may be built using commercial-off-the-shelf (COTS) components. Moreover, the fiber laser architecture may be a platform where SC in the visible, near-infrared/SWIR, or mid-IR can be generated by appropriate selection of the amplifier technology and the SC generation fiber. But until recently, SC lasers were used primarily in laboratory settings since typically large, table-top, mode-locked lasers were used to pump nonlinear media such as optical fibers to generate SC light. However, those large pump lasers may now be replaced with diode lasers and fiber amplifiers that gained maturity in the telecommunications industry.

In one embodiment, an all-fiber-integrated, high-powered SC light source **2000** may be elegant for its simplicity (FIG. **20**). The light may be first generated from a seed laser diode **2001**. For example, the seed LD **2001** may be a distributed feedback (DFB) laser diode with a wavelength near 1542 nm or 1550 nm, with approximately 0.5-2.0 ns pulsed output, and with a pulse repetition rate between one kilohertz to about 100 MHz or more. The output from the seed laser diode may then be amplified in a multiple-stage fiber amplifier **2002** comprising one or more gain fiber segments. In a particular embodiment, the first stage pre-amplifier **2003** may be designed for optimal noise performance. For example, the pre-amplifier **2003** may be a standard erbium-doped fiber amplifier or an erbium/ytterbium doped cladding pumped fiber amplifier. Between amplifier stages **2003** and **2006**, it may be advantageous to use band-pass filters **2004** to block amplified spontaneous emission and isolators **2005** to prevent spurious reflections. Then, the power amplifier stage **2006** may use a cladding-pumped fiber amplifier that may be optimized to minimize nonlinear distortion. The power amplifier fiber **2006** may also be an erbium-doped fiber amplifier, if only low or moderate power levels are to be generated.

The SC generation **2007** may occur in the relatively short lengths of fiber that follow the pump laser. Exemplary SC fiber lengths may range from a few millimeters to 100 m or more. In one embodiment, the SC generation may occur in a first fiber **2008** where the modulational-instability initiated pulse break-up occurs primarily, followed by a second fiber **2009** where the SC generation and spectral broadening occurs primarily.

In one embodiment, one or two meters of standard single-mode fiber (SMF) after the power amplifier stage may be followed by several meters of SC generation fiber. For this example, in the SMF the peak power may be several kilowatts and the pump light may fall in the anomalous group-velocity dispersion regime—often called the soliton regime. For high peak powers in the anomalous dispersion regime, the nanosecond pulses may be unstable due to a phenomenon known as modulational instability, which is basically parametric amplification in which the fiber nonlinearity helps to phase match the pulses. As a consequence, the nanosecond pump pulses may be broken into many shorter pulses as the modulational instability tries to form soliton pulses from the quasi-continuous-wave background. Although the laser diode and amplification process starts with approximately nanosecond-long pulses, modulational instability in the short length of SMF fiber may form approximately 0.5 ps to several-picosecond-long pulses with high intensity. Thus, the few meters of SMF fiber may result in an output similar to that produced by mode-locked lasers, except in a much simpler and cost-effective manner.

The short pulses created through modulational instability may then be coupled into a nonlinear fiber for SC generation. The nonlinear mechanisms leading to broadband SC may include four-wave mixing or self-phase modulation along with the optical Raman effect. Since the Raman effect is self-phase-matched and shifts light to longer wavelengths by emission of optical photons, the SC may spread to longer wavelengths very efficiently. The short-wavelength edge may arise from four-wave mixing, and often times the short wavelength edge may be limited by increasing group-velocity dispersion in the fiber. In many instances, if the particular fiber used has sufficient peak power and SC fiber length, the SC generation process may fill the long-wavelength edge up to the transmission window.

Mature fiber amplifiers for the power amplifier stage **2006** include ytterbium-doped fibers (near 1060 nm), erbium-doped fibers (near 1550 nm), erbium/ytterbium-doped fibers (near 1550 nm), or thulium-doped fibers (near 2000 nm). In various embodiments, candidates for SC fiber **2009** include fused silica fibers (for generating SC between 0.8-2.7 μm), mid-IR fibers such as fluorides, chalcogenides, or tellurites (for generating SC out to 4.5 μm or longer), photonic crystal fibers (for generating SC between 0.4-1.7 μm), or combinations of these fibers. Therefore, by selecting the appropriate fiber-amplifier doping for **2006** and nonlinear fiber **2009**, SC may be generated in the visible, near-IR/SWIR, or mid-IR wavelength region.

The configuration **2000** of FIG. **20** is just one particular example, and other configurations can be used and are intended to be covered by this disclosure. For example, further gain stages may be used, and different types of lossy

elements or fiber taps may be used between the amplifier stages. In another embodiment, the SC generation may occur partially in the amplifier fiber and in the pig-tails from the pump combiner or other elements. In yet another embodiment, polarization maintaining fibers may be used, and a polarizer may also be used to enhance the polarization contrast between amplifier stages. Also, not discussed in detail are many accessories that may accompany this set-up, such as driver electronics, pump laser diodes, safety shut-offs, and thermal management and packaging.

In one embodiment, one example of the SC laser that operates in the SWIR is illustrated in FIG. **21**. This SWIR SC source **2100** produces an output of up to approximately 5 W over a spectral range of about 1.5-2.4 microns, and this particular laser is made out of polarization maintaining components. The seed laser **2101** is a distributed feedback (DFB) laser operating near 1542 nm producing approximately 0.5 nsec pulses at an about 8 MHz repetition rate. The pre-amplifier **2102** is forward pumped and uses about 2 m length of erbium/ytterbium cladding pumped fiber **2103** (often also called dual-core fiber) with an inner core diameter of 12 microns and outer core diameter of 130 microns. The pre-amplifier gain fiber **2103** is pumped using a 10 W laser diode near 940 nm **2105** that is coupled in using a fiber combiner **2104**.

In this particular 5 W unit, the mid-stage between amplifier stages **2102** and **2106** comprises an isolator **2107**, a band-pass filter **2108**, a polarizer **2109** and a fiber tap **2110**. The power amplifier **2106** uses an approximately 4 m length of the 12/130 micron erbium/ytterbium doped fiber **2111** that is counter-propagating pumped using one or more 30 W laser diodes near 940 nm **2112** coupled in through a combiner **2113**. An approximately 1-2 m length of the combiner pig-tail helps to initiate the SC process, and then a length of PM-1550 fiber **2115** (polarization maintaining, single-mode, fused silica fiber optimized for 1550 nm) is spliced **2114** to the combiner output.

If an output fiber of about 10 m in length is used, then the resulting output spectrum **2200** is shown in FIG. **22**. The details of the output spectrum **2200** depend on the peak power into the fiber, the fiber length, and properties of the fiber such as length and core size, as well as the zero dispersion wavelength and the dispersion properties. For example, if a shorter length of fiber is used, then the spectrum actually reaches to longer wavelengths (e.g., a 2 m length of SC fiber broadens the spectrum to about 2500 nm). Also, if extra-dry fibers are used with less O—H content, then the wavelength edge may also reach to a longer wavelength. To generate more spectrum toward the shorter wavelengths, the pump wavelength (in this case around 1542 nm) should be close to the zero dispersion wavelength in the fiber. For example, by using a dispersion shifted fiber or so-called non-zero dispersion shifted fiber, the short wavelength edge may shift to shorter wavelengths.

Although one particular example of a 5 W SWIR-SC has been described, different components, different fibers, and different configurations may also be used consistent with this disclosure. For instance, another embodiment of the similar configuration **2100** in FIG. **21** may be used to generate high powered SC between approximately 1060 nm and 1800 nm. For this embodiment, the seed laser **2101** may be a distributed feedback laser diode around 1064 nm, the pre-amplifier gain fiber **2103** may be a ytterbium-doped fiber amplifier with 10/125 microns dimensions, and the pump laser **2105** may be a 10 W laser diode near 915 nm. A mode field adapter may be included in the mid-stage, in addition to the isolator **2107**, band pass filter **2108**, polarizer **2109** and tap **2110**. The gain fiber **2111** in the power amplifier may be an about 20 m length of ytterbium-doped fiber with 25/400 microns dimension. The pump **2112** for the power amplifier may be up to six pump diodes providing 30 W each near 915 nm. For this much pump power, the output power in the SC may be as high as 50 W or more.

In one embodiment, it may be desirous to generate high power SWIR SC over 1.4-1.8 microns and separately 2-2.5 microns (the window between 1.8 and 2 microns may be less important due to the strong water and atmospheric absorption). For example, the top SC source of FIG. **23** can lead to bandwidths ranging from about 1400 nm to 1800 nm or broader, while the lower SC source of FIG. **23** can lead to bandwidths ranging from about 1900 nm to 2500 nm or broader. Since these wavelength ranges are shorter than about 2500 nm, the SC fiber can be based on fused silica fiber. Exemplary SC fibers include standard single-mode fiber SMF, high-nonlinearity fiber, high-NA fiber, dispersion shifted fiber, dispersion compensating fiber, and photonic crystal fibers. Non-fused-silica fibers can also be used for SC generation, including chalcogenides, fluorides, ZBLAN, tellurites, and germanium oxide fibers.

In one embodiment, the top of FIG. **23** illustrates an exemplary block diagram for an SC source **2300** capable of generating light between approximately 1400 nm and 1800 nm or broader. As an example, a pump fiber laser similar to FIG. **21** can be used as the input to a SC fiber **2309**. The seed laser diode **2301** can comprise a DFB laser that generates, for example, several milliwatts of power around 1542 nm or 1553 nm. The fiber pre-amplifier **2302** can comprise an erbium-doped fiber amplifier or an erbium/ytterbium doped double clad fiber. In this example a mid-stage amplifier **2303** can be used, which can comprise an erbium/ytterbium doped double-clad fiber. A bandpass filter **2305** and isolator **2306** may be used between the pre-amplifier **2302** and mid-stage amplifier **2303**. The power amplifier stage **2304** can comprise a larger core size erbium/ytterbium doped double-clad fiber, and another bandpass filter **2307** and isolator **2308** can be used before the power amplifier **2304**. The output of the power amplifier can be coupled to the SC fiber **2309** to generate the SC output **2310**. This is just one exemplary configuration for an SC source, and other configurations or elements may be used consistent with this disclosure.

In yet another embodiment, the bottom of FIG. **23** illustrates a block diagram for an exemplary SC source **2350** capable of generating light between approximately 1900 nm and 2500 nm or broader. As an example, the seed laser diode **2351** can comprise a DFB or DBR laser that generates, for example, several milliwatts of power around 1542 nm or 1553 nm. The fiber pre-amplifier **2352** can comprise an erbium-doped fiber amplifier or an erbium/ytterbium doped double-clad fiber. In this example a mid-stage amplifier **2353** can be used, which can comprise an erbium/ytterbium doped double-clad fiber. A bandpass filter **2355** and isolator **2356** may be used between the pre-amplifier **2352** and mid-stage amplifier **2353**. The power amplifier stage **2354** can comprise a thulium doped double-clad fiber, and another isolator **2357** can be used before the power amplifier **2354**. Note that the output of the mid-stage amplifier **2353** can be approximately near 1542 nm, while the thulium-doped fiber amplifier **2354** can amplify wavelengths longer than approximately 1900 nm and out to about 2100 nm. Therefore, for this configuration wavelength shifting may be required between **2353** and **2354**. In one embodiment, the wavelength shifting can be accomplished using a length of standard single-mode fiber **2358**, which can have a length between approximately 5 m and 50 m, for example. The

output of the power amplifier **2354** can be coupled to the SC fiber **2359** to generate the SC output **2360**. This is just one exemplary configuration for an SC source, and other configurations or elements can be used consistent with this disclosure. For example, the various amplifier stages can comprise different amplifier types, such as erbium doped fibers, ytterbium doped fibers, erbium/ytterbium co-doped fibers and thulium doped fibers. One advantage of the SC lasers illustrated in FIGS. **20**, **21**, and **23** are that they may use all-fiber components, so that the SC laser can be all-fiber, monolithically integrated with no moving parts. The all-integrated configuration can consequently be robust and reliable.

FIGS. **20**, **21** and **23** are examples of SC light sources that may advantageously be used for near-infrared or SWIR light generation in various spectroscopy, active remote sensing and hyper-spectral imaging applications. However, many other versions of the SC light sources may also be made that are intended to also be covered by this disclosure. For example, the SC generation fiber could be pumped by a mode-locked laser, a gain-switched semiconductor laser, an optically pumped semiconductor laser, a solid state laser, other fiber lasers, or a combination of these types of lasers. Also, rather than using a fiber for SC generation, either a liquid or a gas cell might be used as the nonlinear medium in which the spectrum is to be broadened.

Even within the all-fiber versions illustrated such as in FIG. **21**, different configurations could be used consistent with the disclosure. In one embodiment, it may be desirous to have a lower cost version of the SWIR SC laser of FIG. **21**. One way to lower the cost could be to use a single stage of optical amplification, rather than two stages, which may be feasible if lower output power is required or the gain fiber is optimized. For example, the pre-amplifier stage **2102** might be removed, along with at least some of the mid-stage elements. In yet another embodiment, the gain fiber could be double passed to emulate a two stage amplifier. In this example, the pre-amplifier stage **2102** might be removed, and perhaps also some of the mid-stage elements. A mirror or fiber grating reflector could be placed after the power amplifier stage **2106** that may preferentially reflect light near the wavelength of the seed laser **2101**. If the mirror or fiber grating reflector can transmit the pump light near 940 nm, then this could also be used instead of the pump combiner **2113** to bring in the pump light **2112**. The SC fiber **2115** could be placed between the seed laser **2101** and the power amplifier stage **2106** (SC is only generated after the second pass through the amplifier, since the power level may be sufficiently high at that time). In addition, an output coupler may be placed between the seed laser diode **2101** and the SC fiber, which now may be in front of the power amplifier **2106**. In a particular embodiment, the output coupler could be a power coupler or divider, a dichroic coupler (e.g., passing seed laser wavelength but outputting the SC wavelengths), or a wavelength division multiplexer coupler. This is just one further example, but a myriad of other combinations of components and architectures could also be used for SC light sources to generate near-infrared or SWIR light that are intended to be covered by this disclosure.

Described herein are just some examples of the beneficial use of near-infrared or SWIR lasers for spectroscopy, active remote sensing or hyper-spectral imaging. However, many other spectroscopy and identification procedures can use the near-infrared or SWIR light consistent with this disclosure and are intended to be covered by the disclosure. As one example, the fiber-based super-continuum lasers may have a pulsed output with pulse durations of approximately 0.5-2 nsec and pulse repetition rates of several Megahertz. Therefore, the near-infrared or SWIR spectroscopy, active remote sensing or hyper-spectral imaging applications may also be combined with LIDAR-type applications. Namely, the distance or time axis can be added to the information based on time-of-flight measurements. For this type of information to be used, the detection system would also have to be time-gated to be able to measure the time difference between the pulses sent and the pulses received. By calculating the round-trip time for the signal, the distance of the object may be judged. In another embodiment, GPS (global positioning system) information may be added, so the near-infrared or SWIR spectroscopy, active remote sensing or hyper-spectral imagery would also have a location tag on the data. Moreover, the near-infrared or SWIR spectroscopy, active remote sensing or hyper-spectral imaging information could also be combined with two-dimensional or three-dimensional images to provide a physical picture as well as a chemical composition identification of the materials. These are just some modifications of the near-infrared or SWIR spectroscopy, active remote sensing or hyper-spectral imaging system described in this disclosure, but other techniques may also be added or combinations of these techniques may be added, and these are also intended to be covered by this disclosure.

Wireless Link to the Cloud

The non-invasive blood constituent or analytes measurement device may also benefit from communicating the data output to the "cloud" (e.g., data servers and processors in the web remotely connected) via wired and/or wireless communication strategies. The non-invasive devices may be part of a series of biosensors applied to the patient, and collectively these devices form what might be called a body area network or a personal area network. The biosensors and non-invasive devices may communicate to a smart phone, tablet, personal data assistant, computer, and/or other microprocessor-based device, which may in turn wirelessly or over wire and/or fiber optically transmit some or all of the signal or processed data to the internet or cloud. The cloud or internet may in turn send the data to doctors or health care providers as well as the patients themselves. Thus, it may be possible to have a panoramic, high-definition, relatively comprehensive view of a patient that doctors can use to assess and manage disease, and that patients can use to help maintain their health and direct their own care.

In a particular embodiment **2400** illustrated in FIG. **24**, the physiological measurement device or non-invasive blood constituent measurement device **2401** may comprise a transmitter **2403** to communicate over a first communication link **2404** in the body area network or personal area network to a receiver in a smart phone, tablet cell phone, PDA, or computer **2405**. For the measurement device **2401**, it may also be advantageous to have a processor **2402** to process some of the physiological data, since with processing the amount of data to transmit may be less (hence, more energy efficient). The first communication link **2404** may operate through the use of one of many wireless technologies such as BLUETOOTH, ZIGBEE, WI-FI, IRDA (infrared data association), wireless USB, or Z-WAVE, to name a few. Alternatively, the communication link **2404** may occur in the wireless medical band between 2360 and 2390 MHz, which the FCC allocated for medical body area network devices, or in other designated medical device or WMTS bands. These are examples of devices that can be used in the body area

network and surroundings, but other devices could also be used and are included in the scope of this disclosure.

The personal device **2405** may store, process, display, and transmit some of the data from the measurement device **2401**. The device **2405** may comprise a receiver, transmitter, display, voice control and speakers, and one or more control buttons or knobs and a touch screen. Examples of the device **2405** include smart phones such as the Apple IPHONE or phones operating on the ANDROID or Microsoft systems. In one embodiment, the device **2405** may have an application, software program, or firmware to receive and process the data from the measurement device **2401**. The device **2405** may then transmit some or all of the data or the processed data over a second communication link **2406** to the internet or "cloud" **2407**. The second communication link **2406** may advantageously comprise at least one segment of a wireless transmission link, which may operate using WI-FI or the cellular network. The second communication link **2406** may additionally comprise lengths of fiber optic and/or communication over copper wires or cables.

The internet or cloud **2407** may add value to the measurement device **2401** by providing services that augment the physiological data collected. In a particular embodiment, some of the functions performed by the cloud include: (a) receive at least a fraction of the data from the device **2405**; (b) buffer or store the data received; (c) process the data using software stored on the cloud; (d) store the resulting processed data; and (e) transmit some or all of the data either upon request or based on an alarm. As an example, the data or processed data may be transmitted **2408** back to the originator (e.g., patient or user), it may be transmitted **2409** to a health care provider or doctor, or it may be transmitted **2410** to other designated recipients.

The cloud **2407** may provide a number of value-add services. For example, the cloud application may store and process the physiological data for future reference or during a visit with the healthcare provider. If a patient has some sort of medical mishap or emergency, the physician can obtain the history of the physiological parameters over a specified period of time. In another embodiment, if the physiological parameters fall out of acceptable range, alarms may be delivered to the user **2408**, the healthcare provider **2409**, or other designated recipients **2410**. These are just some of the features that may be offered, but many others may be possible and are intended to be covered by this disclosure. As an example, the device **2405** may also have a GPS sensor, so the cloud **2407** may be able to provide time, data and position along with the physiological parameters. Thus, if there is a medical emergency, the cloud **2407** could provide the location of the patient to the healthcare provider **2409** or other designated recipients **2410**. Moreover, the digitized data in the cloud **2407** may help to move toward what is often called "personalized medicine." Based on the physiological parameter data history, medication or medical therapies may be prescribed that are customized to the particular patient.

Beyond the above benefits, the cloud application **2407** and application on the device **2405** may also have financial value for companies developing measurement devices **2401** such as a non-invasive blood constituent monitor. In the case of glucose monitors, the companies make the majority of their revenue on the measurement strips. However, with a non-invasive monitor, there is no need for strips, so there is less of an opportunity for recurring costs (e.g., the razor/razor blade model does not work for non-invasive devices). On the other hand, people may be willing to pay a periodic fee for the value-add services provided on the cloud **2407**. Diabetic patients, for example, would probably be willing to pay a periodic fee for monitoring their glucose levels, storing the history of the glucose levels, and having alarm warnings when the glucose level falls out of range. Similarly, patients taking ketone bodies supplement for treatment of disorders characterized by impaired glucose metabolism (e.g., Alzheimer's, Parkinson's, Huntington's or ALS) may need to monitor their ketone bodies level. These patients would also probably be willing to pay a periodic fee for the value-add services provided on the cloud **2407**. Thus, by leveraging the advances in wireless connectivity and the widespread use of handheld devices such as smart phones that can wirelessly connect to the cloud, businesses can build a recurring cost business model even using non-invasive measurement devices.

Described herein are just some examples of the beneficial use of near-infrared or SWIR lasers for non-invasive monitoring of glucose, ketones, HbA1c and other blood constituents. However, many other medical procedures can use the near-infrared or SWIR light consistent with this disclosure and are intended to be covered by the disclosure.

Although the present disclosure has been described in several embodiments, a myriad of changes, variations, alterations, transformations, and modifications may be suggested to one skilled in the art, and it is intended that the present disclosure encompass such changes, variations, alterations, transformations, and modifications as falling within the spirit and scope of the appended claims.

While exemplary embodiments are described above, it is not intended that these embodiments describe all possible forms of the disclosure. Rather, the words used in the specification are words of description rather than limitation, and it is understood that various changes may be made without departing from the spirit and scope of the disclosure. Additionally, the features of various implementing embodiments may be combined to form further embodiments of the disclosure. While various embodiments may have been described as providing advantages or being preferred over other embodiments with respect to one or more desired characteristics, as one skilled in the art is aware, one or more characteristics may be compromised to achieve desired system attributes, which depend on the specific application and implementation. These attributes include, but are not limited to: cost, strength, durability, life cycle cost, marketability, appearance, packaging, size, serviceability, weight, manufacturability, ease of assembly, etc. The embodiments described herein that are described as less desirable than other embodiments or prior art implementations with respect to one or more characteristics are not outside the scope of the disclosure and may be desirable for particular applications.

What is claimed is:

1. A measurement system comprising:

a light source configured to generate an output optical beam, comprising:

one or more semiconductor sources configured to generate an input beam;

one or more optical amplifiers configured to receive at least a portion of the input beam and to output an intermediate beam from at least one of the one or more optical amplifiers; and

one or more optical fibers configured to receive at least a portion of the intermediate beam and to communicate at least part of the portion of the intermediate beam to a distal end of the one or more optical fibers to form a first optical beam;

a nonlinear element configured to receive at least a portion of the first optical beam and to broaden a

spectrum associated with the at least a portion of the first optical beam to at least 10 nm through a non-linear effect in the nonlinear element to form the output optical beam with an output beam broadened spectrum; and

wherein at least a portion of the output beam broadened spectrum comprises a near-infrared wavelength between approximately 700 nm and approximately 2500 nm, and wherein at least a portion of the one or more fibers is a fused silica fiber with a core diameter less than approximately 400 microns;

a measurement apparatus configured to receive a received portion of the output optical beam and to deliver to a sample an analysis output beam, which is a delivered portion of the output optical beam and wherein the delivered portion of the output optical beam is a spatially coherent beam;

a receiver configured to receive and process at least a portion of the analysis output beam reflected or transmitted from the sample having a bandwidth of at least 10 nanometers and to generate an output signal; and

a personal device comprising a wireless receiver, a wireless transmitter, a display, a microphone, a speaker, one or more buttons or knobs, a microprocessor and a touch screen, the personal device configured to receive and process at least a portion of the output signal, wherein the personal device is configured to store and display the processed output signal, and wherein at least a portion of the processed output signal is configured to be transmitted over a wireless transmission link.

2. The system of claim **1**, wherein the personal device is selected from the group consisting of a smart phone, a tablet, a personal data assistant, a computer, and a microprocessor-based device.

3. The system of claim **1**, wherein the output signal comprises one or more physiological parameters.

4. The system of claim **1**, further comprising a remote device configured to receive over the wireless transmission link a received output status comprising the at least a portion of the processed output signal, to buffer the received output status, to process the received output status to generate processed data and to store the processed data.

5. A measurement system comprising:

a light source comprising a plurality of semiconductor sources that are light emitting diodes, the light emitting diodes configured to generate an output optical beam with one or more optical wavelengths, wherein at least a portion of the one or more optical wavelengths is a near-infrared wavelength between 700 nanometers and 2500 nanometers,

the light source configured to increase signal-to-noise ratio by increasing a light intensity from at least one of the plurality of semiconductor sources and by increasing a pulse rate of at least one of the plurality of semiconductor sources;

an apparatus comprising a plurality of lenses configured to receive a portion of the output optical beam and to deliver an analysis output beam to a sample

a receiver configured to receive and process at least a portion of the analysis output beam reflected or transmitted from the sample and to generate an output signal, wherein the receiver is configured to be synchronized to the light source;

a personal device comprising a wireless receiver, a wireless transmitter, a display, a microphone, a speaker, one or more buttons or knobs, a microprocessor and a touch screen, the personal device configured to receive and process at least a portion of the output signal, wherein the personal device is configured to store and display the processed output signal, and wherein at least a portion of the processed output signal is configured to be transmitted over a wireless transmission link; and

a remote device configured to receive over the wireless transmission link an output status comprising the at least a portion of the processed output signal, to process the received output status to generate processed data and to store the processed data.

6. The system of claim **5**, wherein at least one of the light emitting diodes emits light with a bandwidth between 20 nanometers to 40 nanometers.

7. The system of claim **5**, wherein the remote device is further configured to transmit at least a portion of the processed data to one or more other locations, wherein the one or more other locations is selected from the group consisting of the personal device, a doctor, a healthcare provider, a cloud-based server and one or more designated recipients, and wherein the remote device is capable of transmitting information related to a time and a position associated with the at least a portion of the processed data.

8. The system of claim **5**, wherein the receiver is located a first distance from a first one of the plurality of light emitting diodes and a different, second distance from a second one of the plurality of light emitting diodes such that the receiver receives a first signal from the first light emitting diode and a second signal from the second light emitting diode.

9. The system of claim**89**, wherein the output signal is generated in part by comparing the first and second signals.

10. The system of claim **5**, wherein the output signal comprises one or more physiological parameters, and the remote device is capable of storing a history of at least a portion of the one or more physiological parameters over a specified period of time.

11. The system of claim **5**, wherein the receiver further comprises one or more filters in front of one of more detectors to select a fraction of the one or more optical wavelengths.

12. The system of claim **5**, wherein the output optical beam comprises a plurality of optical wavelengths, and the output signal is generated in part by comparing signals at different optical wavelengths.

13. A measurement system comprising:

a wearable measurement device for measuring one or more physiological parameters, including a light source comprising a plurality of semiconductor sources that are light emitting diodes, the light emitting diodes configured to generate an output optical beam with one or more optical wavelengths, wherein at least a portion of the one or more optical wavelengths is a near-infrared wavelength between 700 nanometers and 2500 nanometers,

the light source configured to increase signal-to-noise ratio by increasing a light intensity from at least one of the plurality of semiconductor sources and by increasing a pulse rate of at least one of the plurality of semiconductor sources; the wearable measurement device comprising a plurality of lenses configured to receive a portion of the output optical beam and to deliver an analysis output beam to a sample;

the wearable measurement device further comprising a receiver configured to receive and process at least a portion of the analysis output beam reflected or transmitted from the sample and to generate an output

signal, wherein the wearable measurement device receiver is configured to be synchronized to pulses of the light source;

a personal device comprising a wireless receiver, a wireless transmitter, a display, a microphone, a speaker, one or more buttons or knobs, a microprocessor and a touch screen, the personal device configured to receive and process at least a portion of the output signal, wherein the personal device is configured to store and display the processed output signal, and wherein at least a portion of the processed output signal is configured to be transmitted over a wireless transmission link; and

a remote device configured to receive over the wireless transmission link an output status comprising the at least a portion of the processed output signal, to process the received output status to generate processed data and to store the processed data, and wherein the remote device is capable of storing a history of at least a portion of the received output status over a specified period of time.

14. The system of claim **13**, wherein at least one of the light emitting diodes emits light with a bandwidth between approximately 20 nanometers to approximately 40 nanometers.

15. The system of claim **13**, wherein the remote device is further configured to transmit at least a portion of the processed data to one or more other locations, wherein the one or more other locations is selected from the group consisting of the personal device, a doctor, a healthcare provider, a cloud-based server and one or more designated recipients, and wherein the remote device is capable of transmitting information related to a time and a position associated with the at least a portion of the processed data.

16. The system of claim **13**, wherein the receiver is located a first distance from a first one of the plurality of light emitting diodes and a different, second distance from a second one of the plurality of light emitting diodes such that the receiver receives a first signal from the first light emitting diode and a second signal from the second light emitting diode.

17. The system of claim **16**, wherein the output signal is generated in part by comparing the first and second signals.

18. The system of claim **13**, wherein the receiver further comprises one or more filters in front of one of more detectors to select a fraction of the one or more optical wavelengths.

* * * * *